Presenilin signalling in a basic biomedical model

Marthe Helene Regina Ludtmann

This thesis is submitted for the degree of Doctor of Philosophy at Royal Holloway University of London, in November 2012

Declaration of Authorship

I, Marthe Ludtmann, hereby declare that this thesis and the work presented in it is entirely my own. Where I have consulted the work of others, this is always clearly stated.

Signed:

Date:

Abstract

Familial Alzheimer's disease is often caused by mutated forms of one of two highly related presenilin proteins. In order to unravel the effects on signalling pathways caused by these aberrant proteins, a model is required in which all wild-type presenilin protein activity is deleted to enable the investigation of disease-related signal transduction. Deletion of both mammalian presenilin genes is highly problematic, as gene deletion causes lethality at an early embryonic stage. Therefore, this current study set out to develop a model system to aid the understanding of presenilin protein signalling.

Dictyostelium discoideum is the simplest biomedical model possessing two presenilin homologues (PsenA and PsenB). Deletion of either *D. discoideum* presenilin gene did not cause an aberrant developmental morphology, however, deletion of both presenilin genes led to a severe developmental phenotype. This phenotype was rescued by reintroducing *D. discoideum psenB*, suggesting a compensatory mechanism of both *D. discoideum* presenilin proteins.

Functionality of this model in the analysis of the human PS1 (hPS1) was shown through expression of hPS1 in the *D. discoideum* presenilin null background. hPS1 expression restored wild-type development, suggesting the human protein is functional in *D. discoideum*. A conserved function between human and *D. discoideum* proteins was established through a Notch cleavage assay. Analysis revealed that both *D. discoideum* presenilin proteins were able to cleave Notch, confirming a functional conservation.

Calcium dysregulation has previously been linked to FAD and presenilin proteins. The work presented here revealed that calcium influx into the cytosol was significantly upregulated in *D. discoideum* presenilin mutant cells.

This study is the first to describe a conserved function between human and *D. discoideum* presenilin proteins. This model provides therefore an excellent system to further investigate cellular roles of human presenilin in basic cell function and disease-related signalling.

Table of Contents

List of Tables and Figures

Abbreviations

ACA	Adenylate cyclase
AD	Alzheimer's disease
AICD	Amyloid intracellular domain
APC	Adenomatous polyposis coli
Aph-1	Anterior pharynx-defective 1 protein
APP	Amyloid precursor protein
Aβ	Amyloid beta
cAMP	cyclic AMP or 3'-5'-cyclic adenosine monophosphate
cAR	cAMP receptor
CRAC	Cytosolic regulator of adenylate cyclase
DhkA	Histidine kinase
DSH	Dishevelled protein
ecmA	Extracellular matrix A
ecmB	Extracellular matrix B
Egl	Egg-laying deficient
ER	endoplasmic reticulum
FAD	Familial Alzheimer's disease
GSK	Glycogen synthase kinase
Htt	Huntington protein
IP_3	Inositol (1,4,5) trisphosphate
IP_3R	Inositol (1,4,5) trisphosphate receptor
IPLA	Inositol-1,4,5-trisphosphate receptor-like protein
Lin-12	Protein lin-12
Lis-1	Miller–Dieker lissencephaly causing protein
MO	Morpholino knock-down
NICD	Notch intracellular domain
Pen-2	Presenilin enhancer 2 protein
PIP_2	Phosphatidylinositol 4,5-bisphosphate
PIP_3	Phosphatidylinositol 3,4,5-bisphosphate
PKA	Protein kinase A
PKA cat	Protein kinase A catalytic domain
PLC	Phospholipase C
PS1	Presenilin 1
$PS1^{-/-}$	Presenilin 1 knock-out
$PS1^{-/-}/PS2^{-/-}$	Presenilin 1/2 knock-out
PS2	Presenilin 2
$PS2^{-/-}$	Presenilin 2 knock-out
psenA	Presenilin A gene
$psenA^{-}$	Presenilin A knock-out
psenB	Presenilin B gene
$psenB^{-}$	Presenilin B knock-out
$psenB^{-}/A^{-}$	Presenilin B/A knock-out

RegA	Phosphodiesterase
RYR	Ryanodine receptor
TACE	Tumor necrosis factor alpha converting enzyme
ZAK	Zaphod K kinase 1

Acknowledgements

I firstly would like to thank Dr Robin Williams for his idea of this project and invaluable guidance. I would also like to thank Dr Richard Killick for his input and support over the last 4 years. I am grateful to Prof Paul Fisher and the La Trobe Dicty lab for help with the calcium assay and making me feel welcome in Melbourne.

I would like to thank Alzheimer's Research UK who funded this project and the Central research fund and the Helen Shackleton fund for making the research visit to La Trobe University possible.

There are many people who celebrated good results with me, cheered me up when things didn't go to plan and allowed me to have a life outside of the lab. Here are just a few: Tam (Achmed), Nicole (Big 'thank you' for reading this thesis), Sherif, Dan, Dana, Kadda, Ulli, Jessi, Diana, the people in office 404 and the William's lab.

I would like to thank the PCR fairy and Calcium Koala who made the experiments run smoothly at Rhul and La Trobe University.

Ich danke euch, Mami, Lisa, Knut und Lena fuer eure aufmunternden Worte und Unterstuetzung – ohne euch haette ich diese Arbeit nicht abgeschlossen.

Last but not least, I would like to thank Wesley who supported me all the way through my studies and always believed in me. You really do deserve your own doctorate for the encouragement, patience and long days without me. I really couldn't have done it without you!

Introduction

1.1 Alzheimer's disease

Alzheimer's disease (AD) is the most prevalent form of dementia and was first described by Alois Alzheimer in 1907. Dementia currently affects 26 million people worldwide and is predicted to rise to 90 million cases in 2050 worldwide if no cure or prevention is being found (Maccioni et al., 2001; Brookmeyer et al., 2007). The majority of AD cases are sporadic (late-onset) and occur after the age of 65. The cause(s) of sporadic AD are still unknown but genome-wide studies have identified genes which increase the likelihood of developing sporadic AD, such as *apoE4*, which was shown to increase the risk by ~60% by the age of 85 (Bertram et al., 2010). This degenerative disease and the resulting demand of care stretches national health insurance services and the financial burden of dementia amounts to £17 billion a year in the UK (Knapp and Prince, 2007).

1.2 Symptoms

AD causes the loss of brain mass through a decline in neurons of the hippocampus and cortex (Huang and Mucke, 2012). Patients display a substantial pathogenesis and neuronal loss before onset of symptoms, and the disease progress can be divided into three stages (Terry and Davies, 1980):

1. Mild dementia, also referred to as mild cognitive impairment (MCI), can last up to 4 years after onset. It includes symptoms such as difficulties with abstract thinking and language, poor reasoning, depressions, and memory loss along with mood swings.
2. Moderate dementia can last up to 10 years and include symptoms such as amnesia, aggression and loss of fine motor skills. At this stage, patients require carers.
3. Severe dementia is the stage in which patients are bedridden, fully dependent on carers and suffer from exhaustion and apathy. This stage

may last up to three years before patients die of secondary causes such as pneumonia.

1.3 Hypothesis of pathogenesis

The cause(s) of the loss of brain mass in AD that lead to cognitive decline is yet to be unravelled. However, post-mortem analysis of patient brains identified two major pathological changes. Neurofibrillary tangles are found within neuronal cells and amyloid plaques are found in extracellular spaces (Huang and Mucke, 2012). Further, numerous biochemical changes are observed such as oxidative stress and neuroinflammation (Selkoe, 2011). Whether amyloid plaques and neurofibrillary tangles are the cause or consequence of AD remains to be determined.

1.3.1 Amyloid hypothesis

Accumulations of extracellular amyloid proteins consist of conglomerates of 4 kDa peptides with beta sheet structures that derive from a transmembrane protein, the amyloid precursor protein (APP). Three enzyme complexes which process APP proteins have been identified and are directly linked to the aggregation of amyloid plaques: α-secretase, β-secretase and γ-secretase where the latter contains presenilin 1/2 (PS1/PS2), anterior pharynx defective (Aph), presenilin enhancer 2 (pen-2) and nicastrin (Huang and Mucke, 2012). The cleavage of APP can occur in a non-amyloidogenic and an amyloidogenic pathway. The non-amyloidogenic pathway involves α-secretase cleaving APP which gives rise to a large N-terminal fragment (aAPPα) that is released into the extracellular space (Fig. 1.1). The C-terminal is then processed by γ-secretase to produce a short p3 fragment and the amyloid intracellular domain which acts as a transcriptional factor (Selkoe, 1997).

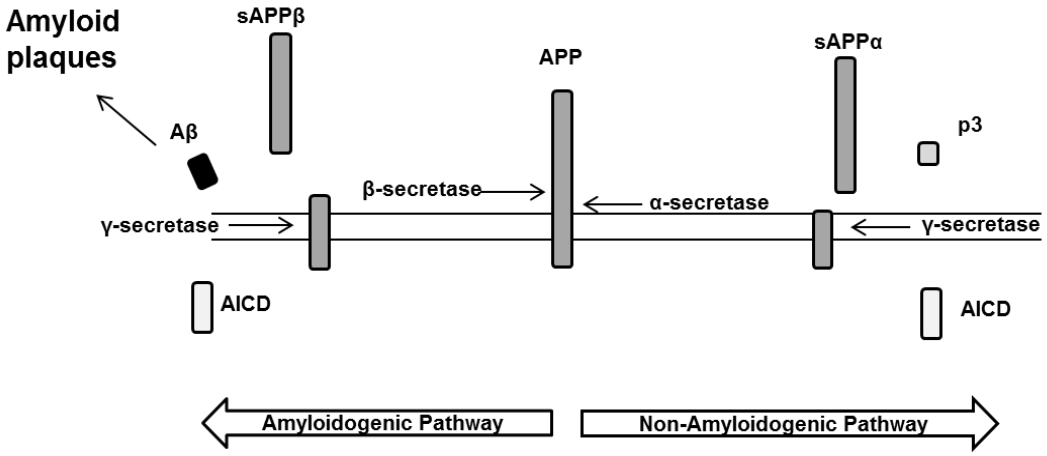

Fig.1.1 Amyloid precursor protein processing. In the non-amyloidogenic pathway APP is cleaved first by α-secretase and then by γ-secretase to produce AICD, sAPPα and p3. The amyloidogenic pathway leads to β-secretase cleavage followed by γ-secretase cleavage generating AICD, sAPPβ and Aβ (36-43) fragment which can then aggregates to form plaques.

In the amyloidogenic pathway however, β-secretase (termed BACE) cleaves APP and the product (sAPPβ) is released into the extracellular medium (Fig. 1.1). The remaining fragment is then cleaved by γ-secretase and Aβ peptides are produced ranging from 36-43 amino acids (Laferla et al., 2007). $A\beta_{40}$ and $A\beta_{42}$ are the predominant isoforms with the shorter isoform being the more common one and the longer isoform the more fibrillogenic (more likely to develop fine fibrils). In AD, a shift towards the amyloidogenic pathway takes place causing an alteration in the $A\beta_{42}$ to $A\beta_{40}$ ratio that leads to an accumulation of $A\beta_{42}$ and extracellular plaques are formed (Gotz and Ittner, 2008). In addition to extracellular Aβ, soluble Aβ fragments within neurons have been identified and mounting evidence suggests that the neurotoxic effects are linked to several biochemical dysregulations in AD brains (Laferla et al., 2007; Swerdlow, 2011).

Genetic analysis has shown that mutations in APP, PS1 and PS2 can cause autosomal dominant AD where mutations trigger an increase of $A\beta_{42}$ fragments thus leading to amyloid plaque deposition (Gotz and Ittner, 2008). This rare form of AD is termed Familial Alzheimer's Disease (FAD) which shares the common pathological hallmarks with the sporadic form of AD but has an onset of disease from as early as 20 years of age. Thus, patients are considered to have FAD if the disease has been diagnosed before the age of 65 and genetic

mutations in AD-associated proteins have been established (Maccioni *et al.*, 2001).

1.3.2 Tau hypothesis

As recently as the 1980s, tau, a micro-tubule-associated protein, was discovered to be a core protein of intracellular neurofibrillary tangles (Maccioni et al., 2001). Researchers have since tried to unravel the clinical importance and cellular pathways of tau regulation. It was found that tau is phosphorylated by serine/threonine kinases such as glycogen synthase kinase-3 beta (GSK-3β) that aids the assembly and stabilisation of microtubules (Hanger and Noble, 2011). In the AD diseased brain, hyperphosphorylation of tau leads to its dissociation from microtubules leading to aggregation and the formation of highly insoluble tangles (Wang et al., 2007). PS1 has been shown to interact and regulate tau phosphorylation through GSK-3β, as FAD mutations in PS1 were found to hyperphosphorylate tau and promote tau tangle aggregation (Takashima et al., 1998). Tau tangles have also been linked to mitochondria dysregulation affecting the electron transport chain and ATP production similar to that seen with Aβ (Ittner et al., 2011). After decades of independent research investigations into tau and Aβ, a link between these proteins has only been recently proposed (Nicholson and Ferreira, 2009). It was shown that Aβ increases neuronal calcium concentrations leading to the activation of kinases that in turn hyperphosphorylate tau leading to tau aggregations within the neuron (Wray and Noble, 2009). The recent understanding of a tau and Aβ interaction further supports the complexity of AD and requires ongoing research efforts in order to find therapeutic agents targeting both proteins (Selkoe, 2011).

1.3.3 Hypothesis of neuroinflammation

In recent years, researchers in the field of AD have begun to widen their investigations outside of tau and Aβ, into inflammation processes which may lead to neuronal loss. Here, microglia activation has gained considerable attention as it is a universal feature of AD and other neurodegenerative diseases and head trauma (Tuppo and Arias, 2005). Microglia cells form part of the immune response of the brain and Aβ has been shown to activate microglia phagocytosis which in turn clears plaques. However, microglia cells have been found to accumulate fragmented DNA which may originate from neuronal injury and death (Mrak, 2012; Li et al., 2004). It has been proposed that microglia activation is initially beneficial in plaque clearance but overexpression of pro-inflammatory cytokines at cytotoxic levels causes acute neuroinflammation, formation of tangles and neuronal death (Mrak, 2012). Pro-inflammatory cytokines have also been linked to calcium dysregulation within neurons and subsequent microglia activation. Furthermore, Aβ has been suggested to stimulate calcium dependent secretory phospholipase A2 resulting in production of arachidonic acid which is then converted into pro-inflammatory eicosanoids which then causes neuronal damage (Paris et al., 2000).

1.3.4 Mitochondrial dysfunction and oxidative stress hypotheses

Another hypothesis of AD aetiology surrounds the neurotoxic effects caused by intracellular Aβ causing calcium dysregulation leading to mitochondrial and synaptic dysfunction and oxidative stress (Hauptmann et al., 2006). Oxidative stress and mitochondrial dysfunction have therefore become a new focus of research in the AD field. It has been shown that intracellular soluble Aβ binds to mitochondria and even accumulates in mitochondria, leading to dysregulated cell functions and cell death. Aβ has been shown to negatively regulate amyloid-binding alcohol dehydrogenase in mitochondria and increased levels of hydrogen peroxides and decreased ATP production (Muirhead et al., 2010). Further, it has been reported that Aβ interacts directly with cyclophilin D on mitochondria that in turn causes calcium dysregulation in mitochondria and

therefore alters synaptic function (Readnower et al., 2011). Aβ has also been suggested to increase reactive protein species which inhibit mitochondrial enzymes such as cytochrome oxidase leading to electron transport chain dysfunction and cell death (Casley et al., 2002).

Despite numerous studies reporting cellular dysregulation affecting numerous signalling pathways, the underlying cause of AD is yet to be determined. Therefore, to help unravel the underlying cause(s) of AD the linking factor(s) between the observed biochemical alterations need to be found.

1.4 Diagnosis and treatment

The lack of definite diagnostic tools and biological markers makes the diagnosis of AD difficult. A combination of neurological and psychiatric tests are currently employed to diagnose AD, however only a post mortem analysis of brain tissue gives unambiguous results (Mayeux, 2003). To date, no cure has been found but therapeutic agents have been marketed such as Memantine and Donezepil which target NMDA receptors or inhibit cholinesterase and improve cognitive functions (Salawu et al., 2011). Immunotherapy is a new strategy in defeating AD and pre-clinical studies in transgenic APP mice have shown a clearance of Aβ plaques but not intracellular Aβ and tau plaques (Schenk et al., 1999; Delrieu et al., 2012). However, translation into human clinical trials did not yield the expected results as plaque clearance did not improve the cognitive decline or side effects caused the trials to be haltered (Delrieu et al., 2012). Nevertheless, development of immunotherapies against plaques and tangles continues with some trial outcomes still outstanding.

1.5 Presenilin

In mammalian systems, presenilin proteins have been shown to interact with a variety of molecules, thus regulating a multitude of signalling pathways. Presenilin proteins are multipass transmembrane aspartic endopeptidases and act either as the catalytic core of the γ-secretase complex or via γ-secretase independent functions (McCarthy et al., 2009). For the γ-secretase complex to

assemble, presenilin proteins are required to undergo endoproteolytic cleavage within exon 9 before they can associate with anterior pharynx-defective 1 protein (Aph-1), presenilin enhancer 2 protein (PEN-2) and nicastrin (De Strooper, 2003). It has been shown that both presenilin proteins can act as the catalytic core of the γ-secretase complex but PS1 has been shown to be more active in APP cleavage than PS2, suggesting overlapping but yet distinct biological processes (Lai et al., 2003). These results were supported by the weaker developmental phenotype in mice lacking $PS2^{-/-}$ when compared to $PS1^{-/-}$ mice (van Tijn et al., 2011). The multimeric γ-secretase complex is responsible for intramembranous cleavage of type I transmembrane proteins such as APP and Notch-1. To date, no uniform target recognition sites for cleavage have been identified for the γ-secretase complex but the multitude of reported substrates suggests a variety of target sites (McCarthy et al., 2009). γ-secretase independent functions for presenilin proteins have emerged but only very few mechanisms have been identified (Parks and Curtis, 2007). One of the best established examples is Wnt-mediated signalling where PS1 acts as a scaffold protein and promotes β-catenin phosphorylation and ultimate degradation (Koo and Kopan, 2004).

1.6 Presenilin in Alzheimer's disease

Presenilin proteins have been linked to FAD due to the discovery of 185 point mutations in PS1 and 13 mutations in PS2 in FAD patients. However, not all reported mutations appear to have a pathological nature (Cruts and Van, 1998). A dominant negative FAD mutation can be caused by insertion, deletion or substitutions of nucleotides resulting in a change of amino acid sequence. The mean age of FAD onset is dependent of the position of the mutation, and can be as early as 20 years of age with 35 years being the mean age of death (Rogaeva et al., 2001). Most of these mutations have been found to increase the $A\beta_{42}$ to $A\beta_{40}$ ratio through the γ-secretase complex and amyloidogenic pathway. Further, FAD mutations cause biochemical and pathological changes which mirrors those observed in sporadic AD. Therefore, understanding of the basic cellular roles of presenilin and their role in disease may help to unravel the underlying cause of AD and may potentially offer a therapeutic target for

drug development studies. To date, presenilin proteins have been linked to a multitude of signalling pathways and a selection of these are discussed in detail in the current study.

1.7 Signalling pathways affected by presenilin dysregulation

1.7.1 Notch signalling

Notch is a transmembrane receptor that, when cleaved, gives rise to an intracellular domain that regulates gene transcription (Robey, 1997). A role for presenilin-dependent Notch cleavage was first found in *Caenorhabditis elegans* where deletion of presenilin produced the same phenotype as the mutant lacking the Notch homologue (Levitan and Greenwald, 1995). Notch itself has first been discovered in *D. melanogaster* and has since been shown in various systems to play a critical role in neuronal development and in the adult brain a role in neurogenesis and neuritic growth (Woo et al., 2009; Selkoe and Kopan, 2003; Robey, 1997). There are four isoforms of the Notch protein (1-4) which are predominantly expressed in the hippocampus and are involved in learning and memory which are both affected in AD patients (Berezovska et al., 1998).

Notch are single pass integral type I receptors and undergo a series of cleavage events (Woo et al., 2009). The first cleavage (S1) is carried out by a furin-like convertase and generates a mature Notch receptor on the cell surface (Fig. 1.2). Delta like or Jagged ligands of neighbouring cells then bind the mature Notch receptor which allows cleavage by tumor necrosis factor alpha converting enzyme (TACE; S2). This then allows the last cleavage event by the γ-secretase complex (S3), which generates the Notch intracellular domain (NICD). This subsequently translocates into the nucleus where it interacts with the C-promoter binding factor-1 (Woo et al., 2009). Presenilin proteins play a key role as part of the γ-secretase complex in Notch cleavage, as S3 cleavage is significantly reduced if not completely abolished in the presence of selected FAD mutations (Moehlmann et al., 2002). These findings together with the involvement of Notch in neurogenesis and memory suggest presenilin and

Notch proteins as an interesting target to investigate the cognitive decline in AD patients.

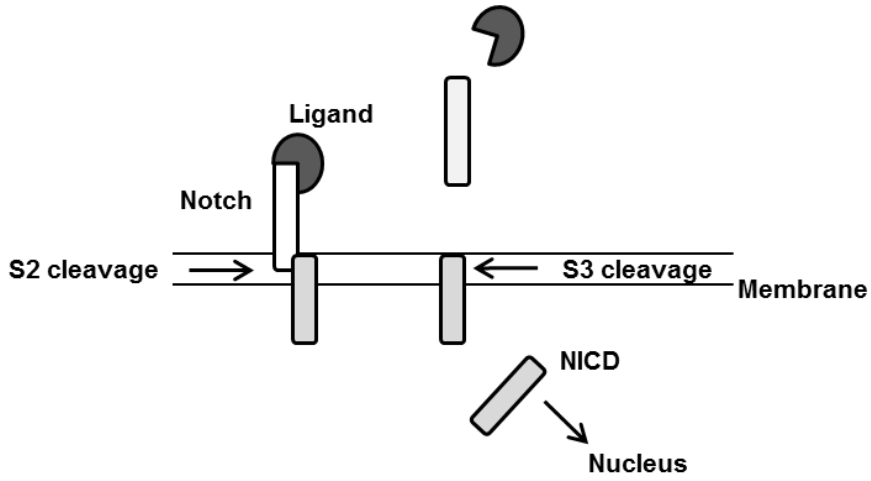

Fig.1.2 Notch reporter cleavage by Tumor Necrosis Factor Alpha Converting Enzyme (TACE) and γ-secretase. A ligand binds to the mature Notch receptor which allows the S2 cleavage by TACE and the shedding of the extracellular domain. The γ-secretase performs then the S3 cleavage, releasing the Notch Intracellular Domain (NICD) which translocates to the nucleus.

1.7.2 Wnt signalling

Several FAD mutations in PS1 potentiate neuronal death through a dysregulation of β-catenin via the Wnt pathway, making this protein interaction interesting to the Alzheimer's disease research community (Zhang et al., 1998). Wnt signalling has been shown to regulate embryogenesis, neurotransmitter release and neuronal plasticity (Murayama et al., 1998). The Wnt protein was first described in *D. melanogaster* where its binding to frizzled receptors leads to a stabilisation of β-catenin within the cell, allowing translocation to the nucleus to control gene transcription (Sharma and Chopra, 1976). For this process, Wnt requires frizzled receptor binding, which in turn activates a dishevelled protein (Dsh) that associates with Axin at the receptor (Fig. 1.3). The association of Axin with the promoter prevents phosphorylation of β-catenin through the GSK-3β/Axin/APC complex and degradation by polyubiquitination and proteasomes (Logan and Nusse, 2004). Soriano et al. (2001) has shown that PS1 interacts with β-catenin and as deletion of PS1 led to a decrease in ubiquitination and therefore stabilisation of β-catenin. Since accumulation of the

phosphorylation of β-catenin took place in PS1 deficient cells, the authors concluded that PS1 interacts directly with ubiquitin ligase (Soriano et al., 2001). Presenilin proteins have also been shown to act as a scaffold that regulates β-catenin stabilisation via a non-canonical Wnt pathway (Boonen et al., 2009). This process involves PS1, protein kinase A (PKA) and GSK-3 which leads to the phosphorylation and degradation of β-catenin (Kang et al., 2002). Here it was shown that mouse fibroblasts lacking PS1 present a hyperproliferation phenotype due to the lack of β-catenin degradation (Soriano et al., 2001). Further, it was shown that γ-secretase inhibitors (inhibiting the catalytic activity of presenilin proteins) did not affect this β-catenin regulation, suggesting that this process is a γ-secretase independent process (Meredith, Jr. et al., 2002).

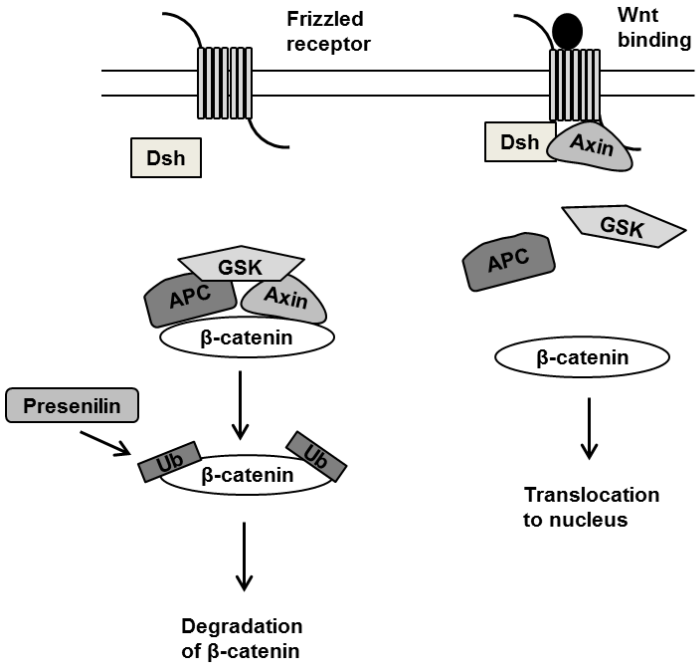

Fig.1.3 The Wnt signalling pathway. In the absence of Wnt binding to the frizzled receptor, APC, Glycogen Synthase Kinase 3β (GSK) and Axin bind and phosphorylate β-catenin. This phosphorylation lead to the ubiquitination and degradation of β-catenin and PS1 is proposed to regulate this process. Upon Wnt binding, dishevelled protein (Dsh) promotes Axin to the receptor which leads to a destabilisation of the APC/GSK-3/Axin complex and stabilisation of β-catenin, allowing translocation to the nucleus.

1.7.3 Calcium signalling

Calcium dysregulation has also been associated with neurodegeneration involved in AD. Oxidative stress and metabolic dysfunction are important contributors to the elevated neuronal calcium levels which are likely to cause neuronal excitation and synaptic death (Mattson and Chan, 2003). The endoplasmic reticulum (ER) regulates cytosolic calcium levels by acting as a calcium store and calcium store overloading was shown in AD models (Ito et al., 1994; Supnet and Bezprozvanny, 2011). As presenilin proteins localise to the ER it has been thought that they play a role in calcium homeostasis (Mattson, 2010). Several different mechanisms have been proposed for this (Fig. 1.4):

It has been shown that PS1 interacts with both the inositol (1,4,5) trisphosphate (IP_3) receptor and ryanodine receptor (RyR), and an increased calcium release into the cytosol has been recorded with FAD mutations or deletion of presenilin proteins (Tu et al., 2006a; Cheung et al., 2008). Although, the exact mechanism of this regulation is still unknown, Tu and collegues (2006a) suggested that presenilin proteins form calcium leak channels independent of the γ-secretase complex. These calcium leak channels are proposed to regulate steady-state ER calcium levels which in the presence of FAD mutated presenilin proteins results in high intraluminal and low cytosolic calcium concentrations. This hypothesis has however been recently challenged by Shilling et al. (2012) as they were unable to find corroborative evidence. Despite this conflicting evidence, calcium dysregulation is a major hallmark of AD and is likely to cause cell death. This outlined research has provided a direct link between calcium homeostasis and presenilin proteins making further investigations necessary.

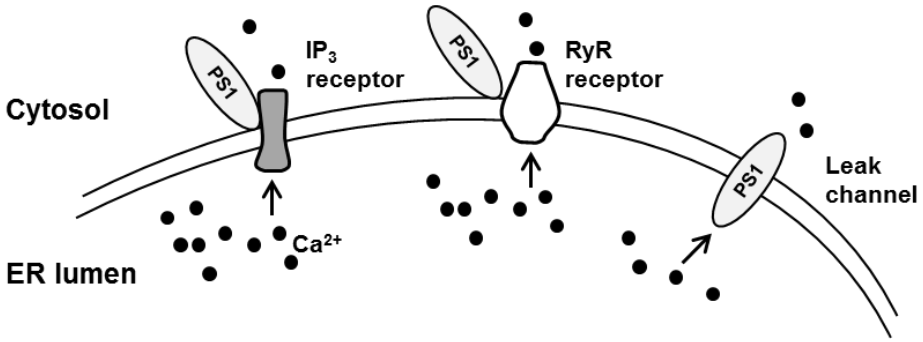

Fig.1.4 ER calcium signalling controlled by PS1. Schematic diagram of selected mechanisms through which PS1 regulates calcium homeostasis. PS1 interacts directly with the inositol (1,4,5) trisphosphate (IP_3) and ryanodine receptor (RyR), thus regulating calcium (black dots) release from the ER. Furthermore, PS1 itself has been shown to channel calcium from the ER into the cytosol through formation of a leak channel.

1.8 Presenilin models

Despite the difference in risk factors for sporadic and inherited forms of AD, presenilin proteins are directly linked to the histopathological changes observed in both forms of AD. Thus, understanding the physiological role of presenilin proteins in their normal and aberrant forms is of high importance to help understand AD and potentially provide a novel drug target.

To date, mice are the most widely used model to understand presenilin proteins and their downstream signalling. Despite advances in developing this research model over the last years, it should be noted that mouse models do not exhibit neurofibrillary tangles and only seldom neuronal loss, although plaque formation can be assessed in FAD transgenic mice (Hall and Roberson, 2011; Qing et al., 2008). Notwithstanding the recent advances in the discovery of therapeutic agents, the basis of presenilin signalling in AD pathologies is yet to be fully established. To investigate presenilin signalling, both presenilin genes need to be deleted in order to establish signalling pathways and proteins controlled by presenilin proteins. This however, proves difficult in mice as both presenilin genes are expressed throughout embryogenesis into adulthood. Deletion of both *ps1* alleles has been shown in mice to be perinatal lethal and down-regulatory to the Notch pathway resulting in a neuronal loss (Shen et al., 1997; Handler et al., 2000). The mouse model lacking both *ps2* alleles does not present a severe phenotype. The ideal model lacking both alleles of *ps1* and

ps2 is not viable, resulting in embryonic death with neural tube disorganisation through a disruption of Notch signalling in early development (Donoviel et al., 1999). One way to overcome this has been suggested using a conditional model lacking both alleles of *ps1* and *ps2* only in the forebrain, allowing investigations into neuronal atrophy and altered cognitive behaviour after 10 months when amyloid plaques have formed (Feng et al., 2004; van Tijn et al., 2011).

Several non-mammalian models have also been shown to provide new insights into presenilin protein function and potential neuropathological changes observed in AD patients. *Caenorhabditis elegans* possesses three presenilin homologues Sel-12, Hop-1 and Spe-4. Sel-12 has fundamentally contributed towards the understanding of presenilin signalling as it provided the first link between presenilin and Notch (Levitan and Greenwald, 1995). This biomedical model presents an egg-laying deficient (Egl) phenotype upon deletion of *sel-12*, through reduction of *lin-12* /notch activity. In this model the human PS1 is able to rescue the observed phenotype, providing evidence of a conserved presenilin function between human and *C. elegans* (Levitan and Greenwald, 1995). In *Drosophila melanogaster*, loss of the only presenilin gene results in lethality at the larval-pupal transition stage which cannot be rescued by expressing human PS1 or PS2. However, FAD *D. melanogaster* mutants have been created by engineering FAD mutations into the *D. melanogaster* presenilin gene, offering a model in which effects of FAD mutations can be assessed by examining head, wing, and retina structures (Seidner et al., 2006). Another cost effective model for presenilin research is *Danio rerio* which possesses two presenilin homologues (van Tijn et al., 2011). Developmental stages are well characterised in this biomedical model, and morpholino antisense-oligonucleotides are employed to knock-down presenilin proteins. *psen1* MO (morpholino knock-down) in *D. rerio* leads to somite defects, defective brain development and loss of Notch target gene *her6* (HES1 orthologue), whereas *psen2* MO leads to reduced melanin pigmentation (Nornes et al., 2008). Interestingly, MO of *psen1* and *psen2* does not result in a more severe phenotype then PS1 alone, which differs from the lethal effect observed in other presenilin models such as the double presenilin knock-out mouse (Nornes et

al., 2009; van Tijn et al., 2011). The reason for this might be the lack of a complete deletion of presenilin protein activity due to the nature of MO.

Another more recent model for presenilin activity is *Dictyostelium discoideum*, a well-established system to investigate development and chemotaxis (Williams et al., 2006). Recently, McMains et al. (2010) have shown that *D. discoideum* encodes two presenilin protein homologues. The authors report that *D. discoideum* presenilin proteins are able to cleave human APP accurately and that presenilin deletion exhibits a developmental phenotype as observed in other biomedical models (van Tijn et al., 2011; Gotz and Ittner, 2008). Furthermore, *D. discoideum* offers a system which can help to find cellular drug targets and potentially identify novel compounds for human disease such as AD (Chang et al., 2012; Ludtmann et al., 2011).

1.9 Dictyostelium discoideum

D. discoideum is a social amoeba and is recognised by the US National Institute of Health (NIH) as a biomedical model. This haploid eukaryote possesses six chromosomes (34Mb) with numerous genes that are homologues to those in higher organisms (Williams et al., 2006). On a phylogenetic scale, Eichinger et al. (2005) have shown that the divergence of *D. discoideum* from a common eukaryotic ancestor took place soon after the plant and animal split, confirming earlier proteomic analysis by Bapteste et al. (2002) (Fig. 1.5). *D. discoideum* can be found in soil, feeding on bacteria and yeast. Upon starvation, amoebae stop dividing and enter a developmental cycle (Weijer, 2004). In this cycle, a single cell in a population will start releasing cyclic AMP (cAMP) in a pulsatile manner and this signal is relayed from surrounding cells enabling chemotaxis to take place. This leads to the aggregation of around 10^5 amoeba, enabling the differentiation into prespore and prestalk cells, and finally form a mature fruiting body. Spores in the fruiting body are ultimately released to germinate in the presence of nutrition (Fig. 1.6) (Weijer, 2004).

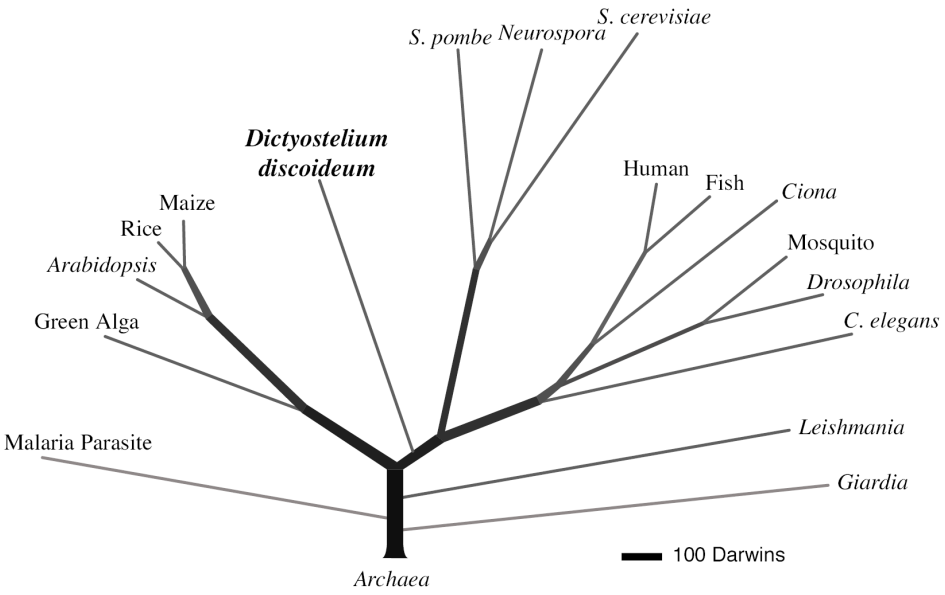

Fig.1.5 Proteome-based eukaryotic phylogeny. *D. discoideum* diverged soon after the plant/animal split but before the divergence of yeast. Taken from Eichinger (2005).

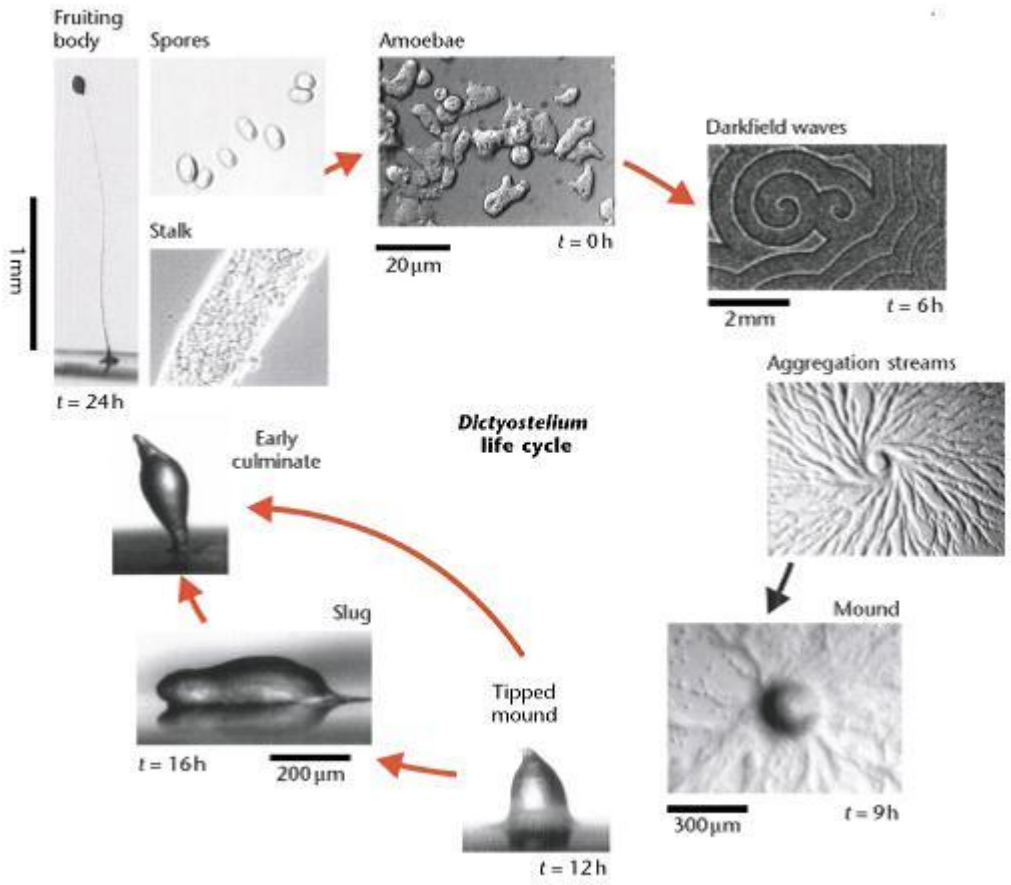

Fig.1.6 Developmental life cycle of *D. discoideum*. Amoeba start to develop upon starvation and chemotax towards an excreted cAMP signal of neighboring cells via aggregation streams. After 9h, cells form a mound before starting to form a slug and develop into stalk cells (dead cells) and a forming a fruiting body after 24h. The fruiting body holds spores which are released to germinate in the presence of a food source. Image from Weijer and Williams (2009).

D. discoideum development can be divided into an early, mid and late stage which depend upon differential regulation of a multitude of genes, allowing chemotaxis, formation of aggregation and differentiation into stalk and spore cells. For a cell to undergo chemotaxis and aggregation it must sense extracellular cAMP. G protein-coupled receptors play a vital role in this process, and in initiating chemotaxis (Kim et al., 1996). *D. discoideum* possess four G protein-coupled receptors that bind extracellular cAMP named cAR1-4 (cAMP receptors 1-4), and these are differently expressed throughout development. cAR1 is the main receptor involved in chemotaxis and streaming during early development in *D. discoideum* and is mainly expressed in the first 2-8h of development (DictyExpress) (Kim et al., 1996). Activation of cAR1 through

cAMP binding leads to a translocation of the Gβγ-subunit to phosphatidylinositol 3-kinase (PI_3K) which in turn phosphorylates phosphatidylinositol 4,5-bisphosphate (PIP_2) to generate phosphatidylinositol 3,4,5-bisphosphate (PIP_3) (Fig. 1.7). PIP_3 is traditionally thought to be involved in chemotaxis but also interacts with cytosolic regulator of adenylate cyclase (CRAC) which in turn activates adenylate cyclase (ACA) and cAMP production (Sun and Devreotes, 1991). The importance of cAR1 in *D. discoideum* development has been shown in a mutant lacking cAR1 and cAR3 which is not able to aggregate (Kim et al., 1997).

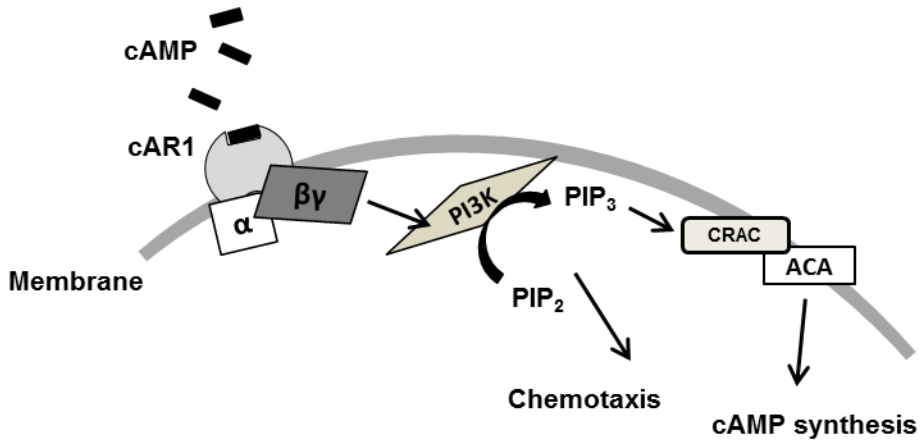

Fig.1.7 Schematic diagram of cAMP binding to the cAR1 receptor and downstream signalling. cAMP binds to the cAR1 receptor which leads to a translocation of the βγ-subunit to phosphatidylinositol 3-kinase (PI3K). PI3K in turn phosphorylates phosphatidylinositol 4,5-bisphosphate (PIP_2) to generate phosphatidylinositol 3,4,5-bisphosphate (PIP_3) which then initiates downstream signalling such as chemotaxis and cAMP synthesis.

The second and third stage of *D. discoideum* development requires initiation of cell fate decisions to allow formation of a mature fruiting body consisting of stalk and spore cells. The decision of which cells develop into pre-stalk or pre-spore cells depends upon the cell cycle phase of each individual cell at the start of starvation. Typically, cells in early stages of the cell cycle develop into pre-stalk cells to eventually form stalk cells. Cells in later stages of the cell cycle differentiate into pre-spore and then mature spore cells (Briscoe and Firtel, 1995). To regulate these cell-fate decisions cAMP and DIF (differentiation-inducing factor) are secreted from cells post-aggregation, where cAMP regulates gene transcription of late-development and pre-spore genes, and DIF

regulates pre-stalk gene transcription. These two morphogens regulate two genes involved in stalk cell production (extracellular matrix A (*ecmA*) and extracellular matrix B (*ecmB*) (Aubry and Firtel, 1999). cAMP has been shown to bind to cAR3 and regulate stalk cell production though a negative regulation of *ecmB* transcription via zaphod K kinase 1 (ZAK-1) and glycogen synthase A (a homologue of GSK-3β) (Fig. 1.8 A). It was further shown that DIF inhibits GSK-A, allowing *ecmB* transcription and stalk cell production (Fig. 1.8 B) (Schilde et al., 2004). These stalk cells are dead vacuolated cells that provide an example of autophagy (programmed cell death) necessary for the formation of mature fruiting bodies (King, 2012).

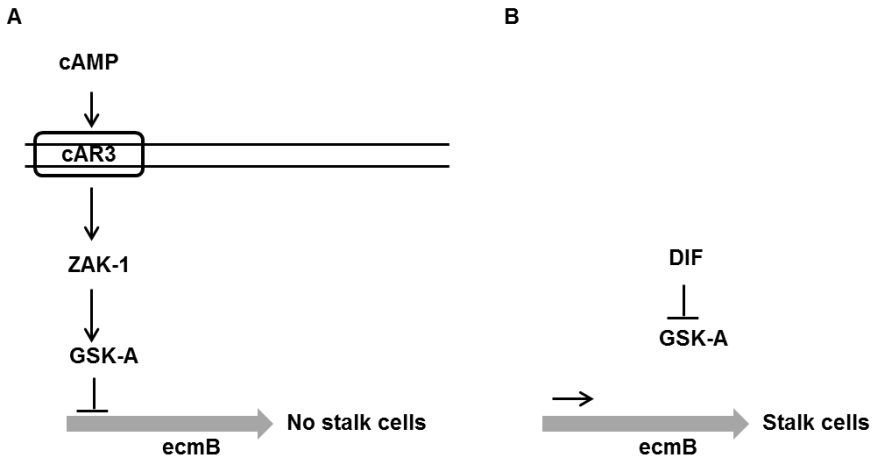

Fig.1.8 Schematic diagram of stalk cell production in *D. discoideum*. (A) The binding of cAMP to the cAR3 receptor leads to a downstream zaphod K kinase 1 (ZAK-1) activation which in turn phosphorylates Gsk-A. Gsk-A inhibition of ecmB gene transcription prevents stalk cell production. (B) Dif inhibits Gsk-A allowing *ecmB* transcription and therefore stalk cell production.

For the final stage of *D. discoideum* development, spore cell production requires high intracellular cAMP in order to activate PKA and induce spore cell production (Loomis, 1998). Intracellular cAMP levels are maintained by ACA which produces cAMP and the phosphodiesterase, RegA, which breaks down cAMP to form 5'AMP (Fig. 1.9) (Thomason et al., 1999a). In *D. discoideum*, RegA activity is inhibited by a histidine kinase (DhkA) to elevate intracellular cAMP levels which leads to spore cell differentiation (Loomis, 1998).

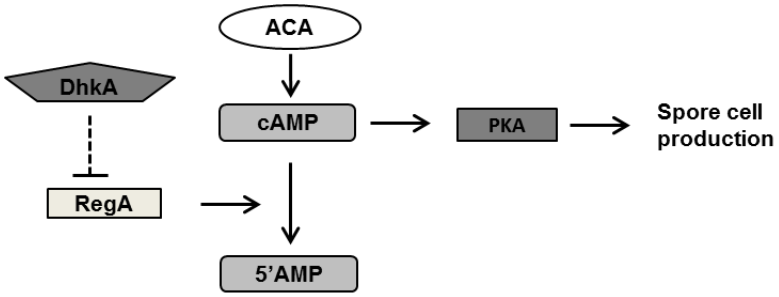

Fig.1.9 Schematic diagram of spore cell production in *D. discoideum*. Intracellular cAMP is produced by adenylate cyclase (ACA) which in turn is broken down by RegA (phosphodiesterase). However in late development, histidine kinase (DhkA) inhibits RegA which allows intracellular cAMP levels to rise, which in turn activates protein kinase A (PKA) to allow spore cell production.

Studies of *D. discoideum* chemotaxis progressed the understanding of eukaryotic cell mobility. It was suggested that calcium may play a role as a chemoattractant as stimulation with cAMP and calcium leads to greater chemotaxis rates (Scherer et al., 2010). Calcium has also been shown to directly regulate velocity and pseudopod formation in this amoeba and global cAMP stimulation of aggregation-competent cells (7h into development) leads to a rapid influx of calcium into the cytosol from the extracellular medium and intracellular stores such as the ER (Wilczynska et al., 2005). The exact mechanism of how calcium influx is regulated is still elusive, but Fisher and Wilczynska (2006) have suggested that calcium influx from the extracellular medium results in a release of calcium stored in the ER. Further, *D. discoideum* possesses homologues of calcium channels and calcium pumps, of which inositol-1,4,5-trisphosphate receptor-like protein (IPLA) is the best studied channel (Traynor et al., 2000). The presence of this calcium channel suggests calcium release from ER stores is facilitated via G protein-coupled receptor activation (such as cAR1) and protein lipase C and IP_3 production during chemotaxis. However, deletion of IPLA did not affect chemotaxis despite a lack of calcium influx from the extracellular medium (Traynor et al., 2000). Although these differing reports leave a role for calcium in chemotaxis and development in *D. discoideum* unclear, calcium has been shown to regulate cell fate decisions in *D. discoideum*, as deletion of IPLA or reduction of intracellular

calcium concentration prevented autophagic death upon DIF stimulation which is required for stalk cell differentiation (Lam et al., 2008; Jaffe, 1999).

D. discoideum has been employed to understand cellular movements and cell fate decisions but development of knock-out techniques allowed multiple gene manipulations within one cell line, allowing more detailed analysis of a multitude of signaling pathways (Parent, 2004; Faix et al., 2004). The sequencing of the *D. discoideum* genome has also opened new directions of research using this model, since it contains proteins encoding homologues associated with a variety of human diseases and disorder (Annesley and Fisher, 2009). For example, Myre et al. (2011) and Wang et al. (2011) have employed *D. discoideum* to investigate cellular functions of the Huntington protein (*htt*) which is a homologue of the disease causing in Huntington's disease. Wang et al. (2011) showed that deletion of *D. discoideum* Htt affects chemotaxis and cytokinesis through a myosin II deficiency. Ongoing studies in this model may help to unravel the biochemical malfunction in Huntington's disease and ultimately help treat this progressive neurological disorder. *D. discoideum* has also aided the understanding of a protein causing Miller–Dieker lissencephaly (LIS1) which is a regulator of dynein. The high similarity of the *D. discoideum* protein to the human disease causing protein allowed the identification of LIS1 binding partners (Rho-GTPase, Rac1A). This research provided the first link of the LIS1 protein to the mechanism causing deficient neuronal actin dynamics observed in lissencephaly (Rehberg et al., 2005). Ongoing work in this area offers a system which allowed analysis of lissencephaly associated mutations in LIS1 and their effects on microtubule interactions and centrosome and nuclei coupling (Williams et al., 2006).

These examples outline the potential of *D. discoideum* to aid the understanding of human disease. Another line of research complements this translational approach, as *D. discoideum* has been employed to investigate drug-sensitive signalling pathways (Williams et al., 2006; Li et al., 2000). For example, lithium and valproate are bipolar disorder treatments, with an unknown mode of action. Exposure of *D. discoideum* to these compounds resulted in altered developmental phenotypes which led to the identification and characterisation of molecular targets of these drugs (Williams et al., 1999). It was shown that

lithium acts inhibitory on inositol (1,4,5) triphosphate levels which supports the inositol depletion theory of bipolar disorder drug action (Williams et al., 1999). Recently, *D. discoideum* has been employed to identify compounds, based on the structure of valproate, that show improved control of seizures in animal models that additionally lack the side effects observed with valproate (Chang et al., 2012). This research was initiated in *D. discoideum* and successfully translated to primary mammalian neurons, clearly indicating the successful translation of research discoveries from *D. discoideum* to mammals.

1.10 Study aims

Presenilin proteins are central to the cleavage of APP and play a role in tau phosphorylation - two key processes associated with AD pathogenesis. Due to the vital nature of these proteins, research into understanding the cellular roles of presenilin proteins have been slow. Understanding the two related presenilin proteins in *D. discoideum*, may help to unravel basic cellular functions of presenilin proteins which translate into mammalian systems.

- Analyse structure and evolutionary relatedness of *D. discoideum* presenilin proteins to those of other species on bioinformatic level.
- Study the role of presenilin proteins in *D. discoideum* development.
- Establish conserved function between human and *D. discoideum* presenilin proteins.
- Investigations into signalling pathways controlled by presenilin proteins.
- Examine a role for presenilin proteins in *D. discoideum* calcium homeostasis.

This study will be beneficial to establish a novel biomedical model for presenilin signalling.

Materials and Methods

2.1 Reagents

Agarose and Taq polymerase were purchased from Bioline (London, UK); Blasticidin and Penicillin/Streptomycin solution from PAA (Pasching, Austria). Calcium chloride, Ethanol and Isopropanol were obtained from VWR (Lutterworth, UK). HL-5 medium, SM agar and SOC broth were purchased from Formedium (Hunstanton, UK) and Ethidium Bromide tablets were from Bio-RAD (Hemel Hempstead, UK). Phusion Hot Start II polymerase was obtained from NEB (Hitchin, UK).T4 DNA ligase, Proteinase K, GeneRuler DNA ladders and all restriction enzymes were obtained from Fermentas (St. Leon-Rot, Germany), whereas Tris/Borate/EDTA buffer was purchased from Fisher (Loughborough, UK). Magnesium chloride, LB Agar Tablets, LB Broth, SYBR Green, cAMP and all other chemicals were obtained from Sigma (Dorset, UK).

2.2 Molecular kits

High Speed Plasmid Maxi, Midi, Mini-prep and Qiaquick Gel Extraction kits were purchased from Qiagen (Crawley, UK). The High Pure RNA Isolation kit was obtained from Roche (Burgess Hill, UK) and the First strand cDNA synthesis kit was bought from Fermentas (St. Leon-Rot, Germany). The DNA-free Dnase kit was obtained from Life Technologies (Grand Island, USA).

2.3 Plasmids

plPBLP and pDEX-NLS-cre were obtained from Dr Jan Faix (Hannover, Germany). CRAC-GFP, pDM317, pDM323, and pDM448 were obtained from Dictybase (Veltman et al., 2009). Prof Paul Fisher (Melbourne, Australia) supplied pPROF120; Dr. Annette Mueller-Taubenberger (Munich, Germany) provided the GSK-GFP plasmid and Prof Jeffrey Williams (Dundee, UK) supplied *ecmA* PKAcat full length, *psA* PKAcat truncated and *psA* full length

plasmids. The human $PS1^{D385A}$ plasmid was supplied by Dr Richard Killick (London, UK) and pFLAG-CMV 5a was obtained from Sigma (Dorset, UK).

2.4 Antibodies

The anti-GFP antibody and GFP-Booster were obtained from ChromoTek (Planegg-Martinsried, Germany), whereas Dr Annette Mueller-Taubenberger (Munich, Germany) supplied the anti-calnexin antibody. The goat anti-mouse IgG (NEB 4409s; Alexa fluor 555) was purchased from NEB (Hitchin, UK).

2.5 Software

Statistical analysis was conducted using Prism 5 (GraphPad Software, Inc.). Phylogenetic analysis was performed using MEGA 5 (Kumar et al., 2008). Microscopic images were captured using Image Pro Plus 6.3 (Media Cybernetics, Inc.). DNA analysis was carried out by employing pDRAW32 (Kjeld, 2006). Image J was employed to analyse CRAC localisation (Rasband, 1997).

2.6 Statistics

Experimental data were shown as means ± standard error of the mean. Statistical analysis between samples was performed using an unpaired Student's t-test after normal distribution was confirmed by employing the Kolmogorov-Smirnov test. Differences were considered to be significantly different if $p < 0.05$ (*).

2.7 Maintenance of *D. discoideum*

D. discoideum (Ax2) cells were stored at -80°C and scrapings were taken at monthly intervals, and grown at 21°C on a SM agar plate (Formedium, UK) containing *Raoultella planticola*. After 3-4 days incubation, a small amount of *D. discoideum* cells from the growth zone was taken and transferred into a liquid dish containing axenic medium (HL-5; 100 µg/ml penicillin/streptomycin). The

dish was kept at 21°C and, when required, adherent cells were washed off the dish and transferred into a 100 ml flask containing 30 ml axenic medium. The culture was then left shaking at 120 rpm (21°C) and harvested in mid-log phase ($4x10^6$ cell/ml). Cell counts were carried out using a Neubauer haemocytometer (Hawksley; Hatfield, UK).

2.8 Development assay

The development assay was performed as previously described by Boeckeler *et al.* (2006) using 10^7 cells. Briefly, cells were put on a black 0.45µm membrane (Millipore; Watford, UK) positioned on an absorbent pad (Millipore; Watford, UK) containing phosphate buffer. After 24h incubation at 21°C, development images were taken using a dissection microscope (Leica; London, UK) and QiCAM (QImaging; Surrey, Canada).

2.9 DNA extraction

Once cells reached confluence, 200 µl of the cell suspension were transferred into a 0.2ml PCR tube and centrifuged at 1000 x g for 3 min. Supernatant was removed, 48µl lysis buffer (50mM KCl, 10mM Tris pH 8.3, 2.5 M $MgCl_2$, 0.45% NP40, 0.45% Tween20) with 2µl Proteinase K (21.4mg/ml) added and mixed. After 5min incubation at room temperature, samples were boiled at 95°C for 1min. 5µl of the crude DNA extract was used to screen for homologous integration by PCR.

2.10 Polymerase chain reaction

DNA of *D. discoideum* was amplified by PCR using NH_4 reaction buffer (670mM Tris-HCl (pH 8.8 at 25°C), 160mM (NH4) 2SO4, 0.1% stabilizer), 1mM dNTPs, 5mM $MgCl_2$, 2units BIOTAQ DNA polymerase, 10pmol of each 3' and 5' primer. PeqSTAR thermocycler (Peqlab; Sarisbury Green, UK) program: 4 min at 94°C denaturation, followed by 30 cycles of denaturation for 30 s at 94°C, annealing for 30 sec (primer dependant temperature) and extension at 72°C (dependent on product length) followed by a final extension of 10 min at 72°C.

2.11 Gel electrophoresis

PCR products were size-fractionated using 1% agarose gels containing ethidium bromide and tris-borate-EDTA buffer. 10 µl of PCR product or 2µl plasmid were loaded on to the gel with 1x DNA loading dye. 5µl of either 100bp Plus or 1Kb GeneRuler DNA ladder were used as molecular weight markers. The gel was run at 100 Volts for 40 min and samples were visualized using a BIO-RAD Gel Documentation 2000 system.

2.12 RNA extraction

D. discoideum cells ($1x10^7$ *) were developed on filters (Millipore; Watford, UK) and harvested at predetermined time points (see individual experimental results). RNA was then extracted using the High Pure RNA Isolation Kit according to the manufacturer's instructions. * $2x10^7$ cells were extracted for 24h time points to ensure sufficient amounts of RNA.

2.13 Reverse transcriptase PCR

RNA was treated with the DNA free kit to remove residual genomic DNA and coding DNA (cDNA) was synthesised by employing the First Strand cDNA Synthesis kit. For the expression profile, presenilin genes were amplified from the generated cDNA and expression was quantified using ImageJ (Rasband, 2007).

2.14 Mutagenesis and overlap extension PCR

Overlap extension PCR was employed to create wild type human PS1 and insertion of FAD mutations into *D. discoideum psenB* (Ho et al., 1989). PCRs for two overlapping PCR fragments were performed using Phusion Hot Start II polymerase (1x HF buffer, 200µl dNTPS, 0.5µM of each Primer, 1unit polymerase; 15 cycles) and products were gel purified. A full length product was then amplified using 2µl of each purified PCR fragments and two outside primers (15 cycles).

2.15 Creating a knock-out construct

Two ~500bp fragments were PCR amplified from wild type genomic DNA using Taq polymerase. The primers used contained enzyme restriction sites so that the fragments could be ligated into the plpBLP vector backbone (Faix et al., 2004). The PCR product was then purified using a MicroSpin column (GE Healthcare Life Sciences; Little Chalfont, UK) before the product and vector were double-digest by employing suitable restriction enzymes. Subsequently, the digested fragment was ligated into vector using T4 DNA ligase at various vector:insert ratios and incubated overnight which was followed by an heat inactivation (Fig. 2.1). 5µl of the resultant construct was then transformed into chemically competent *E. coli* cells. The plasmids from resultant colonies were then prepared and digested with restriction enzymes to verify the presence of vector and insert. Upon this confirmation, the second fragment was ligated into the previously prepared plasmid in the same way as described above.

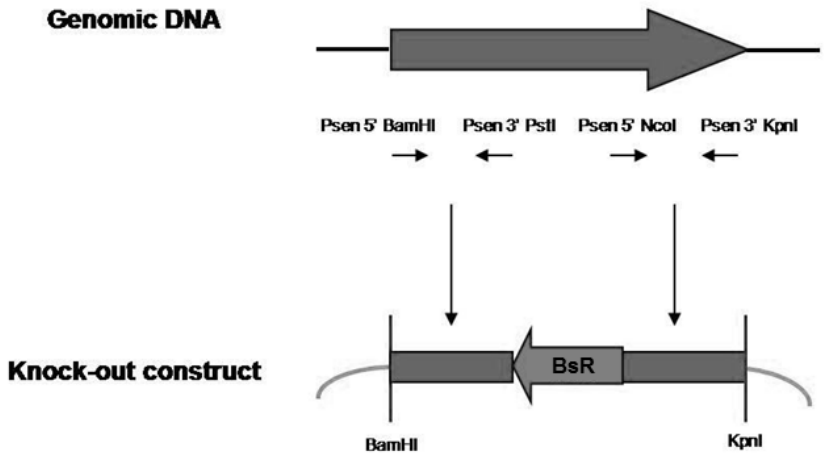

Fig.2.1 Creation of a knock-out construct. Genomic presenilin gene fragments were amplified, restriction sites (BamHI, PstI NcoI, KpnI) inserted, and fragments ligated into pLPBLP vector containing a blasticidin resistance cassette.

2.16 Transformation of *D. discoideum* by electroporation

The knock-out construct was double digested with BamHI and KpnI, purified using isopropanol precipitation and added into a 4mm electroporation cuvette. Before electroporation, $1x10^7$ cells were counted and pre-chilled on ice for

10min and centrifugated for 3 min at 800xg (4°C). Next, cells were washed three times with ice cold sterile phosphate buffer and resuspended in 700µl electroporation buffer (10mM $NaPO_4$, 50mM sucrose). Cells were then transferred to the electroporation cuvette containing 10µg of the digested knock-out construct. This was followed by one pulse (0.85kV, 25 µF) using a GenePulser Xcell electroporator (BIO-RAD, Hemel Hempstead, UK) after which the cuvette containing the cells was placed on ice for 10min. 8 µl $MgCl_2$ (0.1M) and $CaCl_2$ (0.1M) were added to the cells, followed by a 15min incubation and transferral of cells into into 10 ml of axenic medium (HL-5 medium) containing penicillin and streptomycin. 100 µl of the cell suspension was then transferred into each well of a 96 well plate (Peqlab; Sarisbury Green, UK) and placed into a 21°C incubator over night. The next day, 100µl of double concentrated blasticidin (20µg/ml) was added to each well to select for transformed cells. The media was then changed every week (10µg/ml blasticidin) and cells were grown to confluence before PCR screens were performed.

2.17 Screening for potential knock-out and knock-in mutants

PCR screens with three primer sets were performed on DNA extracted from transformants growing in the presence of blasticidin (Fig. 2.2). The first primer set (3' outside primer + 5' inside primer) amplifies a genomic control. The second primer pair amplifies a vector control band (3' inside primer and 5' BsR primer). The third primer set amplifies knock-out diagnostic product which is only present in homologous integrants (3' outside primer + 5' BsR primer). All PCR screens were performed employing Taq polymerase and a normal PCR protocol (30 cycles).

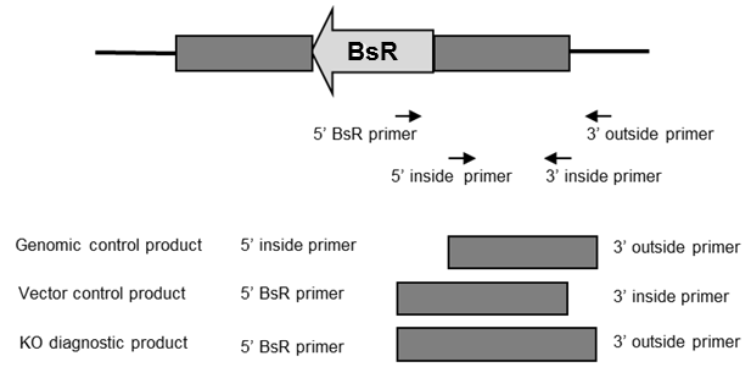

Fig.2.2 Knock-out screen using three primer sets. The first set amplifies a genomic control band and is amplified in wild type as well as all transformed cells. The second set produces a vector control product which is only amplified in transformed cells; whereas the third primer set amplifies a diagnostic band only produced in homologous integrants.

2.18 BsR excision

BsR cassettes were excised to allow multiple gene deletion in one cell line. To do so, 10^7 knock-out mutant cells were harvested and prepared for electroporation as previously described (2. 16) (Fig. 2.2). Cells were then electroporated with 30µg of pDEX-NLS-cre vector using two pulses of 0.75KV (25µF) with a 5sec interval. After electroporation, 0.5ml of HL-5 medium was added and cuvettes were incubated on ice for 5min. The content of cuvettes was transferred into a petri dish containing 12ml HL-5 medium and incubated over night at 22°C. Subsequently, 20µg/ml of G418 antibiotic was added to the dish to act as a selection agent for cells containing the pDEX-NLS-cre vector. Selection media was changed at day 3 and day 5. Once colonies were visible, the entire plate was harvested and washed once and resuspended in 1ml KK2 buffer (16.16mM KH_2PO_4, 4.01mM K_2HPO_4). Various dilutions of this cell suspension were plated onto SM agar plates containing *Raoultella planticolla* which were then incubated at 22°C for 3-7 days. Colonies were then transferred into a 24 well dish and selective antibiotic was added to select for transformants containing the vector.

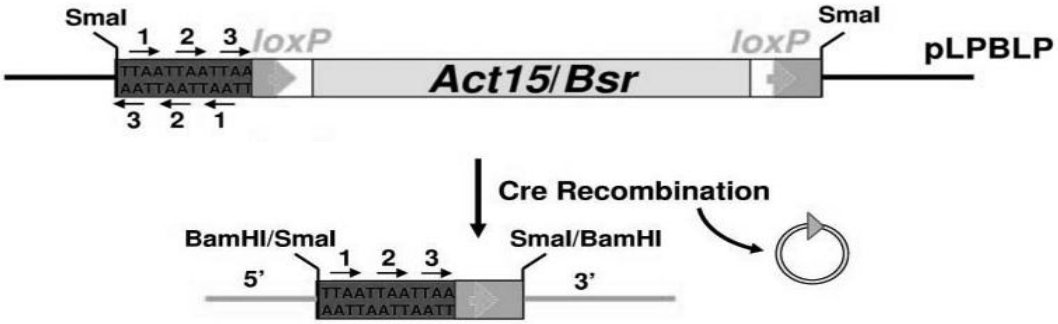

Fig.2.3 BsR excision through introduction of a Cre-loxP recycling cassette. The knock-out construct contains a BSR cassette which is framed by loxP sites. The Cre protein (pDEX-NLS-cre vector) is employed to recycle the BSR cassette which leaves a single LoxP site and stop codons in all six reading frames behind (Faix et al., 2004).

2.19 Overexpressing constructs

Overexpression constructs were created to express green fluorescently tagged presenilin proteins. To do so, full-length cDNA was amplified using Phusion Hot Start II polymerase and appropriate enzyme restriction sites were inserted through primers. These PCR products were then cloned into GFP overexpressing vectors (pDM317 and pDM323, or pDM448). PCR products had to be in frame at the 5' end and contain a stop codon at the 3' end to ensure an N-terminal tagged GFP expression. For the C-terminal tagged vectors, the PCR product did not contain a 3' end stop codon ensuring expression of a C-terminal GFP tagged protein. All constructs were sequenced to ensure mutation-free expression (GATC Biotech; London, Germany).

2.20 Transformation of *D. discoideum* by calcium chloride precipitation

Overexpression constructs were transformed into *D. discoideum* cells using $CaCl_2$ transformation. Axenic grown cells (10^7 cells) were transferred into a 9cm tissue culture dish and allowed to settle on the surface for 30min. The medium was exchanged to 10ml MES-HL5 (0.6% (w/v) yeast, 22.2mM glucose, 1% (w/v) bacterial peptone, 6.65mM MES; pH7.1) and incubated for 1.5h at RT. The DNA was prepared by adding 15µg DNA to 600µl dH_2O and 600µl 2x HBS (273mM NaCl, 9.65mM KCL, 1.66mM $Na_2H_2PO_4$, 41mM HEPES, 11.1mM D-Glucose; pH 7.05) and precipitated using 76µl 2M $CaCl_2$. The solution was left

for 25min at room temperature. Subsequently, MES-HL5 was removed and 1.2ml DNA solution was directly added to the culture dish. After 30min incubation at room temperature, 10ml MES-HL5 was gently added and cells were incubated for a further 3h at room temperature. The medium was removed, 2ml of a 15% glycerol stock (2.5ml 60%glycerol, 2.5ml dH_2O, 5ml 2xHBS) were added to the culture dish and gently distributed by rocking of plate. After 2min all glycerol was carefully removed and 10ml axenic medium added. Cells were allowed to recover over night before being equally distributed onto 10 *Micrococcus luteus* lawn (G418 resistant) SM plates (25µg/ml) and incubated at room temperature.

2.21 Knock-in construct

For the wild type knock-in cassette, 5' and 3' *psenB* flanking regions were amplified and enzyme restriction sites inserted by PCR. The fragments were ligated into pLPBLP vector resulting in a BsR cassette being inserted into the first intron of *psenB* upon homologues integration. For the knock-in cassette carrying a FAD mutation (L-V), overlap extension PCR (2. 14) was employed to insert the mutation into the 3' *psenB* flanking region. The electroporation, PCR screening and BsR excision were carried out as described in 2.16, 2.17 and 2.18.

2.22 Monolayer stalk cell assay

For a monolayer stalk cell assay, $1x10^6$ cells per condition were washed twice and re-suspended in 1.5ml stalk cell buffer [1x stalk salts (200mM $NaCl_2$, 1M KCl, 100mM $CaCl_2$); 10mM MES, 1u/ml Penicillin/Streptomycin) before being transferred into a 6cm cell culture dish. Cells were incubated for 24h with the addition of 5mM cAMP at 22°C. The following day, the cells were rinsed twice with stalk cell buffer followed by the addition of stalk cell buffer containing either 5mM cAMP or 5mM cAMP and 100nM DIF. After a further 24h, stalk cell counts were carried out, using an Olympus IX71 bright field microscope.

2.23 SDS-PAGE and Western Blotting

For western blots, $1x10^7$ *D. discoideum* cells were lysed by addition of 1x sample buffer (62.4mM Tris pH6.8, 2% (w/v) SDS, 2% (v/v) β-mercaptoethanol, 5% (v/v) glycerol, bromophenol blue). The samples were boiled for 10min and placed onto ice prior to addition of phosphatase inhibitor. Sodium Dodecyl Sulfate (SDS) PolyAcrylamide Gel Electrophoresis (SDS-PAGE) was carried out using a separate stacking and resolving gel. The resolving gel contained 0.375M Tris-HCl (pH 8.8), 9% (v/v) acrylamide, 0.1% (w/v) SDS, 0.25% (v/v) TEMED and 0.3% (w/v) ammonium persulphate (APS). The stacking gel contained 0.125M Tris (pH 6.8), 7% (v/v) acrylamide, 0.1% (w/v) SDS, 0.25% (v/v) TEMED and 0.3% (w/v) APS. The protein samples (15µl) and PageRuler Plus standard (4µl) were loaded onto the gel. The chamber was then connected to a power pack (BioRad; Hemel Hempstead, UK) and the gel run at 150 Volts/35mA for 90min.

After electrophoresis the separated proteins were transferred to a PVDF membrane using a TRANS-BLOT SD semi-dry transfer apparatus (BioRad). Four 10cm x 7cm pieces of blotting paper and PVDF membrane were soaked in blotting buffer (20mM Tris, 0.2M Glycine, 20% (v/v) Methanol). After loading of the blotting cassette, the whole apparatus was attached to a power pack (BioRad; Hemel Hempstead, UK) and the transfer was carried out at 15 Volts/300mM for 90min.

To block non-specific antibody binding sites, the membrane was incubated on a platform in 5% (w/v) semi-skimmed dried milk in Tween/Tris buffered saline (TTBS; 15 mM Tris, 0.1% (v/v) Tween-20, 0.15M NaCl) for 1h. The membrane was then incubated with gentle agitation with anti-GFP antibodies (1:1000) over night at 4°C.The next day, the membrane was washed three times with TTBS and incubated with secondary anti-rat antibody (1:5000; IRDye800) for 1h at room temperature. This was followed by three washes with TTBS and protein-antibody complexes were visualised using an Odyssey SA Infrared Imaging System (LI-COR Biosciences; Lincoln, USA).

2.24 Fluorescence microscopy

Monoclonal antibodies against calnexin were kindly provided by Annette Müller-Taubenberger. For immunofluorescence labelling, overexpressor cell lines were allowed to settle to cover slip for 20min prior to 4% paraformaldyhyde fixation for 10min and permeabilization using 0.5% TritonX-100 for 5min. Subsequently, cells were washed three times with PBS Tween20, blocked with BSA before labelling with anti-calnexin antibodies over night at room temperature in a humidified chamber. Cells were washed with PBS Tween20 and incubated with goat anti-mouse secondary antibody for 30min. The GFP-signal was enhanced by incubation with a GFP-booster for 1h. Subsequently, cells were washed three times with PBS Tween20 and nuclei were stained using DAPI. Fluorescence microscopy was carried out using Olympus IX71 at 60x magnification with a QImaging RetigaExi Fast1394 digital camera.

2.25 Quantative RT-PCR

Total RNA of *D. discoideum* RNA was extracted using the High Pure RNA Isolation kit. cDNA was amplified using First Strand cDNA Synthesis Kit as previously described. The qPCR was set up in a QIAgility (Qiagen; Crawley, UK) to ensure accurate pipetting. Real-time amplification with SYBR Green was performed using a Rotor-Gene 6000 (Qiagen; Crawley, UK). Triplicate samples were collected at each time point and two qRT-PCR technical replicates were carried out and levels of transcription were quantified using the $2^{-\Delta\Delta C}{}_{T}$ method.

2.26 Calcium assay

To assess calcium homeostasis in *D. discoideum* cells, the plasmid pPROF120 encoding the calcium sensitive apoaequorin was transformed into these cells by employing calcium chloride precipitation and the calcium assay was performed as described in (Allan and Fisher, 2009). In brief, 10^8 cells were incubated in 5ml of MES development buffer (10mM MES of pH 6.2, 10mM KCl, 0.25mM CaCl) containing coelenterazine-*h* (0.5µg/ml dissolved in 20% w/v Pluronic F-127) for 7h in shaking suspension. This was followed by one wash with MES

development buffer to remove residual coelenterazine-*h*. The coelenterazine-*h* allows an in vivo reconstitution of the functional photoprotein which upon calcium binding results produces luminescence which can be detected by a photometer. In order to measure calcium influx upon cAMP stimulation, the total light emission possible was determined to normalise the aequorin luminescence signals. These values allowed calculation of an in vitro calcium concentration-effect curve upon 1µM cAMP stimulation. All measurements were carried out in a New Brunswick ATP Photometer as described in (Allan and Fisher, 2009) and analysed by employing the R statistical package (R Core Team, 2012).

Chapter 3

D. discoideum contains two presenilin genes (PsenA and PsenB) and no detailed bioinformatic characterisation has previously been carried out on either of these proteins. This chapter investigates the structure and homology of *D. discoideum* presenilin proteins and compares it to presenilin proteins of other species using sequence alignments, domain structure analysis, hydropathy and phylogenetic analysis.

3.1 Homology of D. discoideum presenilin proteins

To establish an evolutionary link between presenilin proteins of *D. discoideum* other species the NCBI Basic Local Alignment Search Tool (BLAST) was employed (Altschul et al., 1990). This program aligns *D. discoideum* presenilin amino acid sequences to presenilin protein sequences of other species and generates overall identity and similarity scores and e-values according to their relatedness (Table 3.1, 2). The results showed that both *D. discoideum* presenilin proteins are similar to those of other species such as *D. melanogaster* (fruit fly) and *B. floridae* (lancelet) but to a lesser extend to *C. elegans* (nematode; Hop-1). Furthermore, the analysis revealed that PsenA shares greater homology with the PS2 (highest identities; Table 3.1); whereas PsenB shows highest identities to human PS1 (Table 3.2). It should be noted that the homology identities/scores did not change when only highly conserved regions (i.e. peptidase domain) were analysed (data not shown).

Species	Length of Protein (aa)	Identity %	Positives %	E-value
***D. discoideum* PsenA**	**622**	**100**	**100**	**0**
D. discoideum PsenB	473	38	59	1e-64
Human PS1	467	27	48	3e-53
Human PS2	448	40	64	2e-42
C. elegans Sel-12	444	29	49	5e-51
C. elegans Hop-1	358	26	45	1e-34
P. patens Psen	477	28	51	5e-55
D. rerio PS1	456	30	50	2e-51
D. rerio PS2	441	36	59	1e-42
D. melanogaster Psen	541	31	55	2e-61
A. thaliana PsenA	453	30	55	6e-55
A. thaliana PsenB	337	31	52	2e-54
B. floridae Psen	525	32	52	3e-74
O. sativa Psen	459	30	51	2e-50

Table 3.1 BLAST analysis of full length *D. discoideum* PsenA. The table shows the name of organism and presenilin homologue, protein length, identity (%), similarity (%) and e-value. The results represent comparisons of PsenA to presenilin proteins spanning across several kingdoms.

Species	Length of Protein	Identity %	Positives %	E-value
***D. discoideum* PsenB**	**473**	**100**	**100**	**0**
D. discoideum PsenA	622	38	59	2e-74
Human PS1	463	34	58	2e-48
Human PS2	448	30	50	9e-49
C. elegans Sel-12	444	31	55	4e-22
C. elegans Hop-1	358	27	46	4e-29
P. patens Psen	477	35	55	8e-28
D. rerio PS1	456	34	56	8e-37
D. rerio PS2	441	31	50	1e-55
D. melanogaster Psen	541	35	59	9e-33
A. thaliana PsenA	453	35	54	1e-25
A. thaliana PsenB	337	38	58	2e-32
B. floridae Psen	467	40	59	8e-40
O. sativa Psen	478	33	52	1e-29

Table 3.1 BLAST analysis of full length *D. discoideum* PsenB. The table shows the name of organism and presenilin homologues, protein length, identity (%), similarity (%) and e-value. The results represent comparisons of PsenB to presenilin proteins spanning across several kingdoms.

3.2 Phylogenetic analysis

To further characterise the relatedness of both *D. discoideum* presenilin proteins to those of other species, the Molecular Evolutionary Genetics Analysis program (MEGA5) was employed to reconstruct a phylogenetic tree (Kumar et al., 2008). Using the neighbour-joining method, a wide range of presenilin proteins from several kingdoms were analysed using a bacterial signal peptide, peptidase-like 2A, to root the resultant tree (Fig. 3.1). The analysis revealed that both *D. discoideum* presenilin proteins are basal to the animal clade and are distinctly different from presenilin proteins of the plant clade. The phylogenetic analysis, with high confidence in the bootstrapped

tree, reveals a close relatedness of *D. discoideum* to human presenilin proteins.

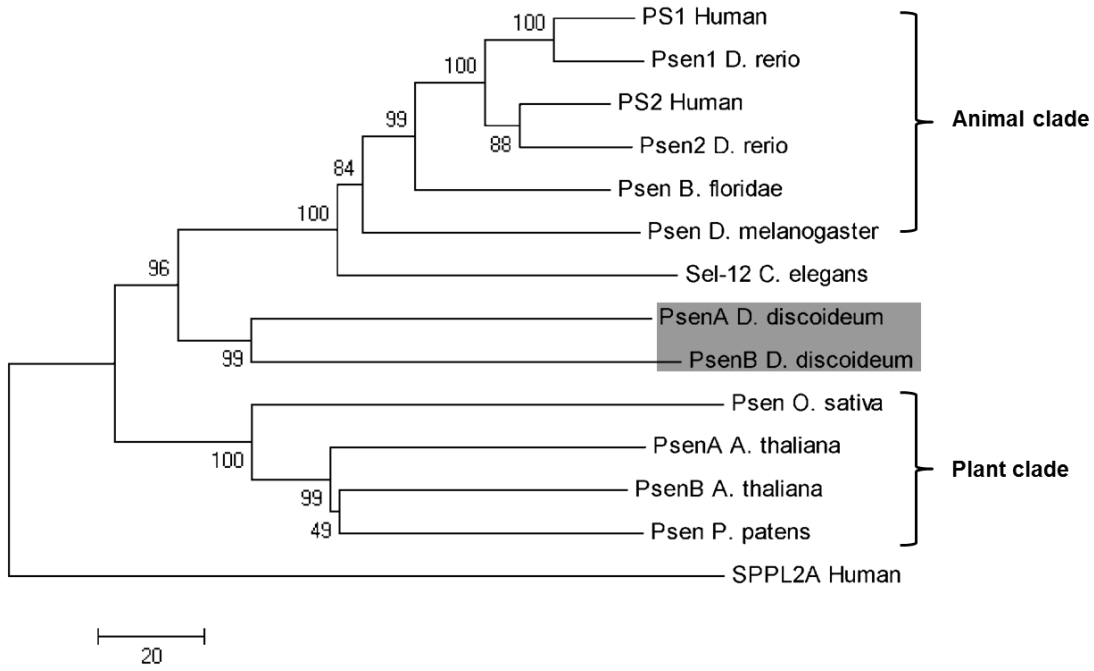

Fig.3.1 Phylogenetic tree of aspartic acid peptidases. Presenilin genes of various species were used reconstruct a tree using neighbouring-joining method with a bootstrap (500): PS1 *Human* (Uniprot accession number: P49768); PS2 *Human* (P49810); PsenA *D. discoideum* (Q54ET2); PsenB *D. discoideum* (Q54DE8); PS1 *Danio rerio* (Q9W6T7); PS2 *Danio rerio* (Q90ZE4); Sel-12 *Caenorhabitis elegans* (P52166); Psen *Drosophila melanogaster* (O02194); PsenA *Arabidopsis thaliana* (O64668); PsenB *Arabidopsis thaliana* (Q9SIK7); Psen *Oryza sativa* (Q6AUZ8); Psen *Physcomitrella patens* (A9S846). The tree was rooted using signal peptide peptidase-like 2A (Q8TCT8). *C. elegans* Hop-1 and Spe-4 were omitted as the high evolutionary rate might cause a long-branch attraction artefact. *D. discoideum* presenilin proteins are basal to the animal clade, whilst plant presenilin proteins are part of a separate clade.

3.3 Presenilin protein domain structure

Since the BLAST analysis and phylogenetic analysis suggested conservation between human and *D. discoideum* presenilin proteins, a more detailed domain analysis was carried out. In agreement with BLAST and phylogenetic analysis, aligning *D. discoideum* and human presenilin amino acid sequences using ClustalW, identified highly conserved regions (Fig. 3.2). Human presenilin proteins possess a A22A-type peptidase domain and this domain was found to be highly conserved in both *D. discoideum* presenilin proteins (Fig. 3.2; yellow box) (Page and Di, 2008). Within this domain, in mammalian systems, presenilin proteins require two conserved catalytic

aspartic acid residues which are found in the transmembrane motif 'YD' towards the N-terminal and in a 'GLGDF' motif towards the C-terminal of the proteins. The alignment revealed that both *D. discoideum* presenilin proteins possess conserved motifs containing aspartic acid sites (Fig. 3.2; red box). Furthermore, PsenA as well as PsenB possess a 'PAL' sequence which, in mammalian systems, is required for γ-secretase assembly (Fig. 3.2; green box).

Fig.3.2 Partial amino acid alignment of human and *D. discoideum* presenilin proteins. The presenilin peptidase domain (yellow) is conserved in *D. discoideum* presenilin proteins. Further, both aspartic acid residues (orange) and 'PAL' (green) sequence are present in *D. discoideum* and human presenilin proteins."*" identical residue; ":" conserved substitution; "." Semi-conserved substitution.

3.4 Transmembrane region analysis

It is well established that presenilin proteins are transmembrane proteins with a cytosolic loop (De Strooper and Annaert, 2010). The topology of these presenilin proteins is still subject to debate but in recent years, nine transmembrane regions have been the favoured model for presenilin proteins (Henricson et al., 2005). A similar topology was found for *D. discoideum*

presenilin proteins since the domain structure analysis revealed multiple conserved regions resembling transmembrane domains of human presenilin proteins. Using the hydrophobicity analysis tool DAS, the properties of each amino acid sequence was analysed and secondary structure topology predictions for human and *D. discoideum* presenilin proteins were made (Cserzo et al., 2002). This analysis revealed that both human presenilin proteins possess 10 transmembrane regions in comparison to 9 regions seen in both *D. discoideum* proteins (Fig. 3.3). However, when assessing the hydrophobicity plot of both human presenilin proteins, two twin peaks are observed, suggesting this region may contain only one transmembrane domain rather than two. PsenA and PsenB were predicted to comprise 9 transmembrane regions with extended cytosolic N-termini and extracytosolic C-termini. Further, PsenA was predicted to have a large cytosolic loop similar to that seen in human presenilin proteins, whereas PsenB appeared to possess only a small cytosolic region. An additional analysis (ClustalW) of the predicted transmembrane regions revealed that PsenA transmembrane regions are more similar to PS1 and PS2 than PsenB regions (Table 3.3; (Chenna et al., 2003)).

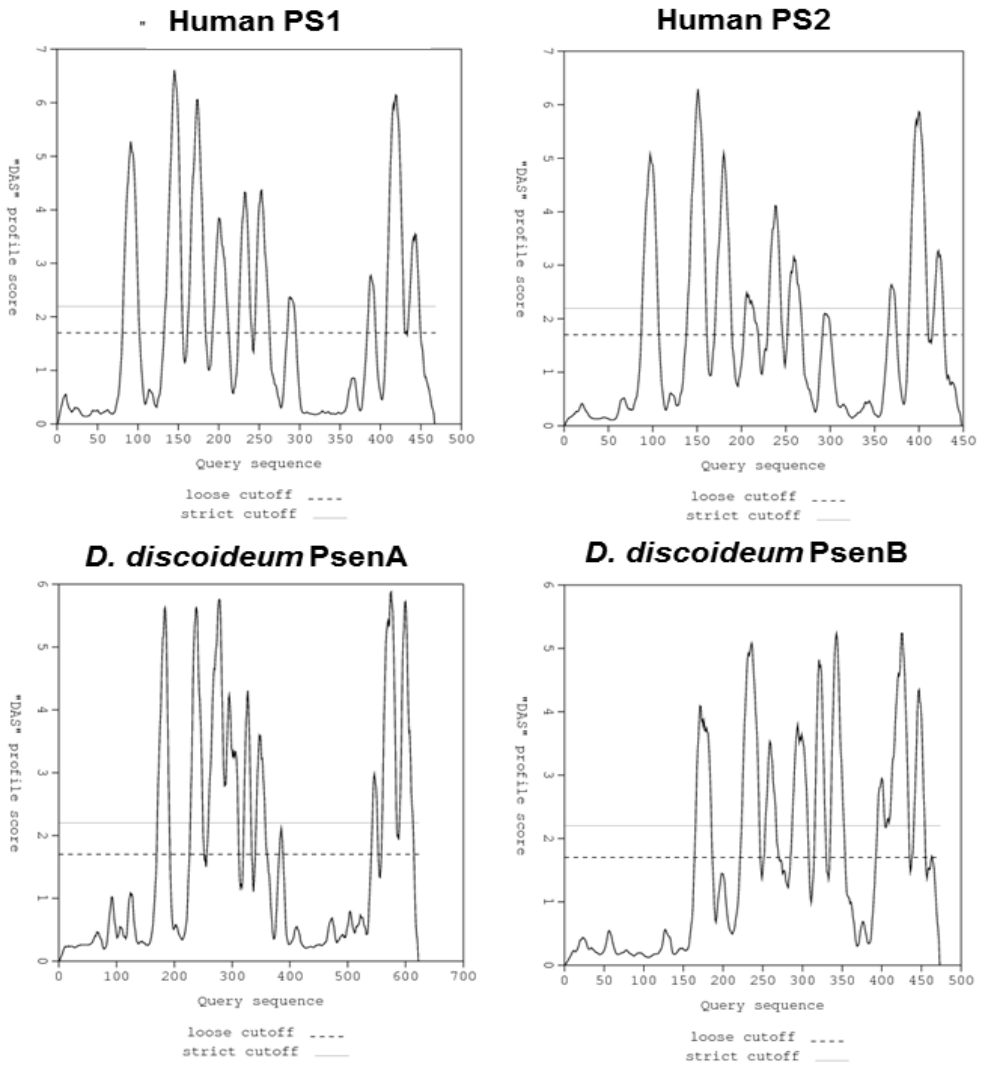

Fig.3.3 Hydrophobicty plot of human and *D. discoideum* presenilin proteins. Analysis revealed that both *D. discoideum* presenilin proteins are predicted to have 9 transmembrane regions (peaks). X-axis represents amino acid numbers, whereas the y-axis shows the transmembrane score.

	PS1	PS2	PsenA	PsenB		PS1	PS2	PsenA	PsenB
TM 1	100	91	**33**	27	**TM 1**	91	100	27	27
TM 2	100	85	**45**	40	**TM 2**	85	100	**50**	35
TM 3	100	66	**44**	27	**TM 3**	66	100	33	38
TM 4	100	55	38	**55**	**TM 4**	55	100	**50**	22
TM 5	100	100	**66**	44	**TM 5**	100	100	**66**	44
TM 6	100	77	**55**	44	**TM 6**	77	100	**50**	38
TM 7	100	100	66	**75**	**TM 7**	100	100	66	**75**
TM 8	100	90	57	**66**	**TM 8**	90	100	61	61
TM 9	100	85	45	45	**TM 9**	85	100	50	50

Table 3.3 Homology of transmembrane regions in human and *D. discoideum* presenilin proteins. This table shows ClastalW alignment scores of *D. discoideum* presenilin and human presenilin TM regions. TM regions of human presenilin proteins are more conserved in PsenA than PsenB (highlighted scores).

3.5 FAD mutations in presenilin

The continuously updated Alzheimer disease and frontotemporal dementia mutation database currently lists (retrieved 1st July 2012) 185 Familial Alzheimer's Disease (FAD) mutations for PS1 affecting 101 amino acids (Cruts and Van, 1998), whereas 18 amino acids are reported to be affected in PS2. Analysis of cellular changes caused by these mutations is difficult and biomedical models are being developed to investigate signalling pathways affected by FAD mutations. One of these models is *D. melanogaster*, where FAD mutations were engineered into the presenilin gene and phenotypes assessed (Seidner et al., 2006). To assess whether similar work could be carried out *D. discoideum*, conserved amino acids in *D. discoideum* presenilin proteins were identified which are affected by FAD mutations in human presenilin proteins.

A full length amino acid alignment of both human and *D. discoideum* presenilin proteins was generated using the ClustalW alignment tool. Further, each individual amino acid that is altered in FAD was highlighted in the *D. discoideum* presenilin amino acid sequence. Analysis of 101 amino acid residues revealed that 52% of these residues are conserved in PsenA, PsenB or both (Fig. 3.4, 3.5). Further analysis of 18 FAD-inducing mutations in PS2 showed that 34% of the residues are conserved in both *D. discoideum* presenilin (Fig. 3.4). Furthermore, most of the conserved sites are located in transmembrane regions and key catalytic domains of both *D. discoideum* presenilin proteins (Fig. 3.5).

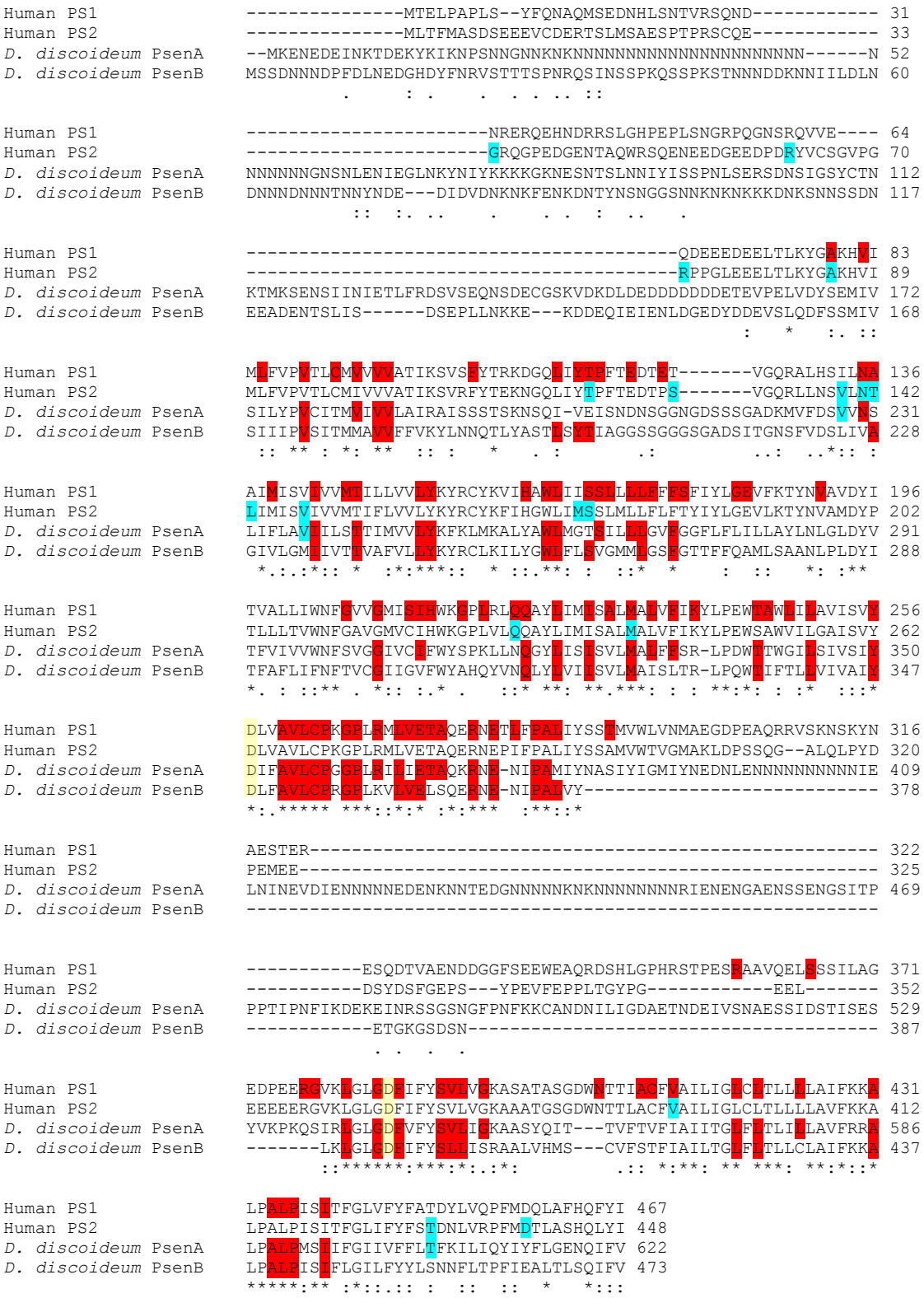

Fig.3.4 Amino acid alignment of full length human and *D. discoideum* presenilin proteins. Highlighted amino acids represent reported residues affected by missense mutations in PS1 (red) and in PS2 (blue). Amino acid residue highlighted in yellow indicate endoproteolytic cleavage site.”*” identical residue; “:” conserved substitution; “.” semi-conserved substitution.

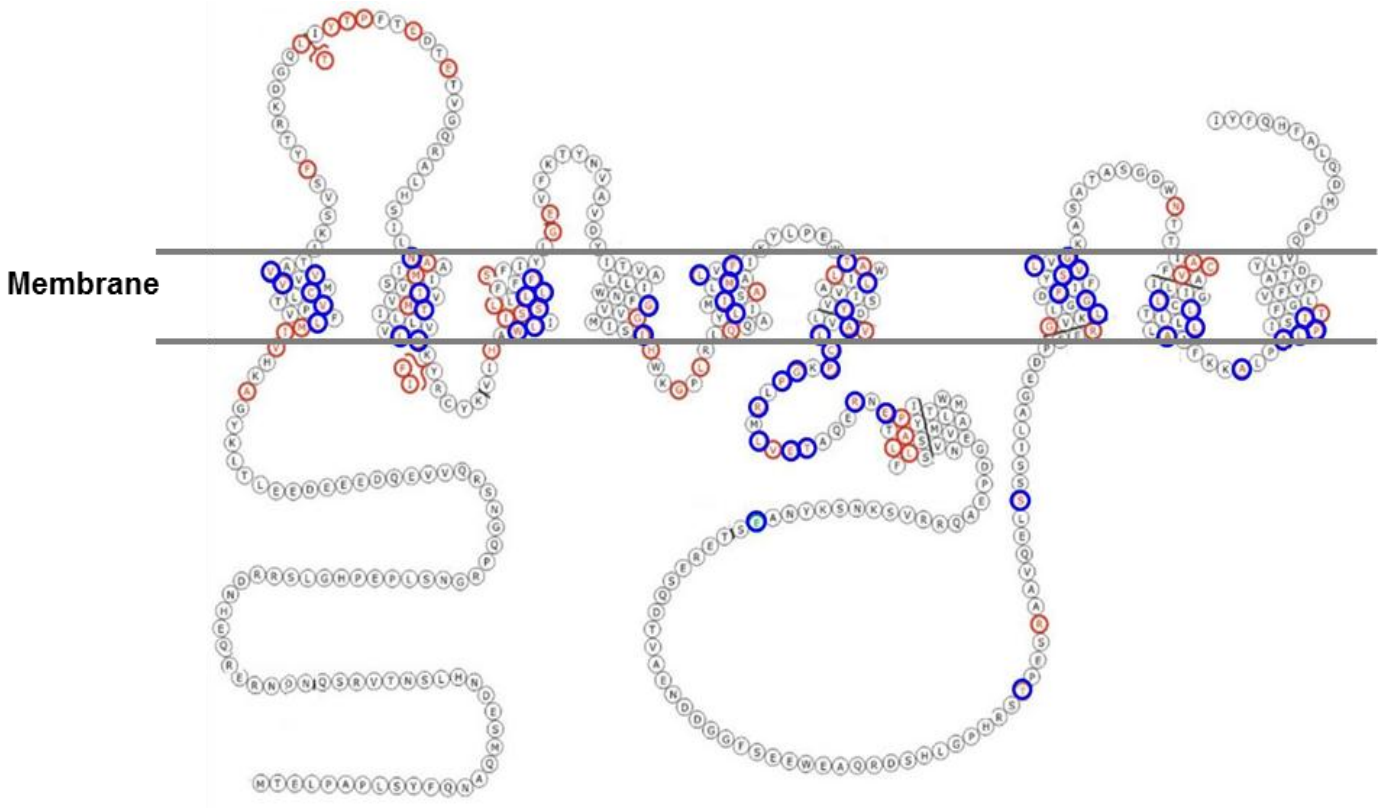

Fig.3.5 Secondary structure of human PS1. Amino acids affected by FAD mutations in PS1 are highlighted in red, and those conserved in both *D. discoideum* presenilin proteins are highlighted in blue. *D. discoideum* presenilin proteins possess 52% of the amino acids affected by FAD [modified from Cruts and Van (1998)].

3.6 Discussion

This chapter analysed the structure and homology of the two *D. discoideum* presenilin proteins. Bioinformatic tools employed in this analysis allowed catalytic domain structure, transmembrane regions and phylogenetic analysis of both *D. discoideum* presenilin proteins.

3.6.1 Conservation of presenilin proteins across kingdoms

To investigate potential structural conservation between *D. discoideum* presenilin proteins and those of other species, a BLAST analysis was carried out. Regions of high similarity were found by this analysis and revealed that *D. discoideum* presenilin proteins are similar to those of other species such as *D. melanogaster* and *B. floridae*. Further, PsenA was shown to be more similar to human PS2 than PS1 as similarities and identities were higher. PsenB was more similar to human PS1 as identities and similarities were higher in comparison to human PS2.

A phylogenetic tree was reconstructed to support the relatedness between *D. discoideum* presenilin proteins to those of other species. Amoebozoa are one of the earliest eukaryotic branches and the phylogenetic analysis found that *D. discoideum* PsenA and PsenB are basal to the animal clade, thus showing relatedness to human presenilin proteins. Further, this tree resembles the tree of life where the branch of amoebozoa diverged after the split between animals and plants (Chisholm et al., 2006). Many organisms such as human, *D. rerio* and *A. thaliana* possess two presenilin gene copies, whereas other species such as *D. melanogaster* and *O. sativa* possess only one presenilin gene (Tandon and Fraser, 2002). Hashimoto-Gotoh et al. (2003) have attempted to unravel the approximate time of this gene duplication event and different phylogenetic tree methods suggested that presenilin gene duplications occurred independently in different phyla. The gene duplication event is suggested to have occurred in the vertebrate lineage after the split from cephalochordates (Martinez-Mir et al., 2001). Hashimoto-Gotoh et al. (2003) suggest that a gene duplication event occurred independently in the plant lineage as, for example,

A. thaliana possesses two presenilin genes and *O. sativa* only one. These independent gene duplications in different phyla, including *D. discoideum*, suggest a functional requirement for these events to have taken place. To date, lower organisms such as yeast, fungi or bacteria are not known to possess presenilin genes (Hashimoto-Gotoh et al., 2003).

3.6.2 Presenilin protein structure

Presenilin proteins belong to the subfamily A22A of endopeptidases which comprise a peptidase domain, two catalytic aspartic acid residues and a 'PAL' sequence for endoproteolytic cleavage and γ-secretase function (Wang et al., 2006). To confirm that *D. discoideum* presenilin proteins are 'true presenilin proteins' possessing these catalytic regions and to further support conservation between human and *D. discoideum* presenilin proteins, a domain structure analysis was carried out. This analysis revealed that PsenA and PsenB possess a peptidase domain, both containing fully conserved catalytic aspartic acid residues as well as a 'PAL' sequence. Since PsenA and PsenB amino acids are moderately conserved, one would expect to observe a similar one-dimensional topology as seen in human presenilin proteins. To analyse the one-dimensional structure, hydropathy plots were generated and transmembrane regions compared. This analysis predicted 9 transmembrane regions for both *D. discoideum* presenilin proteins showing a high resemblance to the transmembrane regions of human presenilin proteins as they also were predicted to comprise 9 transmembrane regions (Spasic et al., 2006; Henricson et al., 2005). Furthermore, the hydropathy analysis predicted that PsenA contains a large cytosolic loop, characteristic for presenilin proteins, whereas PsenB is predicted to have only a small cytosolic loop. To fully establish the one-dimensional structure of *D. discoideum* presenilin proteins, X-ray crystallography needs to be carried out, however, this work is still outstanding for human presenilin proteins due to large hydrophobic domains of presenilin and the γ-secretase complex (Takagi et al., 2010).

Structural analysis of *D. discoideum* presenilin proteins revealed conservation of key catalytic sites, which support the assertion that *D. discoideum* presenilin

protein localisation and function might be similar to those seen in mammalian systems (Wolfe et al., 1999). These functions may involve assembly of a γ-secretase complex and cleavage of type I transmembrane proteins since *D. discoideum* possesses all other subunits required for this protease complex (Nicastrin (Q54JT7), Aph-1 (Q55FS3), and Pen-2 (Q54BR1)). Despite the presence of all γ-secretase subunits, to date there are no known endogenous integral membrane proteins such as APP and Notch-1 that are cleaved by *D. discoideum*. Nevertheless, McMains et al. (2010) have shown that *D. discoideum* is able to cleave truncated APP which was overexpressed in this amoeba supporting the theory of γ-secretase functions in *D. discoideum*.

3.6.3 FAD mutations

The pathological and biochemical changes of sporadic AD phenocopy the alterations observed in FAD. Therefore, analysis of biochemical changes caused by FAD mutations might give a deeper insight into the aetiology of AD. This current study showed that 52% of all amino acids affected by FAD in human PS1 and a further 34% of all amino acids affected in PS2 are conserved in PsenA and PsenB. Therefore, FAD mutations could be engineered into *D. discoideum* presenilin genes similar to the work seen in *D. melanogaster* (Seidner et al., 2006). Recent work by Kim and Kim (2008) showed that one third of all reported PS1 FAD mutations are located to amino acid residues which are conserved in a wide variety of species (*D. discoideum* not analysed). Further, the group found that 75% of all FAD mutations occur in TM regions which are likely to cause damage to the presenilin protein function which was also found in this current study. Histopathological changes, such as presence of amyloid plaques and tau tangles, have been reported for many of these mutations however, it should be assumed that each mutation affects more than one signalling pathway since presenilin proteins have been linked to numerous downstream targets (Parihar and Hemnani, 2004; McCarthy et al., 2009). Thus, the majority of biochemical alterations caused by FAD mutations remain to be identified. The current study revealed suitable sites for mutagenesis in PsenA and PsenB such as the leucine residue 392 in PsenB which corresponds to the residue 286 in PS1. In mammalian cell lines, research showed that the

mutation L268V caused an imbalance in phospholipid and calcium homeostasis which can both be analysed in *D. discoideum* (Landman et al., 2006; Guo et al., 1996; Allan and Fisher, 2009; Pawolleck and Williams, 2009).

This bioinformatics analysis here presented suggests that *D. discoideum* presenilin proteins share related peptidase structures with the human and presenilin proteins of other species. Therefore, *D. discoideum* offers a system that allows analysis of presenilin signalling in the absence of Notch-1, APP and tau homologues. Further, this novel presenilin model may enable the analysis of altered cell signalling caused by FAD mutations. Ultimately, the development of this promising presenilin model may provide a deeper insight into biochemical changes of AD.

Chapter 4

Presenilin proteins play a critical role in growth and development in animal models (Parks and Curtis, 2007). To investigate the role of presenilin in growth and development in *D. discoideum*, this chapter describes the deletion of *D. discoideum* presenilin genes. Gene expression, growth and development were assessed in these mutants, and phenotypes were then rescued by complementation.

4.1 Expression of *D. discoideum* presenilin genes throughout development

Presenilin gene expression was investigated in *D. discoideum* throughout development. A semi-quantitative Reverse Transcriptase PCR (RT-PCR) study was carried out to generate an expression profile for *psenA* and *psenB*. RNA was extracted at four hourly intervals throughout development and cDNA was synthesised. To ensure an equal amount of cDNA was analysed from each sample, a constantly expressed housekeeping gene (glycogen synthase) was amplified from each sample as a loading control (Iranfar et al., 2003). This control also served as an indicator of genomic DNA contamination within the cDNA sample. To assess transcription of each *D. discoideum* presenilin gene, primers were designed to amplify across *psenA* and *psenB* specific cDNA regions. Semi-quantitative analysis was carried out by measurement of the intensity of each amplified presenilin cDNA fragment. Both presenilin genes were transcribed in vegetative cells (0h; Fig. 4.1A, B). At 4-12h, *psenA* transcription levels increased and stayed constant throughout the remaining development stages (Fig. 4.1A, B). *psenB* showed a constant high gene transcription throughout development when compared to *psenA*. Assuming identical primer binding and amplification rates of both gene products, *psenA* transcription is significantly lower expressed than *psenB* in the vegetative stage (0h) and early developmental stages (4h). The developmental expression patterns are consistent with dictyExpress

database for gene expression obtained by RNA sequencing (Rot et al., 2009) (Fig. 4.1C).

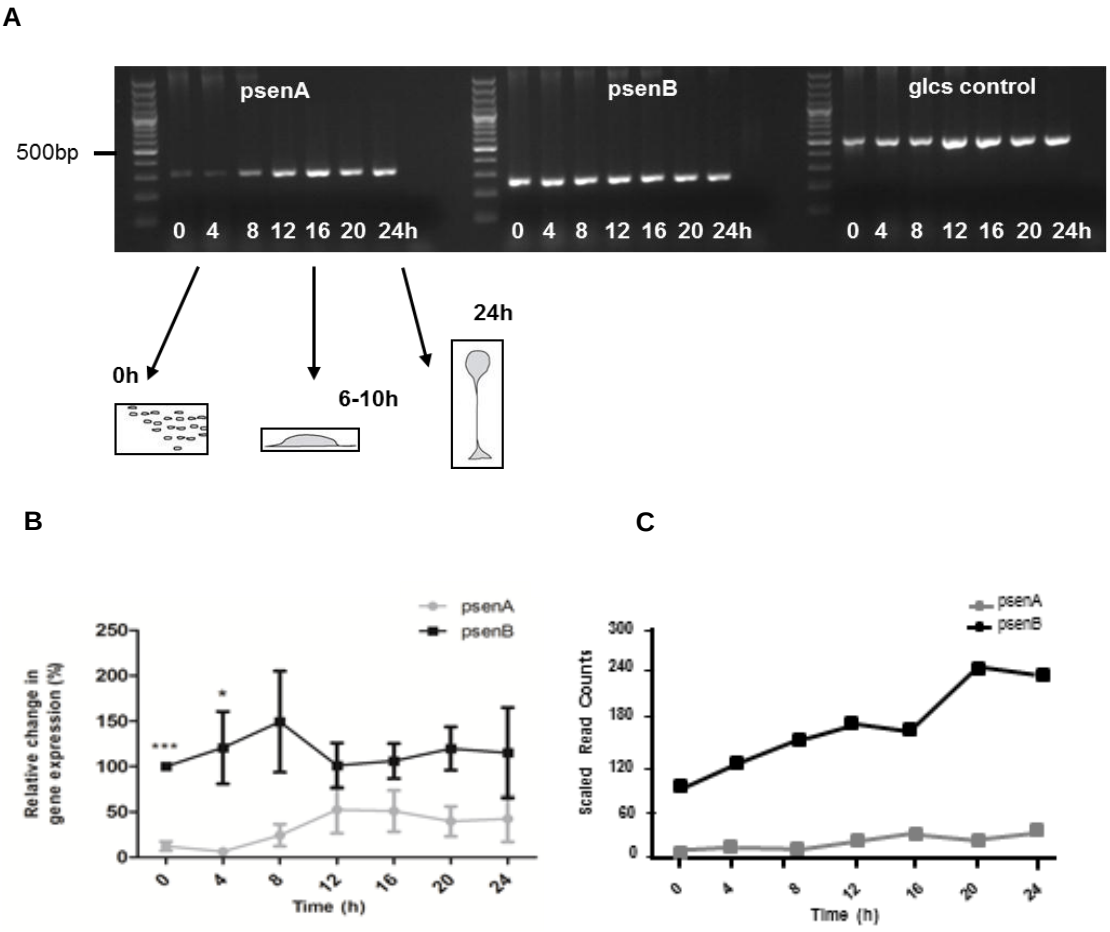

Fig.4.1 Gene expression of *psenA* and *psenB* throughout development. (A) A representative gel image of *psenA*, *psenB* and glycogen synthase (glcs; loading control) PCR products. Drawings represent multicellular structures at stated times. (B) Quantification of presenilin gene expression. Numbers indicate hours into development; average percent expression of both genes compared to *psenB* expression at 0h. (C) Expression profile of *psenA* and *psenB* adapted from Run dictyExpress. Values shown are means (±S.E.M; n=3) *** p<0.001; ** p<0.01; * p<0.05.

4.2 Creating presenilin knock-out cassettes

In order to investigate the cellular and developmental role of *psenA* and *psenB*, knock-out cell lines were created using the pLPBLP/Cre-loxP system (Faix et al., 2004). For this approach, knock-out cassettes were created with a region of each gene replaced by a Blasticidin resistance cassette (BsR cassette; Fig. 4.2A). Both 5' and 3' targeting fragments (~500bp) of each gene were amplified by PCR with appropriate restriction sites introduced by PCR primers. Each PCR product was then cloned into the pLPBLP vector on

either site of the BsR cassette (Fig. 4.2A, B) (Faix et al., 2004). This was followed by restriction digests to verify each gene-specific plasmid before transformation into wild type *D. discoideum* took place (Fig. 4.2C, D).

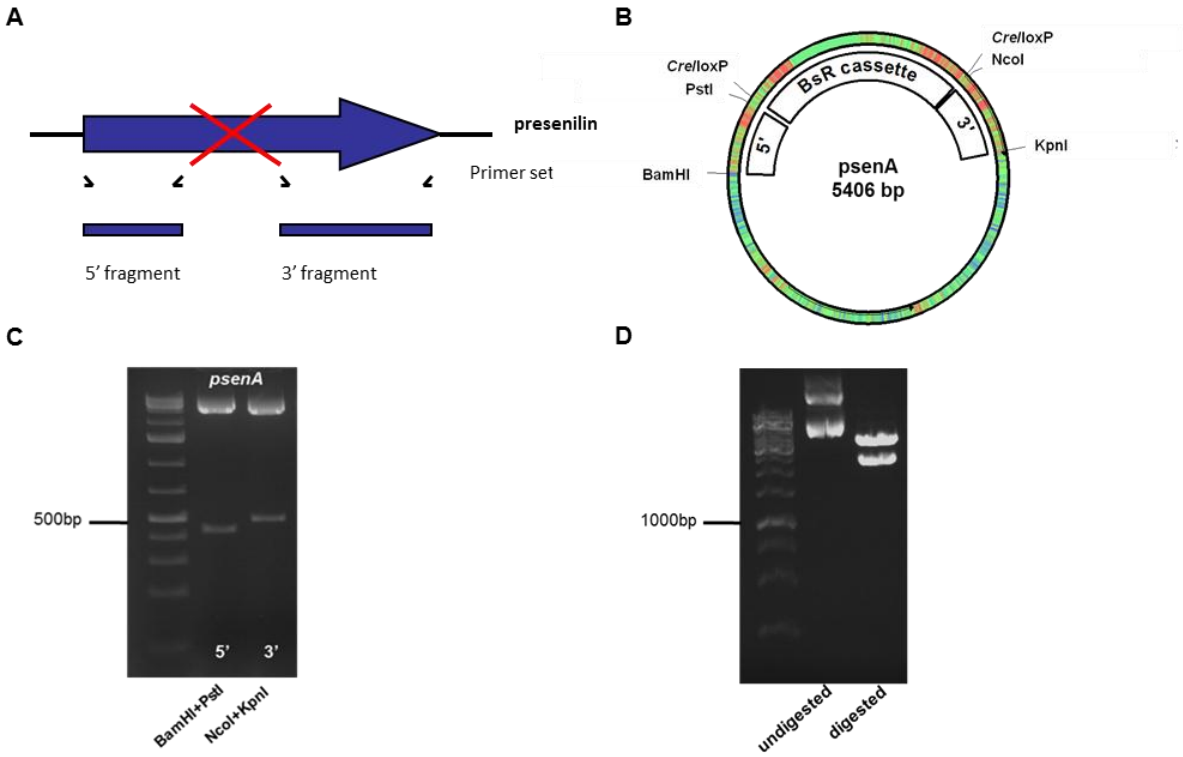

Fig.4.2 Preparing a presenilin knock-out construct. (A) Schematic of presenilin targeting fragments amplified to generate knock-out vectors. (B) *psenA* knock-out construct containing a 442bp 5' and a 500bp 3' targeting fragment. *Cre/LoxP* sites indicate start of the BsR cassette. (C) Restriction digest of *psenA* knock-out construct using BamHI and PstI to cut out the 5' targeting fragment and NcoI and KpnI to cut out the 3' targeting fragment. (D) Restriction enzyme digest of knock-out construct using BamHI and KpnI resulting in a linearised knock-out cassette and vector backbone, whereas the undigested constructs shows supercoiled DNA.

4.3 Creation of single presenilin knock-out mutants

To ablate each presenilin gene, wild type (Ax2) cells were transformed with a BamHI and KpnI digested knock-out construct targeting either *psenA* or *psenB* and selected for integration by resistance to antibiotic (Blasticidin; Fig. 4.2D). Resultant transformants were PCR screened for homologous integration of the knock-out construct (Adley et al., 2006). In brief, DNA

derived from transformants grown in 96 well plates was amplified using three sets of primer: a genomic control primer set annealing outside and inside of the knock-out cassette flanking region (G); a vector control primer set consisting of a primer inside of the BsR cassette and inside of the knock-out cassette flanking region (V); and a knock-out diagnostic primer set (KO) using a primer annealing outside the knock-out cassette region and inside the BsR cassette (Fig. 4.3A, B). Genomic and vector control bands were present in non-homologous integrants, whereas genomic, vector control and knock-out diagnostic products were amplified in homologous integrants only (Fig. 4.3A). This PCR screening method was performed on both termini of the knock-out cassette to verify homologous integration into the targeted gene.

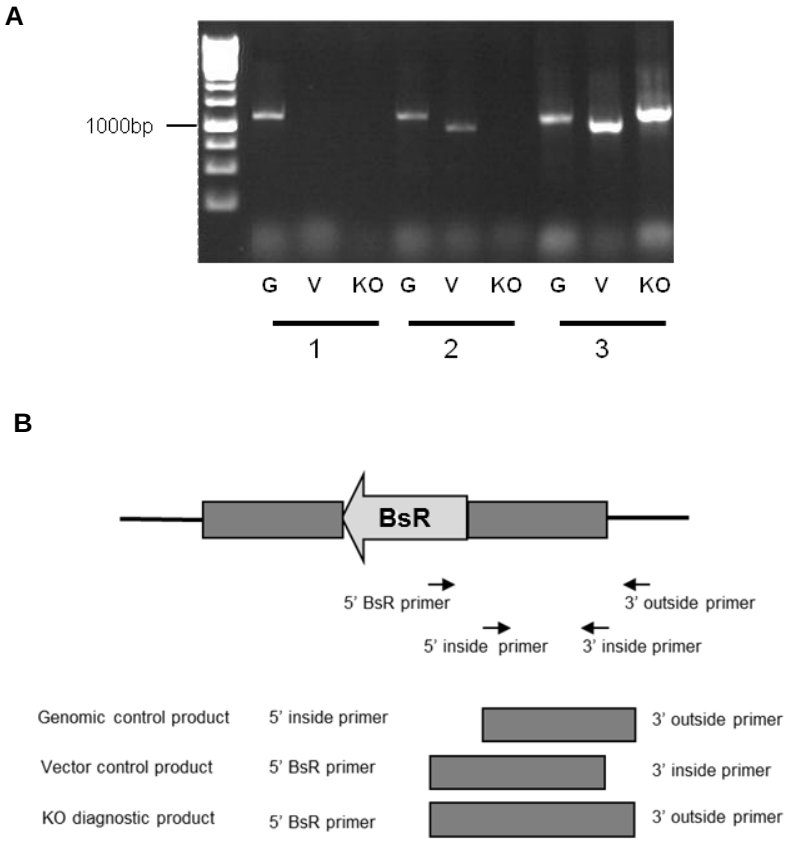

Fig.4.3 PCR screen of *D. discoideum* colonies growing in the presence of Blasticidin following transformation with a presenilin knock-out construct (shown for *psenB*). (A) Untransformed cells not growing in presence of Blasticidin (1) show a PCR product for the genomic control (G) only. Non-homologous transformants (2) show a PCR product for the genomic and vector (V) controls. Homologous integrants (3) show a PCR product for genomic, vector controls and a knock-out (KO) diagnostic band. (B) Schematic of PCR screen using genomic, vector control and knock-out diagnostic primer sets. BsR=Blasticidin resistance.

The frequency of homologous integration events for each of the presenilin genes was very low. This led to a modification of the transformation protocol in which gel purification of the digested knock-out constructs removed the pLPBLP backbone (2895bp) ensuring transformation of the knock-out cassette only (2446bp). Furthermore, different wild type *D. discoideum* laboratory strains and double electro-pulses were tested to improve homologous integration rates; however, none of these approaches were successful. Screening of in excess of 3000 clones identified two *psenA*$^-$ and one *psenB*$^-$ cell line. These transformants were then sub-cloned and PCR screened on both termini of the knock-out cassette to ensure isogenic cell lines (Fig. 4.4A). To verify gene disruption of the identified *psenB*$^-$ and *psenA*$^-$ mutants, a RT-PCR on cDNA was carried (Fig. 4.4B).

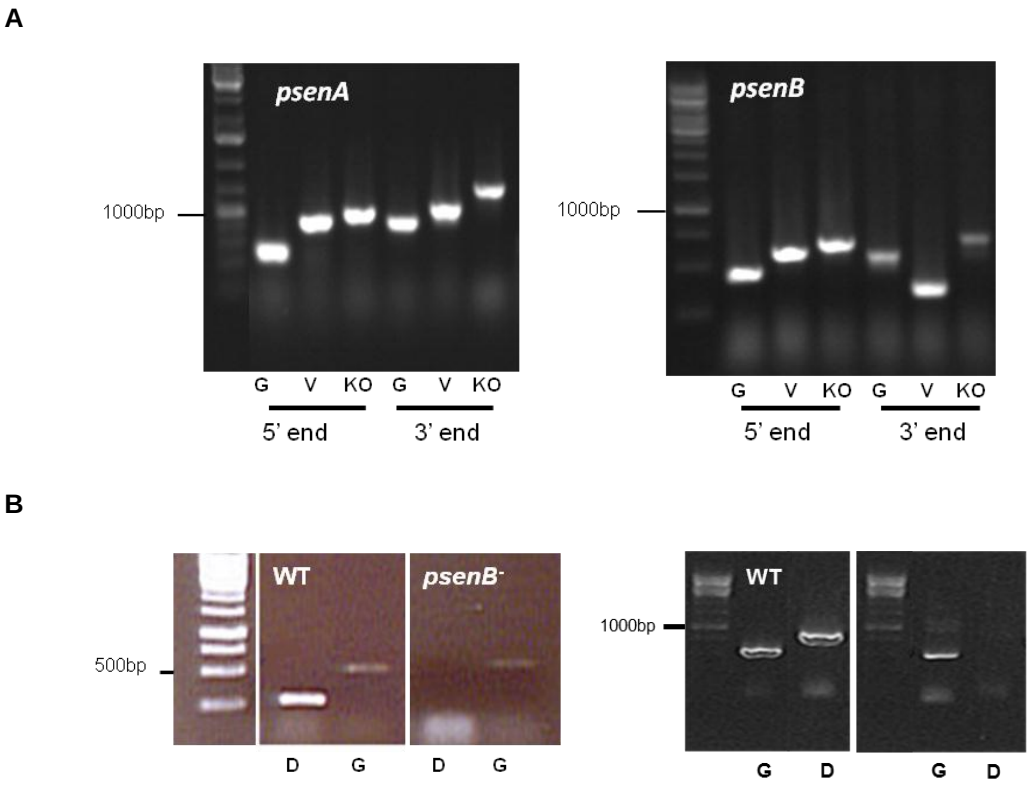

Fig.4.4 PCR identification of *psenA* and psenB knock-out mutants. (A) For both isogenic *psenA*$^-$ and *psenB*$^-$ mutants, 5' and 3' termini were screened for homologous integration with the above outlined six primer sets (genomic (G) control, vector (V) controls, and knock-out (KO) diagnostic band). (B) Reverse Transcriptase PCR analysis of the *psenB* in wild type (WT) *psenA*$^-$ and *psenB*$^-$ mutants after BsR excision, using a primer pair amplifying across the deleted region (D). Amplification of *glcs* was chosen as an internal control (G).

4.4 Developmental analysis of single presenilin knock-out mutants

To determine whether deletion of either presenilin gene causes a developmental defect in *D. discoideum*, each deleted cell line was developed on nitrocellulose filters and fruiting body morphology was assessed after 24h. Both independently identified *psenA*$^-$ and the single *psenB*$^-$ cell lines showed wild type fruiting body formation, with sori and stalks showing no gross change when compared to the parent strain (Fig.5).

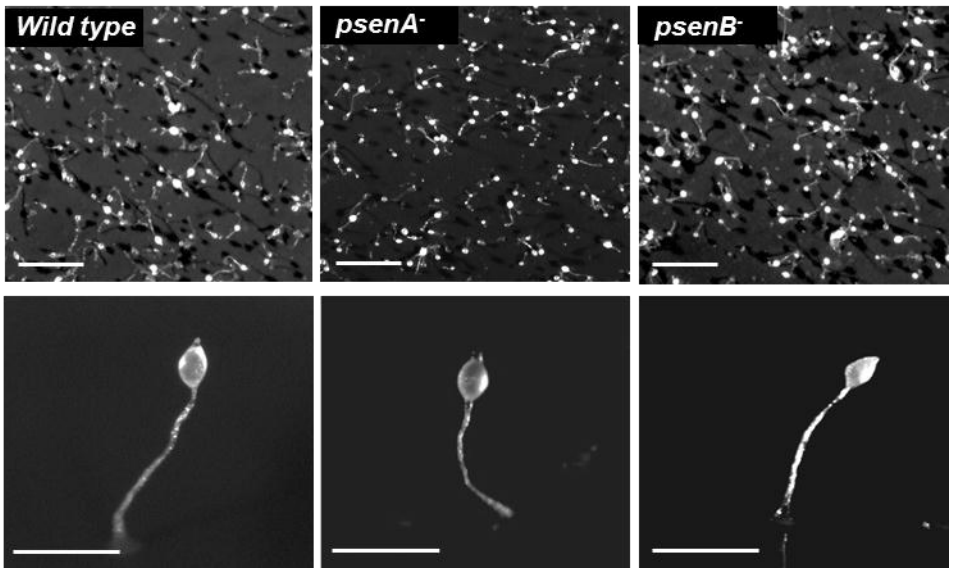

Fig.4.5 Effects of single presenilin gene deletion on development of *D. discoideum*. Wild type and single presenilin mutant cell lines developed on nitrocellulose filters and fruiting body morphology was assessed. Wild type, *psenA*$^-$ and *psenB*$^-$ cell lines developed mature fruiting bodies within 24h with no gross change in development; seen from an aerial view at low magnification (top) and from a side angle at high magnification (bottom). Size bar= 1mm.

4.5 Blasticidin resistance cassette excision

Since no developmental phenotype was observed for each single presenilin mutant cell line, a double presenilin knock-out mutant was created. Excision of the BsR cassette in a single presenilin knock-out mutant is necessary for the ablation of a second presenilin gene in a single cell line. For this excision process, *psenB*$^-$ clones were transformed with a pDEX-NLS-Cre construct encoding Cre-recombinase and transformants were selected over a period of

26 days (Faix et al., 2004). Dilution plating of the resultant resistant colonies enabled the identification of isogenic colonies sensitive to Blasticidin (suggests excision of BsR cassette). PCR amplification across the deleted region in the *psenB*$^-$ cell line produced an 875bp fragment, compared to a fragment of 1156bp for the wild type cell line (Fig. 6). The *psenB*$^-$ (non BsR excised) cell line would be predicted to show a 2398bp fragment in this amplification but this was not achieved due to rich AT regions in the BsR cassette (data not shown).

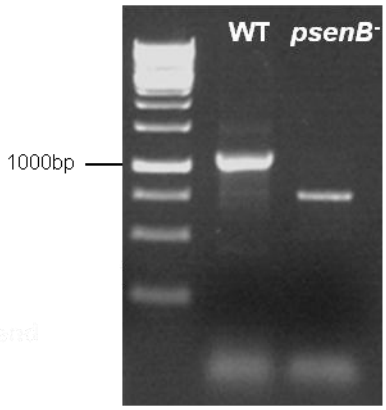

Fig.4.6 PCR analysis of *D. discoideum psenB* in wild type and *psenB*$^-$ cells following BsR excision. A primer pair flanking the BsR cassette, amplifying across the deleted region of *psenB*$^-$, was employed to identify BsR excised *psenB*$^-$ mutant cells. The primer pair amplified an 1156bp PCR product in wild type cells and an 875bp product in BsR excised *psenB*$^-$ mutant cells.

4.6 Creation of a double presenilin knock-out mutant

To delete both presenilin genes in a single *D. discoideum* cell line, the BsR excised *psenB*$^-$ cell line was transformed with the *psenA* knock-out construct. Again, transformants growing in the presence of Blasticidin were PCR screened for homologous integration of the *psenA* knock-out cassette. As for ablation of *psenB* in wild type cells, several thousand Blasticidin resistant clones were screened yielding one double presenilin knock-out clone (*psenB*$^-$*/A*$^-$; Fig. 4.7A).

Repeating the BsR cassette excision of the *psenA*$^-$ BsR cassette in the *psenB*$^-$/*A*$^-$ cell line allowed PCR amplification across both deleted gene regions to confirm deletion of a central part from each presenilin gene in this cell line (Fig. 4.7B).

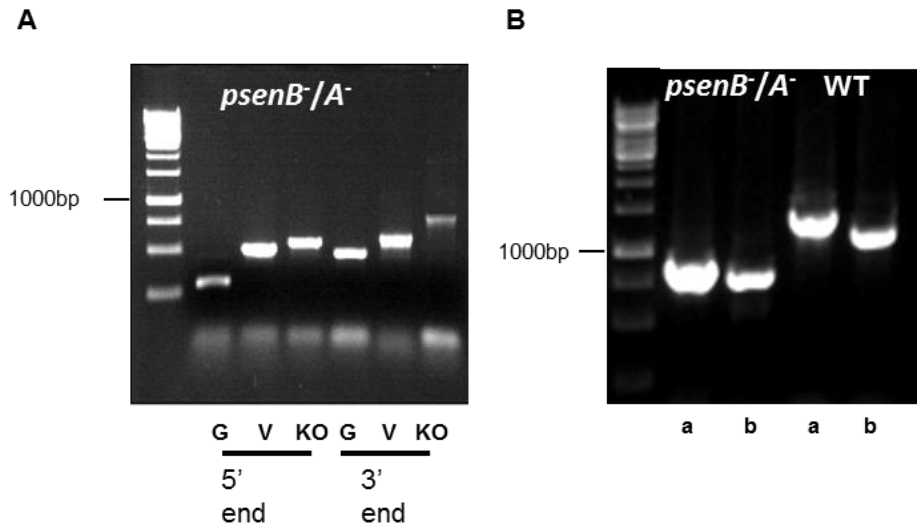

Fig.4.7 PCR analysis of *D. discoideum psenB*$^-$/*A*$^-$ mutant. (A) Homologous integration of *psenA* knock-out cassette in a *psenB*$^-$ background identified by PCR analysis amplifying genomic (G), vector (V) and knock-out (KO) products for both 5' and 3' termini of *psenA* knock-out cassette. (B) Amplification across *psenA* (a) and *psenB* (b) in *psenB*$^-$/*A*$^-$ after BsR cassette excision produced smaller PCR products showing deletion of large gene regions in comparison to wild type cells.

4.7 Developmental analysis of a double presenilin knock-out mutant

Development of the *psenB*$^-$/*A*$^-$ mutant was assessed to establish a potential role for presenilin proteins in *D. discoideum* development. As previously described, fruiting body structure was assessed 24h into starvation, revealing that mutant cells were able to aggregate (early development) but not able to develop mature structures (late development). The observed aggregates of the *psenB*$^-$/*A*$^-$ mutant did not show stalks or sori in comparison to the wild type cells which did produce mature fruiting bodies (Fig. 4.8). Furthermore, streaming of wild type and *psenB*$^-$/*A*$^-$ mutant cells was assessed over 8h. Here, *psenB*$^-$/*A*$^-$ mutant cells did not appear to form streams, whilst forming smaller aggregation territories when compared to wild type cells (Fig 4.9).

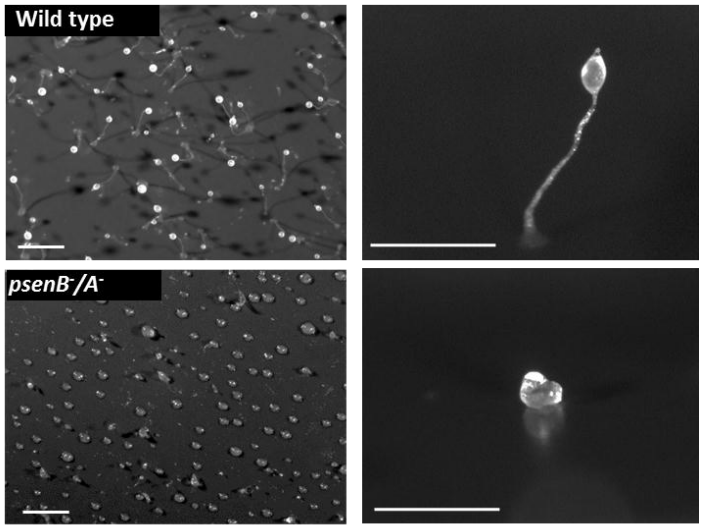

Fig.4.8 Effects of double presenilin deletion on development of *D. discoideum*. Wild type and *psenB*$^{-}$*/A*$^{-}$mutant cells were developed on nitrocellulose filters and assessed using an aerial view at low magnification (left) and side view using a high magnification (right). Wild type cells produce mature fruiting bodies, whereas *psenB*$^{-}$*/A*$^{-}$ mutant cells form aggregates with no visible stalks or sori. Size bar=1mm.

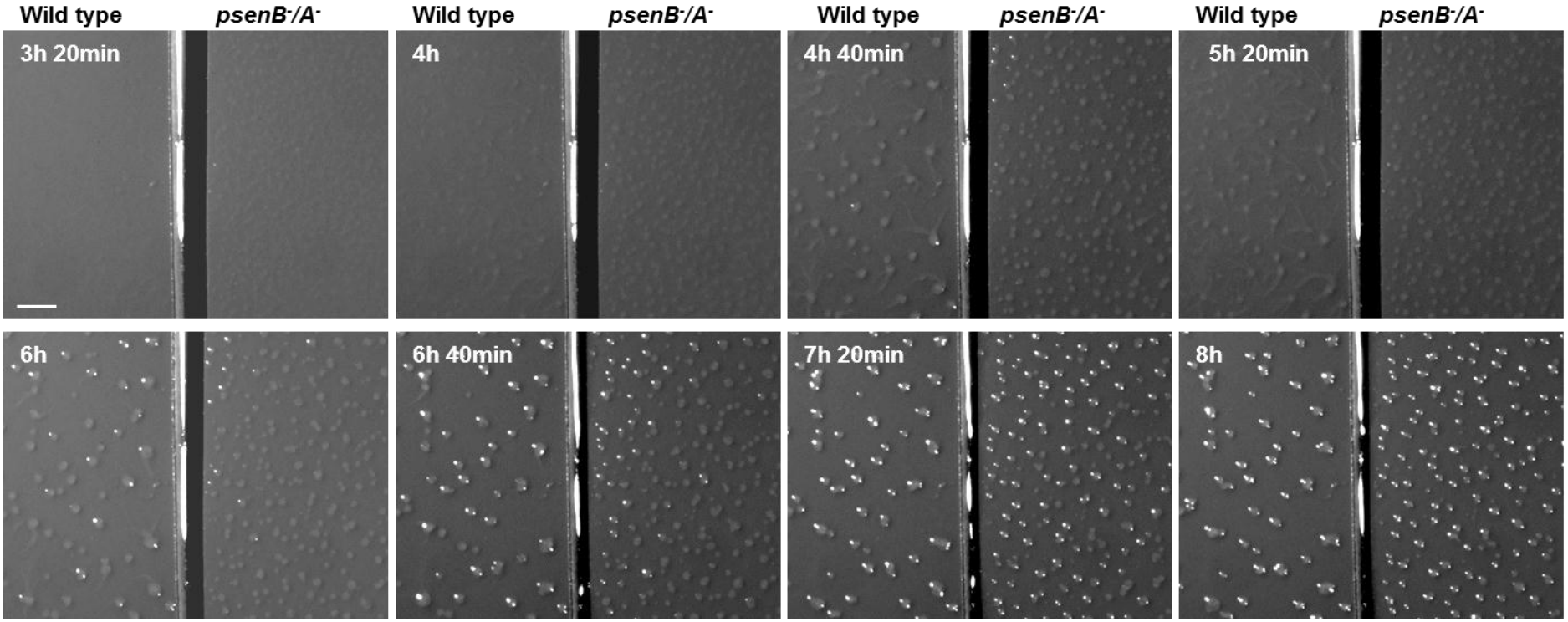

Fig.4.9 Time-lapse images of streaming wild type and *psenB*$^{-}$*/A*$^{-}$ mutant cells. Wild type (left) and *psenB*$^{-}$*/A*$^{-}$mutant (right) cells were developed on nitrocellulose filters and streaming was assessed. *psenB*$^{-}$*/A*$^{-}$ mutant cells appeared to not stream efficiently and form smaller aggregates 4h, when compared to wild type cells. Size bar=1mm.

4.8 Developmental rescue

In order to confirm that the *psenB*$^{-}$*/A*$^{-}$ cell line is a genuine knock-out mutant and that the developmental phenotype is caused by deletion of both presenilin genes, a *psenB* overexpression vector was created to rescue the developmental defect. This vector allowed transcription of *psenB* under the control of a strong *actin*15 promoter with an *actin*8 terminator (pDM vector series (Veltman et al., 2009).

To create an overexpression construct, mutation-free cDNA of *psenB* was amplified using a proof-reading polymerase. This process initially proved difficult, since 40 independent clones (in an intermediary vector; pCR2.1-TOPO) from three separate amplification reactions using Bio-X-Act (Bioline) were sequenced and no mutation-free cDNA was identified. Repeating this approach using reduced PCR cycles (20 instead of 28) still failed to produce a mutation free cDNA. To overcome this, replacing the polymerase with Phusion Hot Start II polymerase (NEB) enabled amplification of mutation-free PsenB with restriction sites within primers for subsequent cloning into an overexpression vector.

Two non-integrating overexpressing vectors were chosen to express *psenB* cDNA tagged with green fluorescence protein (GFP) at either the N- (pDM317) or C- (pDM323) terminal end. The approach of using N- as well as C-terminal tagged GFP vectors was chosen to identify and avoid potential interference of the GFP tag in localisation and/or protein function. Ligation of the PCR product into the pDM vectors was difficult and required transformation into highly competent *E. coli* cells (XL10-Gold Ultracompetent cells; Agilent).

To rescue the observed *psenB*$^{-}$*/A*$^{-}$ mutant phenotype, the N- or C-terminal tagged PsenB overexpressing vectors were transformed into the presenilin null cells. The calcium chloride transformation method was employed to ensure a high plasmid copy number in transformants. Selection for transformants on *Micrococcus luteus* lawns allowed isolation of multiple independent transformants. To confirm that transformants express PsenB-GFP in the *psenB*$^{-}$*/A*$^{-}$ background, Western blot analysis was carried out using anti-GFP

antibodies to probe for PsenB-GFP. The molecular weight of PsenB-GFP is predicted to be approximately 80kDa (PsenB 52kDa; GFP 28kDa). A ~80kDa protein was successfully detected in the lysate of *psenB*$^{-}$*/A*$^{-}$ overexpressing PsenB-GFP mutant cells (Fig. 4.10B). Development of transformants containing either N- or C-terminal GFP tagged PsenB revealed that both GFP tagged PsenB rescued the developmental phenotype observed in the *psenB*$^{-}$*/A*$^{-}$ mutant, thus allowing development of wild type mature fruiting bodies (Fig. 4.10A; images for N-terminal PsenB-GFP not shown). This rescue suggests that the PsenB-GFP is fully functional and that the GFP tag does not interfere with cellular functions of PsenB. Further, PsenB-GFP was overexpressed in wild type cells to assess whether constitutively expression of PsenB-GFP affects *D. discoideum* development. These transformants also developed within 24h and no gross changes in fruiting body morphology was observed when compared to wild type cells (Fig, 4.10A).

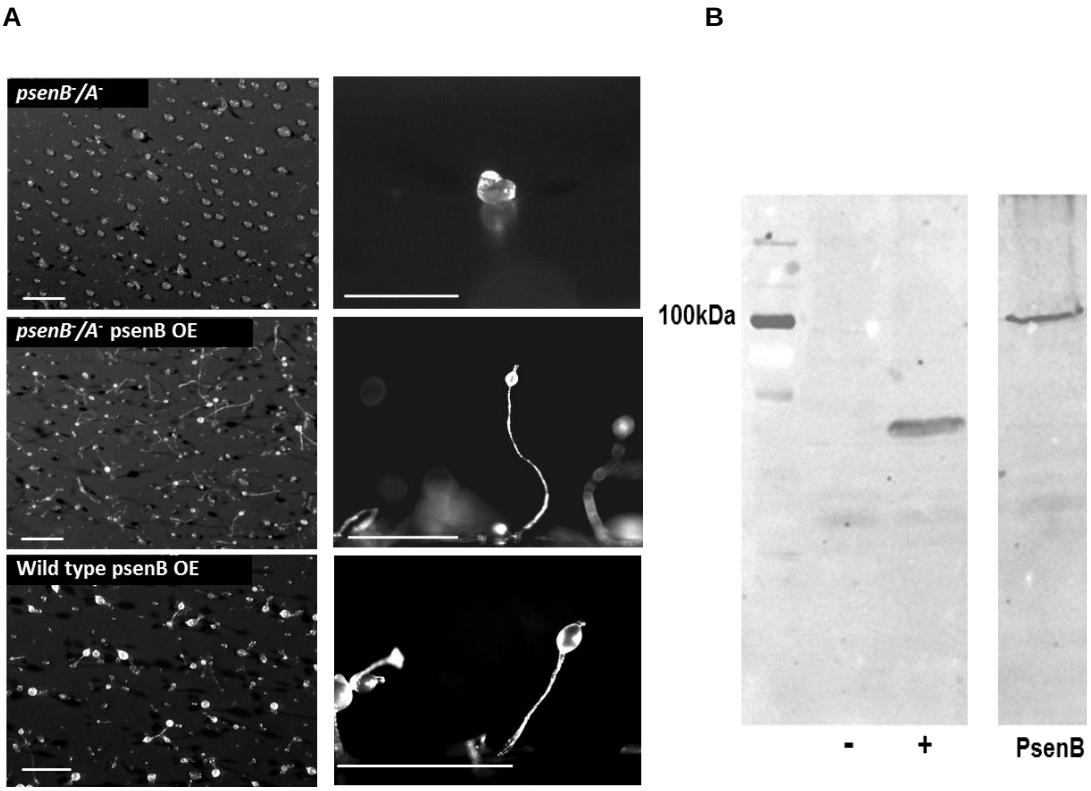

Fig.4.10 PsenB-GFP overexpression in *psenB⁻/A⁻* mutant cells. (A) Developmental rescue of *psenB⁻/A⁻* by PsenB-GFP overexpression. *psenB⁻/A⁻* mutant cells overexpressing PsenB-GFP (N-terminal tagged) were developed on nitrocellulose filters and developmental morphology was assessed using an aerial view (left) and side view (right). Overexpression of *psenB* in the *psenB⁻/A⁻* cell line allowed development of mature fruiting bodies. PsenB-GFP overexpression on wild type development did have no effect on fruiting body morphology. Size bar=1mm. (B) Western blot analysis of *psenB⁻/A⁻* overexpressing PsenB-GFP mutant cells. An anti-GFP antibody was employed to probe against the GFP tag of PsenB in the *psenB⁻/A⁻* overexpressing mutant (~80kDa). Probing untransformed wild type cell lysate (-) for GFP shows no unspecific binding, whereas probing for GFP in lysates of cells overexpressing Crac PH domain (GFP tagged; ~41kDa) shows specificity of the antibody (+).

4.9 Localisation of presenilin B in *D. discoideum*

To investigate the localisation of PsenB-GFP in *D. discoideum*, live cell imaging was initially used. Both *psenB⁻/A⁻* mutants containing either N- or C-terminal GFP tagged PsenB, were starved (4h) and light and fluorescence images were taken (Fig. 4.11). Live cell fluorescence imaging revealed that both, the N- and C-terminal GFP tagged PsenB localized to membrane structures which resemble the endoplasmic reticulum (ER). To verify that the protein localises to the ER, cells were fixed and probed for calnexin, an ER and nuclear envelope specific protein (Muller-Taubenberger et al., 2001). An overlay of PsenB-GFP and calnexin localisation images revealed both proteins co-localised to the ER and nuclear envelope (Fig. 4.12).

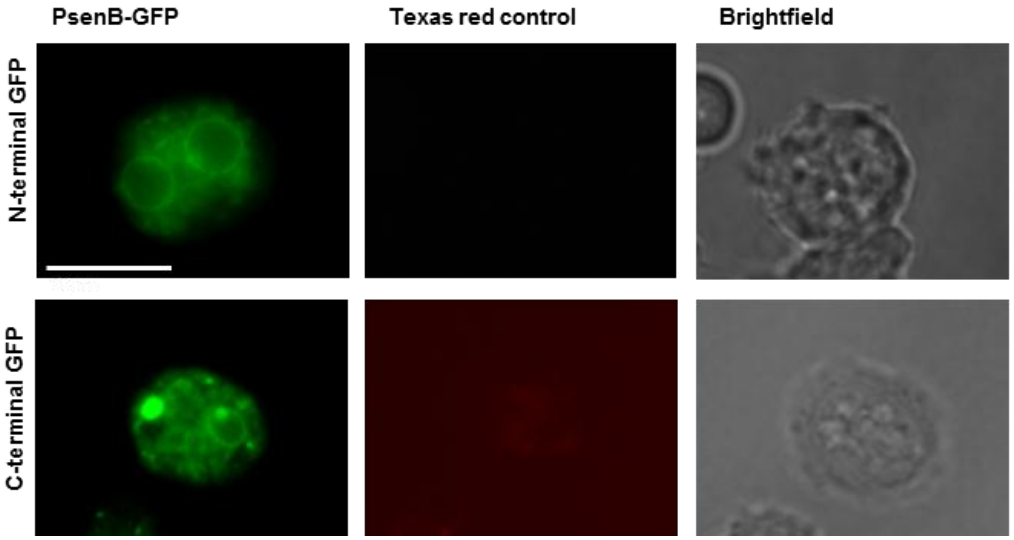

Fig.4.11 Live cell fluorescence images of *psenB⁻/A⁻* cells overexpressing PsenB-GFP 4h into starvation. Both N- or C-terminal GFP allowed localisation of PsenB to structures which resemble the ER and nuclear envelope. Not all cells express PsenB-GFP at detectable levels. Texas red channel (615nm) shows auto-fluorescence caused by residual media within the cell. Size bar=10µm.

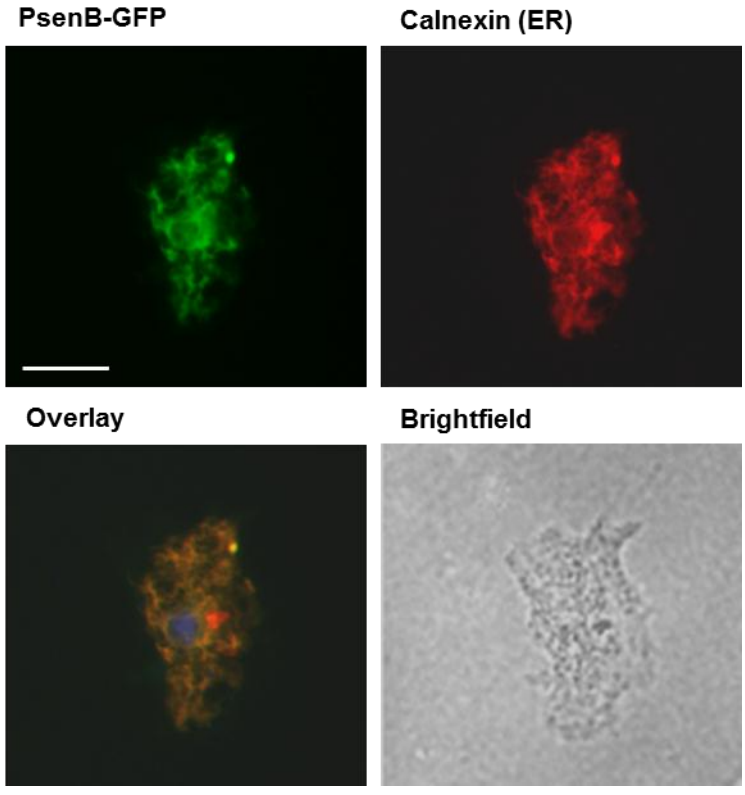

Fig.4.12 Fluorescence images of PsenB-GFP expressed in *psenB⁻/A⁻* cells. Cells were fixed and permeabilized using paraformaldehyde and TritonX-100 and co-stained using an anti-calnexin antibody (ER marker). The overlay image suggests co-localisation of PsenB-GFP and calnexin to the ER. DAPI stained the nucleus and provides evidence that PsenB-GFP and calnexin localise to the nuclear envelope. Size bar=10µm.

4.10 Growth of presenilin mutant cell lines

To further characterise the role of presenilin proteins in *D. discoideum* cell function, growth generation times of single and double presenilin mutants were assessed in shaking culture (Fig. 4.13A, B). In this experiment, cells were counted twice per day over a period of 4 days. Generation times for *psenA*$^-$ mutant cells (10.65h) and *psenB*$^-$ (9.65h) were not significantly different to wild type cells (10.57h). Furthermore, the *psenB*$^-$*/A*$^-$ mutant took 10.80h for one generation to duplicate which was again not significantly different to wild type cells.

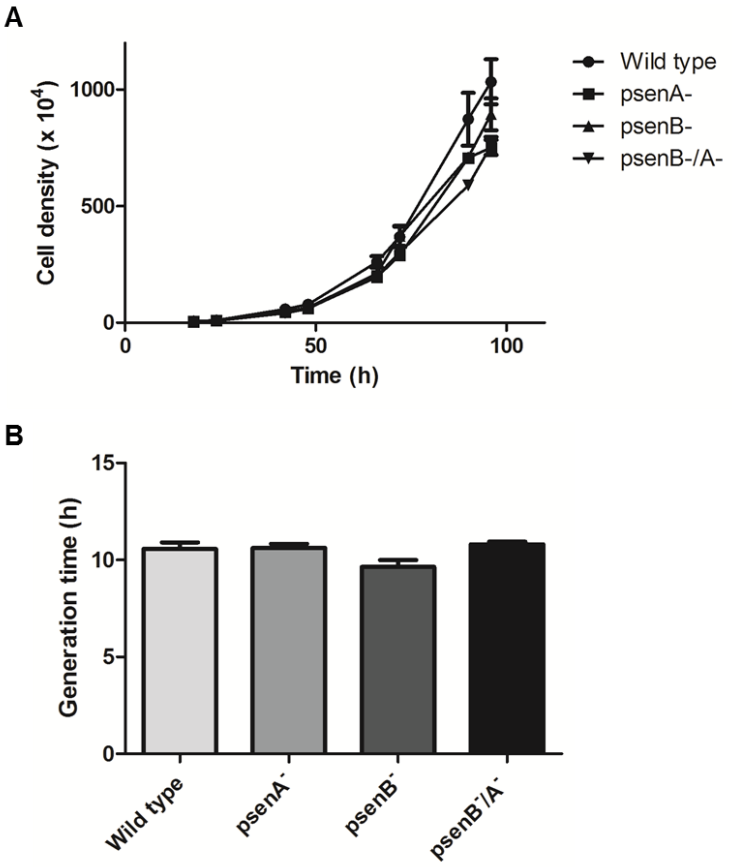

Fig.4.13 Generation times of wild type, psenA$^-$, psenB$^-$ and psenB$^-$/A$^-$ cell lines. (A) Cells were grown in shaking culture and cells were counted over a period of 96h. Graph represents cell growth reaching log-phase. (B) Generation times were calculated and no statistical significance was found when comparing wild type to mutant cell lines (±S.E.M; n=3).

4.11 Discussion

In this chapter, the role of presenilin proteins was examined in development and growth of *D. discoideum*, the simplest biomedical model possessing two presenilin genes. After analysis of presenilin gene transcription throughout development, mutants were created lacking one or both presenilin genes. Development and growth were assessed in these mutants and results suggest a redundant role for these proteins in development. Functional redundancy was then confirmed by overexpression of PsenB and this protein was localised to the ER.

4.11.1 A role for presenilin in *D. discoideum* development

To investigate a role for presenilin in *D. discoideum* development, gene transcription was assessed throughout this developmental process by Reverse Transcriptase PCR analysis. This analysis revealed that both *psenA* and *psenB* are expressed in vegetative, growing cells. *psenA* transcription increases between 4 to 12h and is constantly expressed in mid to late development. This upregulation suggests a role for *psenA* in *D. discoideum* mid to late development. High transcription levels were found for *psenB* throughout growth and development. In contrast to *psenA*, *psenB* transcription levels imply a cellular function in growing as well as developing cells. When directly comparing transcription levels of both genes, *psenB* transcription levels were significantly higher than *psenA* in growth and early development. A differential transcription pattern for both presenilin genes may suggest at least partially independent roles in growth and development.

Presenilin genes have been shown to be differentially transcribed throughout development in a variety of organisms. In human development, both presenilin genes are expressed in the fetal cortex with high *ps1* transcription levels (Lee et al., 1996). Lee et al. (1996) found that in young adult and aged brain tissue both genes are expressed at similar levels. Further, transcription levels of *ps1* and *ps2* are similar in a variety of other tissues, such as spleen and lung in the developing fetus. The authors suggest that the differential expression patterns

of both genes show at least partial independent functions in human development. Presenilin gene expression profiles were assessed in a variety of other organisms. For example, *Xenopus tropicalis* is a widely used model to study embryological development and possesses two copies of presenilin (*psα* and *psβ*) (Hashimoto-Gotoh et al., 2003). Both presenilin genes are transcribed at high levels in early oocytes with decreasing levels of *psα* in maturing oocytes, whereas *psβ* transcription levels remain high (Tsujimura et al., 1997). Again, these results suggest independent roles for each of the *X. tropicalis* presenilin genes in development. In the nematode, *C. elegans*, three presenilin genes (*sel-12*, *hop-1*, *spe-4*) are also differentially regulated throughout development (Levitan and Greenwald, 1995). Levitan and Greenwald (1995) showed that transcription of *sel-12* is uniform from embryonic to adult stages, whereas *spe-4* is only expressed in the larval stage 4 where sperm is produced. Further, the last presenilin gene, *hop-1*, is weakly expressed in embryos with increasing levels in L2-L4 and high levels in the adult stage. These results show differential presenilin gene expression, suggesting partial independent cellular functions. In the parasite, *Schistosoma mansoni*, only one presenilin gene is present. Here, gene transcript levels were found to be high in eggs of this parasite thus implying a role for presenilin in embryogenesis (Magalhaes et al., 2009). The gene transcription results presented in this current study suggest that *D. discoideum* presenilin proteins have independent roles in development.

In this current study, analysis of transcriptional gene expression was carried out by Reverse Transcriptase PCR, although quantitative PCR (qPCR) has recently surpassed this method as a more accurate mean to quantify gene expression. Nevertheless, the data produced here by Reverse Transcriptase PCR was supported by the dictyExpress database (RNA sequencing analysis) and Northern blot analysis by McMains *et al*. (2010) which were both published shortly after this study was carried out. However, it should be noted that analysis of gene transcription does not necessary translate to protein levels (Greenbaum et al., 2003). Western blot analysis would provide information about total presenilin protein present throughout development and assist in the understanding of the role in *D. discoideum* development. However, commercially available antibodies binding to the N, C-terminal or intracellular

loop of human PS1 cannot be used as these regions are weakly conserved in *D. discoideum*, thus antibodies would have to be raised against *D. discoideum* presenilin protein.

To assess the effects of deleting presenilin genes in *D. discoideum,* single and double presenilin knock-out mutants were produced. Initially knockout constructs for each presenilin gene were created. PCR amplification of open reading frames allowed creation of *psenA* and *psenB* knock-out cassettes containing 5' and 3' gene regions flanking a BsR cassette. These knock-out cassettes allowed deletion of large gene regions upon homologous integration into the genome, thus deletion of presenilin genes and protein function. The rate of homologous integration on both sides of the knock-out cassette was found to be very low (<0.1%) requiring the PCR screening of in excess of 5000 transformants. The vast majority of transformants contained the knock-out cassette non-homologously integrated into the genome, showing that electroporation of the construct into the cells was successful but homologous integration was highly infrequent. Literature describing the use of pLPBLP/Cre-loxP system (Faix et al., 2004) suggest that non-essential genes can be deleted at high frequency in *D. discoideum*. This low knock-out frequency allowed identification of only a small number of independent presenilin mutants. Therefore, to ensure correct gene deletion several molecular techniques were employed; PCR analysis of transformants using six primer pairs ensured the correct position and knock-out of the presenilin genes. Reverse transcriptase PCR on RNA level across this deleted gene region after BsR excision showed correct gene disruption for *psenA*$^-$ and *psenB*$^-$ strains.

To assess a role for presenilin proteins in *D. discoideum* development, fruiting body morphology was recorded in single and double presenilin knock-out mutants. *D. discoideum* cell lines lacking either *psenA* or *psenB* showed no apparent developmental defects since wild type fruiting bodies were observed. However, deletion of both presenilin in one cell line resulted in a severe developmental defect, as only aggregate structures were observed. These structures did not contain visible stalk nor sori structures. These results indicate that presenilin proteins play an important role in *D. discoideum* development. Analysis of early developmental streaming of *psenB*$^-$*/A*$^-$ mutant cells revealed

aberrant streaming and aggregation of smaller mounds when compared to wild type cells. These results may suggest that presenilin proteins may regulate or maintain streams and aggregation territories. A similar deficient streaming phenotype has been observed in other *D. discoideum* such as the cell number regulator mutant strain (Tang and Gomer, 2008). Furthermore, since a developmental defect was caused by deletion of both presenilin genes but not either one individually suggests a redundant role for both proteins, despite differential gene expression. It would be of interest to assess gene transcriptional levels of *psenA*$^-$ in a *psenB*$^-$ background (and vice versa). This analysis may show an upregulation of the intact gene, to provide a compensatory mechanism during development of *D. discoideum*.

A functional redundancy for both presenilin proteins has been observed in other species. In mice, deletion of both *ps1* alleles was shown to down-regulate the Notch-1 pathway resulting in a neuronal loss and perinatal lethality (van Tijn et al., 2011). The mouse model lacking both *ps2* alleles is viable, displaying only mild pulmonary fibrosis (Herreman et al., 1999). Deleting both presenilin (all alleles) genes leads to neural tube disorganisation and disrupted Notch-1 signalling resulting in death of mice at the embryonic stage (Hall and Roberson, 2011). A developmental defect is also seen in *C. elegans* where deletion of *sel-12* leads to an egg-laying deficiency phenotype via reduction of *lin-12*/Notch-1 activity (Levitan et al., 1996). Deletion of *sel-12* and *hop-1* leads to a more severe phenotype including germ-line proliferation defects and embryonic lethality (Westlund et al., 1999). Another biomedical model possessing two presenilin genes is *D. rerio*. Morpholino knock-down of *psen1* leads to somite defects and defective brain development, whereas *psen2* morpholino knock-down results in reduced melanin pigmentation (Nornes et al., 2008). Knock-down of both presenilin genes does not result in a more severe phenotype which may be due to the nature of knock-down studies where small amounts of gene products are present in the cell (Nornes et al., 2009).

In other organisms, presenilin has been shown to regulate development and display functional redundancy (Selkoe and Kopan, 2003; Donoviel et al., 1999). The study presented here suggest that *D. discoideum* presenilin proteins

regulate development and may possess a functional redundancy as only the double presenilin mutant displays a severe developmental defect.

4.11.2 Complementation and localisation of presenilin

To confirm the deletion and developmental phenotype of the *psenB⁻/A⁻* mutant, GFP tagged PsenB was overexpressed in this cell line. Resulting transformants developed into mature fruiting bodies within 24h. Both the N- and C-terminal PsenB overexpression rescued the developmental phenotype, suggesting that the GFP tag at either end of the protein did not interfere with presenilin protein functions. PsenB-GFP was also overexpressed in wild type cells to investigate a potential effect of constitutively expressed PsenB-GFP in *D. discoideum* development. Developmental analysis of these transformants did not reveal a gross change in fruiting body morphology. These results combined indicate that *psenB⁻/A⁻* mutant is a genuine knock-out cell line and developmental changes in this cell line were caused by loss of both presenilin genes. Furthermore, phenotype rescue of the *psenB⁻/A⁻* mutant by overexpression of PsenB-GFP supports the hypothesis of functional redundancy of presenilin proteins in *D. discoideum* development. However, in other organisms such as *C. elegans* presenilin proteins were found to possess dissimilar abilities to compensate for lost presenilin function (Westlund et al., 1999). Therefore, to further characterise *D. discoideum* presenilin redundancy, PsenA needs to be overexpressed in *psenB⁻/A⁻* mutant to establish its role in development and ability to compensate.

Since overexpression of GFP-tagged PsenB complemented the developmental phenotype observed in the *psenB⁻/A⁻* mutant, live cell imaging was initially employed to establish its cellular localisation. PsenB-GFP was found to localise to membrane structures which resemble the ER and nuclear envelope and this was confirmed by calnexin co-localisation (Muller-Taubenberger et al., 2001). This localisation to the ER and nuclear envelope appears to be conserved widely throughout animal species as shown in human and *C. elegans* (Li et al., 1997; Walter et al., 1996; Arduengo et al., 1998) . The role of presenilin at the ER is still under investigation but recent studies suggest a role in passive calcium leak formation (Tu et al., 2006b). Since the ER is the central site for

phospholipid synthesis (Fagone and Jackowski, 2009), a possible link between presenilin protein and phospholipids synthesis has also been proposed (Landman et al., 2006). This study reported here provides evidence of a conserved presenilin protein localisation in human and *D. discoideum*.

4.11.3 Growth of presenilin mutant cell lines

Since a role for presenilin in regulating cell growth was shown in several wide ranging models, such as mouse and moss, a similar role for presenilin was investigated in *D. discoideum* (Khandelwal et al., 2007; Soriano et al., 2001). Generation times of wild type, single and double presenilin mutant cells were examined in shaking axenic culture. No gross changes in generation times were observed, despite a developmental defect in *D. discoideum* lacking all presenilin. These results indicate that cytokinesis and pinocytosis, a process which is required to take up nutrients in shaking culture, is not affected by deletion of presenilin.

Cell proliferation has been shown to be regulated through PS1 and β-catenin as part of the Wnt signalling pathway in mammalian systems (Soriano et al., 2001). β-catenin binds to the cytosolic loop of presenilin which negatively regulates β-catenin activity. Upon deletion of presenilin or the intracellular loop of this protein, β-catenin stabilises, leading to hyperproliferation in embryonic mouse fibroblasts lacking *ps1* (Soriano et al., 2001; Murayama et al., 1998). Similar observations were made in moss, *P. patens*, where deleting the only presenilin gene resulted in longer shoots and a greater number of leaves despite a weakly conserved intracellular loop (Khandelwal et al., 2007). These studies suggest that despite the large evolutionary distance between mice and *P. patens*, presenilin proteins regulate cytokinesis through the Wnt pathway in both systems.

Since *psenB* is highly transcribed in the vegetative stage, it would therefore be likely to have a role in growing cells. Whilst the work here reported was carried out, McMains et al. (2010) confirmed that deletion of presenilin in *D. discoideum* does not affect growth in shaking culture. However, McMains et al. (2010) showed that deletion of presenilin (*psenA*$^-$ and *psenB*$^-$/*A*$^-$) leads to a significant

decrease in phagocytic capture of yeast. To further establish a role for presenilin proteins in growing cells, cell adhesion (Bozzaro and Ponte, 1995) or induction of morphogenesis (Weijer, 2004) could be investigated.

4.11.4 Published *D. discoideum* presenilin mutant data

In 2010, whilst this current work was undertaken, a collaborator published data on *D. discoideum* presenilin mutants (McMains et al., 2010). Despite regulated naming of genes (Dictybase), the authors named *D. discoideum* presenilin genes as follows: *ps1* (*psenB*) and *ps2* (*psenA*). These gene names reflect the order of discovery and not homology to either of the human presenilin genes (personal communication with McMains). From this published work, deletion of *psenA* (*ps2*) produced a phenotype with a developmental arrest at the slug stage (produces slugs only), whereas deletion of *psenB* (*ps1*) had no effect on development or fruiting body morphology. Deletion of both presenilin genes in one cell line (*ps1*$^-$/*ps2*$^-$) mirrored the phenotype described in the *psenA*$^-$(*ps2*$^-$) mutant. The differences in phenotypes observed in the work submitted here to that published by McMains et al. (2010) may be due to background strains used, since this current study was based in an Ax2 cell line, and McMains et al. (2010) failed to report a strain background. Further differences may have arisen due to a different knock-out construct design by McMains *et al*. (2010), since the current study created mutant strains lacking large parts of the gene, thus ensuring gene disruption, whereas MacMains et al. (2010) created mutants by insertional mutagenesis (without deletions). Similar discrepancies in developmental phenotypes following ablation of the same gene have been reported by two research groups deleting glycogen synthase kinase A (GSK-A) (Schilde et al., 2004; Harwood et al., 1995). Here, Schilde *et al*. (2004) argued that the milder developmental phenotype of GSK-A$^-$ mutant cell line was due to differences in the parent strains.

Chapter 5

Bioinformatic analysis of both *D. discoideum* presenilin proteins suggests common cellular functions to those of human presenilin proteins. Analysis of the two *D. discoideum* presenilin proteins showed a role for these proteins in development. This chapter investigates a conserved role for human PS1 (from here onwards PS1) in development and the complementation of the *D. discoideum psenB*$^{-}$*/A*$^{-}$ mutant. This was achieved by overexpression of PS1-GFP in the mutant background to assess developmental rescue and localisation. Furthermore, mutant cell lines were assessed for abnormalities in stalk and spore cell numbers and quantitative PCR (qPCR) was employed to assess developmental gene transcription. To establish whether the role for presenilin proteins in *D. discoideum* development is dependent upon the proteolytic activity, overexpression of proteolytic inactive PS1 in a *psenB*$^{-}$*/A*$^{-}$ mutant and western blot analysis were performed.

5.1 Developmental rescue using human presenilin 1

In order to investigate whether *D. discoideum* and human presenilin proteins possess common cellular functions, a *psenB*$^{-}$*/A*$^{-}$ mutant cell line overexpressing PS1 was created. For this experiment, a *D. discoideum* vector expressing PS1 from a highly expressed constitutive promoter was prepared from a human PS1^{D385A} cDNA clone (isoform 2) where the aspartic acid 385 (D385A) was eliminated through overlap extension PCR to construct the wild type gene (Fig. 5.1).The resultant PS1 cDNA was then cloned into pDM448 (N-terminal GFP tag) and sequenced to ensure the construct was mutation free.

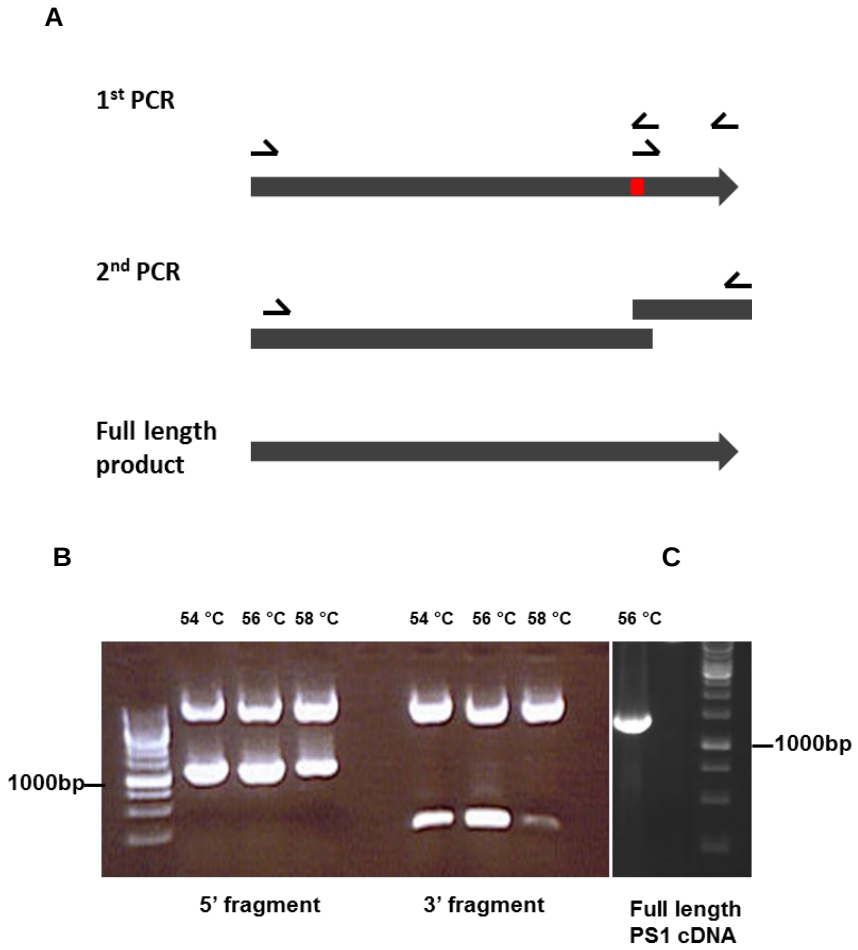

Fig.5.1 Overlap extension PCR to create mutation free *ps1* cDNA. (A) Schematic overview of the overlap extension PCR where the two primer pairs correct the mutated nucleotides of $ps1^{D385A}$ cDNA and were used to amplify two wild type fragments of *ps1*. These products were then combined to amplify full length, mutation free *ps1* cDNA. (B) Gel electrophoresis image of 5' and 3' fragments which were amplified using a mammalian vector containing $ps1^{D385A}$ as a template at various annealing temperatures. (C) 5' and 3' fragments were used as templates to amplify full length wild type *ps1* cDNA.

In this experiment, $psenB^{-}/A^{-}$ mutant cells were transformed with the created PS1-GFP overexpression construct and colonies growing in the presence of antibiotic were screened by PCR for the presence of PS1-GFP in a $psenB^{-}/A^{-}$ background. Amplification across the deleted regions of *psenA* and *psenB* produced smaller fragments in the presenilin null background (confirming deletion of the presenilin genes) when compared to the wild type background. Furthermore, a PCR primers annealing to *ps1* did amplify a PCR product in $psenB^{-}/A^{-}$ mutant cells overexpressing PS1 only (Fig. 5.2).

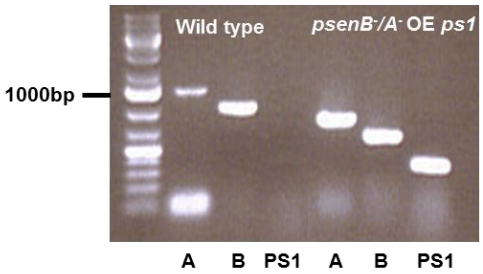

Fig.5.2 PCR screen of *D. discoideum* wild type and *psenB*$^{-}$*/A*$^{-}$ mutant cells for the presence of human *ps1*. Primer sets amplify across the deleted region of *psenA* (A), *psenB* (B) and human *ps1* (PS1). DNA of non-transformed cells produced wild type length *psenA* and *psenB* PCR product and not a *ps1* product. DNA of transformed cells produced smaller, knock-out PCR products for *psenA* (A), *psenB* (B) and a product *ps1* (PS1) confirming the presence of the *ps1* overexpressing vector.

D. discoideum psenB^{-}*/A*$^{-}$ cells expressing PS1-GFP were then developed on nitrocellulose filters and fruiting body morphology was assessed after 24h (Fig. 5.3). These transformants developed into mature fruiting bodies comprising wild type stalks and sori, thus showing rescue of the *psenB*$^{-}$*/A*$^{-}$ developmental phenotype. Furthermore, wild type cells overexpressing *ps1* did not produce an altered developmental phenotype when compared to wild type cells.

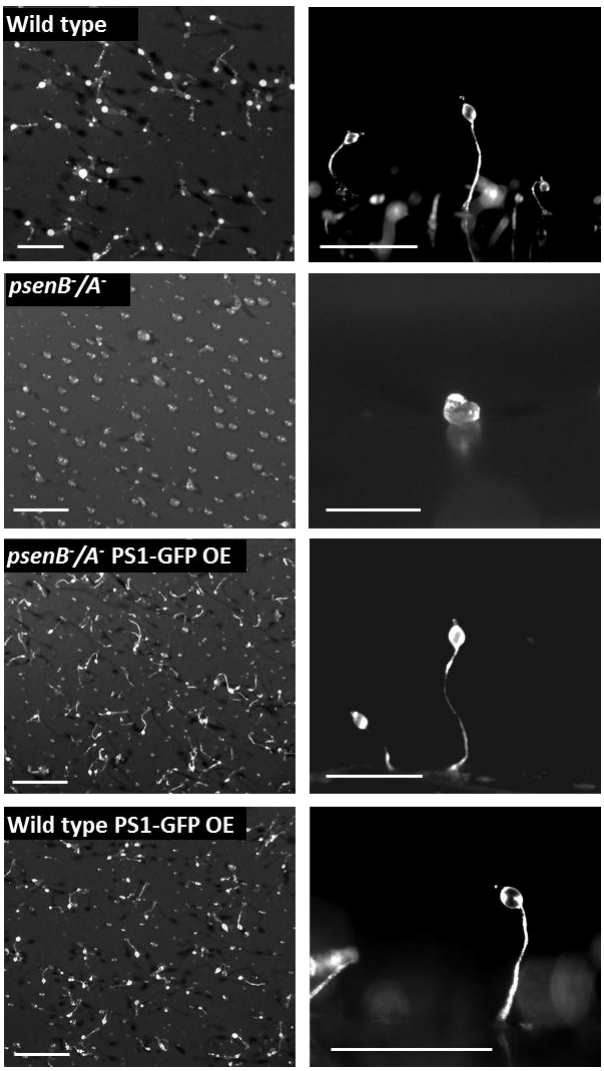

Fig.5.3 Developmental rescue of *psenB*$^{-}$*/A*$^{-}$ mutant cells through human PS1 overexpression. Wild type, *psenB*$^{-}$*/A*$^{-}$, *psenB*$^{-}$*/A*$^{-}$ overexpressing PS1 and wild type overexpressing PS1 (N-terminal tagged GFP) were developed on nitrocellulose filters and developmental morphology was assessed using an aerial view (left) and side view (right). Overexpression of human *ps1* in the *psenB*$^{-}$*/A*$^{-}$ cell line allows development of mature fruiting bodies. Expression of PS1 in wild type cells did not produce a developmental phenotype. Size bar=1mm.

5.2 Localisation of human presenilin 1 in *D. discoideum*

Since the *D. discoideum* PsenB-GFP localises to the ER and nuclear envelope in *psenB*$^{-}$*/A*$^{-}$ cells (Chapter 4), the localisation of PS1-GFP was also assessed using fluorescence imaging. This analysis revealed localisation to cellular structures resembling the ER and nuclear envelope (Fig. 5.4).

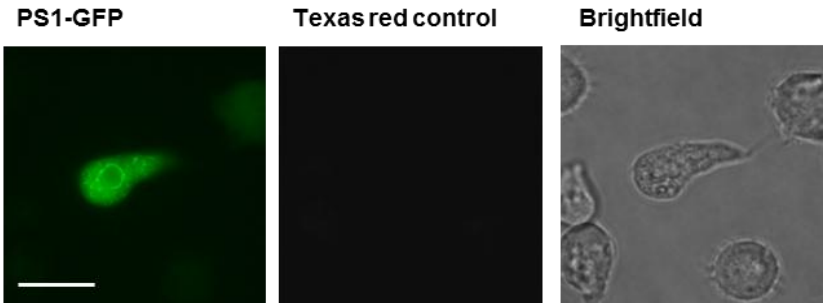

Fig.5.4 Live cell fluorescence images of *psenB⁻/A⁻* cells overexpressing PS1. PS1 was tagged with an N-terminal GFP to allow localisation using live cell imaging. PS1-GFP localised in structures which resemble the ER and nuclear envelope. Not all cells express PS1-GFP at detectable levels. Texas red channel (615nm) was used as an internal auto-fluorescence control. Size bar=10µm.

To verify whether PS1-GFP localises to the ER and nuclear envelope, *psenB⁻/A⁻* PS1-GFP overexpressing cell were fixed and probed for calnexin as described in Chapter 4. The overlay of PS1-GFP and calnexin images demonstrates a co-localisation of PS1-GFP to the ER and nuclear envelope in *D. discoideum* (Fig. 5.5).

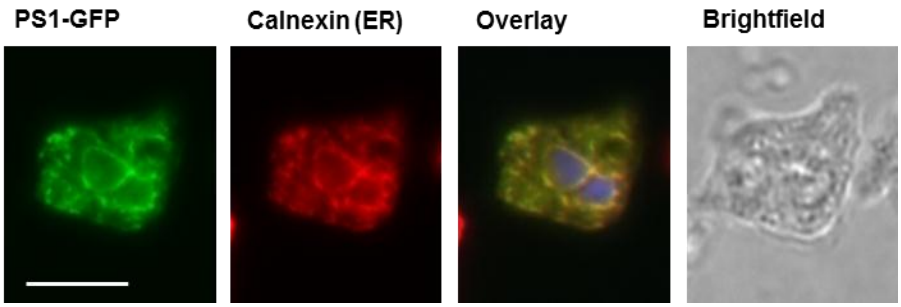

Fig.5.5 Fluorescence images of PS1-GFP overexpressed in *psenB⁻/A⁻* cells. Cells were fixed and permeabilized using paraformaldehyde and TritonX-100 and co-stained using an anti-calnexin antibody (ER marker). The overlay image suggests co-localisation of PS1 and calnexin to the ER. DAPI stained the nucleus and provides evidence that PS1 and calnexin localise to the nuclear envelope. Size bar=5µm.

5.3 Stalk cell analysis

To assess the developmental phenotype observed in *psenB⁻/A⁻* mutant cells, a more detailed phenotypic analysis was carried out. *D. discoideum* offers a system in which the analysis of individual developmental stages such as stalk cell production is possible. Stalk cells production can be induced using DIF enabling assessment of stalk cell production in a low-density monolayer. This

stalk cell production is inhibited by the addition of cAMP which acts through a Gsk-A-dependant inhibition (GSK-3β homologue) (Williams et al., 1999). Quantification of stalk cells revealed that ablation of either of the presenilin genes did not affect stalk cell production, whereas deletion of both presenilin genes resulted in 31% fewer stalk cells ($p \leq 0.05$) when compared to wild type cells (Fig. 5.6) (Harwood, 2008). Analysis of the inhibition of stalk cell production using cAMP revealed that the *psenB⁻/A⁻* mutant cells produced 84% ($p \leq 0.01$) less stalk cells when compared to wild type cells. Expression of either PsenB-GFP or PS1-GFP in the *psenB⁻/A⁻* background restored stalk cell production back to wild type levels (Fig. 5.6).

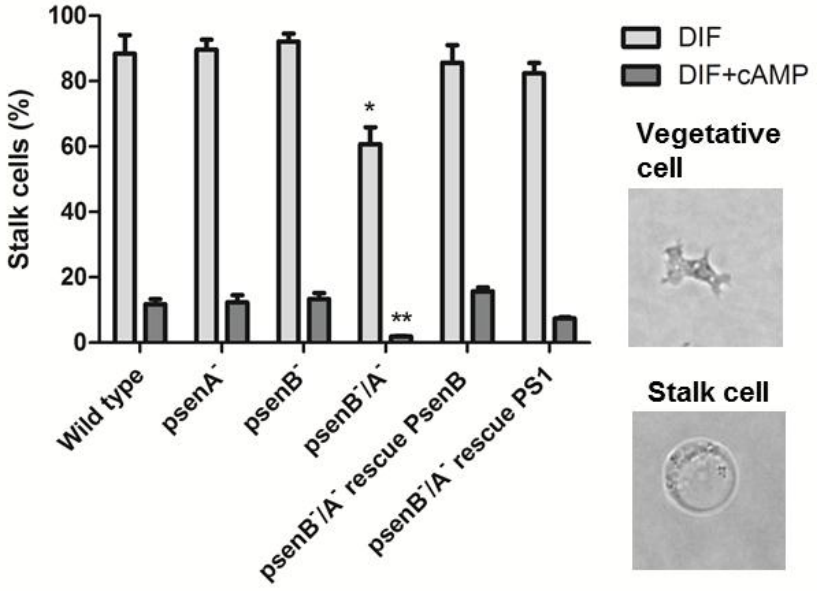

Fig.5.6 Stalk cell analysis of presenilin mutant strains. DIF induces whereas cAMP inhibits stalk cell production in *D. discoideum*. Ablation of one presenilin gene did not affect stalk cell production but ablation of both presenilin genes showed a significant reduction in stalk cell number. This effect was rescued by overexpression of PsenB-GFP and PS1-GFP. Images represent cell types, where stalk cells are round and vacuolated. Values shown are means (±S.E.M; n=3) *** p<0.001; ** p<0.01; * p<0.05.

5.4 Spore cell analysis

To further characterise the developmental phenotype observed in *psenB⁻/A⁻* mutant cells, spore cell production was assessed. To do so, wild type and presenilin mutant strains were developed for 24h on nitrocellulose filters and resultant fruiting bodies (or aggregates) were lysed with detergent to remove all non-spore cells. Spore counts revealed that *psenA⁻* and *psenB⁻* cell lines produced 40% less spores than wild type cells (p≤ 0.001; Fig. 5.7). In the *psenB⁻/A⁻* mutant cell line 98% decrease in spore cell production was observed when compared to wild type spore production. However, spore cell production was restored to single knock-out cell lines levels when PsenB-GFP or PS1-GFP was overexpressed in the *psenB⁻/A⁻* background (Fig. 5.7). It should be noted that PsenB-GFP is able to restore these levels more efficiently when compared to PS1-GFP (p≤ 0.05).

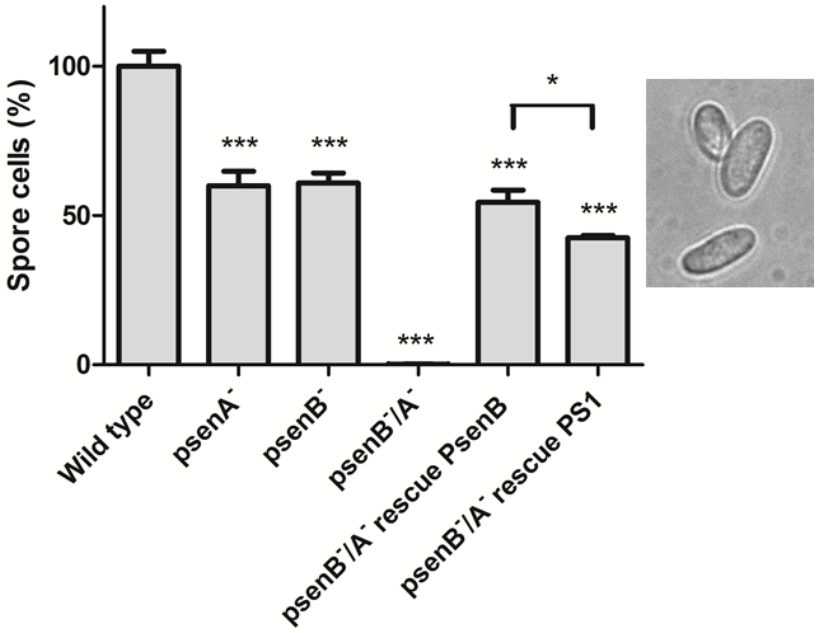

Fig.5.7 Spore cell analysis of wild type and presenilin mutant strains. All strains were developed on nitrocellulose filters and developmental structures were treated with detergent (lyses non spore cells). Spore cell numbers in single presenilin knock-out cell lines were found to be significantly decreased with complete ablation of spore cell production in *psenB⁻/A⁻* mutant cells. Overexpression of PS1-GFP and PsenB-GFP restored spore production to single presenilin gene knock-out strain levels. Image represents spore cells. Values shown are means (±S.E.M; n=3) *** p<0.001; ** p<0.01; * p<0.05.

5.5 qPCR analysis of developmental regulated genes in presenilin mutants

To independently assess developmental changes caused by deletion of both presenilin genes, transcriptional gene regulation of developmental markers was assessed using quantitative PCR (qPCR). The developmental genes assessed by this method are markers for specific developmental stages during early, mid and late development of *D. discoideum* (*carA-1*, *ecmA*, *psA*). In these experiments, wild type, *psenB*$^-$/*A*$^-$, *psenB*$^-$/*A*$^-$ overexpressing PsenB-GFP and *psenB*$^-$/*A*$^-$ overexpressing PS1-GFP cells were developed on nitrocellulose membranes (Fig. 5.8), and RNA was extracted at six hourly intervals over a period of 24h. This RNA was used as a template for cDNA synthesis and gene transcription levels were analysed by qPCR.

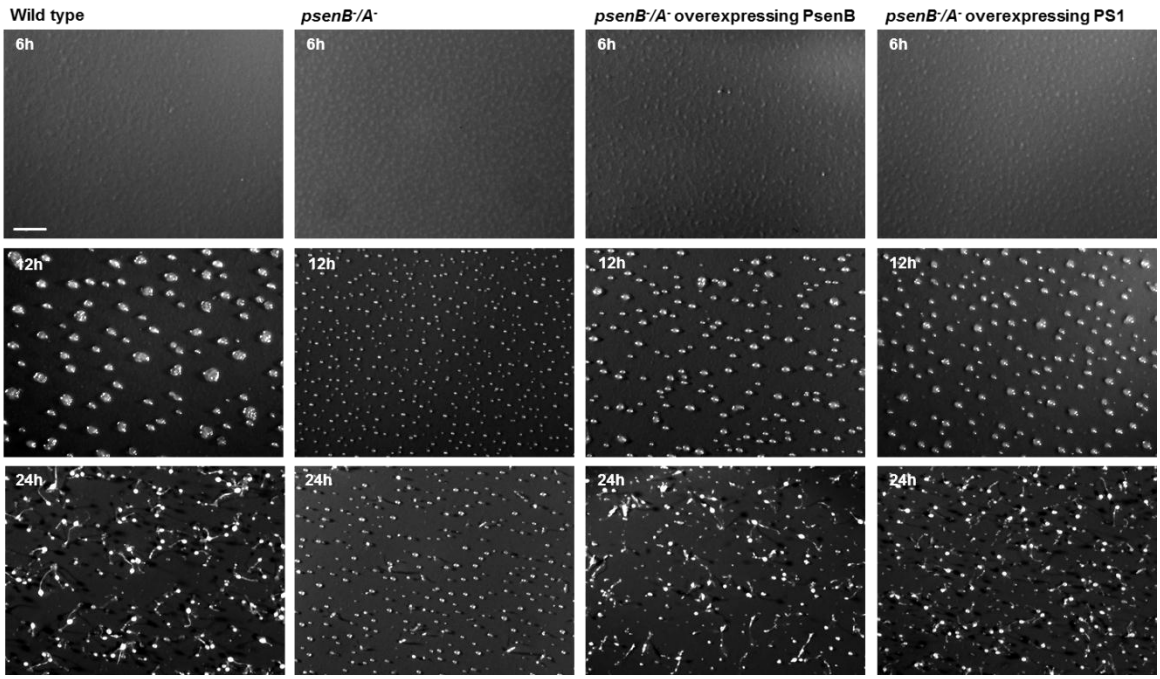

Fig.5.8 Development of wild type, *psenB*$^-$/*A*$^-$ mutant cells and *psenB*$^-$/*A*$^-$ mutant cells expressing either PsenB or PS1 for qPCR analysis. Cells were washed off the nitrocellulose filters at six hourly intervals over a period of 24h. This was followed by RNA extraction and cDNA synthesis. No images were taken of cells at 0h as no structures are visible on nitrocellulose filters at this time point. Development was assessed using an aerial view. Size bar=1mm.

To analyse the early development, expression of the cAMP receptor (*car1*) was assessed as it is required for the streaming phase. This analysis showed that *psenB*$^-$/*A*$^-$ mutant cells had a threefold increase in *car1* expression ($P < 0.001$) at

6h compared to wild type cells (Fig. 5.9 A). Throughout mid and late development, *car1* transcription levels stay higher (P<0.001) when compared to wild type cells. The transcription levels of stalk cell marker (*ecmA*) showed a significant decrease (P< 0.001) in *psenB*$^{-}$/*A*$^{-}$ mutant cells throughout early and mid-development when compared to wild type expression (Fig. 5.9 B). Analysis of the pre-spore specific marker (*psA*) and late development showed increased transcription levels in early and late development for *psenB*$^{-}$/*A*$^{-}$ mutant cells at 24h (Fig. 5.9 C).

Gene expression analysis of the rescued strains revealed that the elevated *car1* observed in *psenB*$^{-}$/*A*$^{-}$ transcription was downregulated in the rescued *psenB*$^{-}$/*A*$^{-}$ cells (Fig. 5.9 A). At 6 and 12h, overexpression of *psenB* results in a restored transcriptional regulation of *car1*, when compared to *psenB*$^{-}$/*A*$^{-}$ mutant and wild type cells. Transcription of *ecmA* in *psenB*$^{-}$/*A*$^{-}$ overexpressing PsenB-GFP was upregulated and resembles wild type transcription of this gene at 12h (Fig. 5.9 B). However, at 24h, overexpression of *psenB* resulted in a significant transcriptional upregulation of *ecmA* (p< 0.001) when compared to wild type and *psenB*$^{-}$/*A*$^{-}$ mutant cells. The spore cell marker (*psA*) is significantly upregulated in *psenB*$^{-}$/*A*$^{-}$ overexpressing *psenB* at 12 and 24h (Fig. 5.9 C; p< 0.01).

Overexpression of PS1-GFP in the *psenB*$^{-}$/*A*$^{-}$ background led to a downregulation of *car1* transcription but did not fully restore wild type *car1* transcription at 6 and 24h (Fig. 5.9 A). *ecmA* transcription levels were upregulated in *psenB*$^{-}$/*A*$^{-}$ cells overexpressing PS1-GFP but wild type levels were not fully restored at 12h (Fig. 5.9 B). However, *ecmA* expression was significantly upregulated at 24h when overexpressing PS1-GFP in the *psenB*$^{-}$/*A*$^{-}$ background, similar to that observed in *psenB*$^{-}$/*A*$^{-}$ cells overexpressing PsenB-GFP (p< 0.001). The spore cell marker transcription levels (*psA*) was as well significantly upregulated at 12 and 24h (p< 0.001) in *psenB*$^{-}$/*A*$^{-}$ cells overexpressing PS1-GFP when compared to wild type and *psenB*$^{-}$/*A*$^{-}$ cells (Fig. 5.9 C).

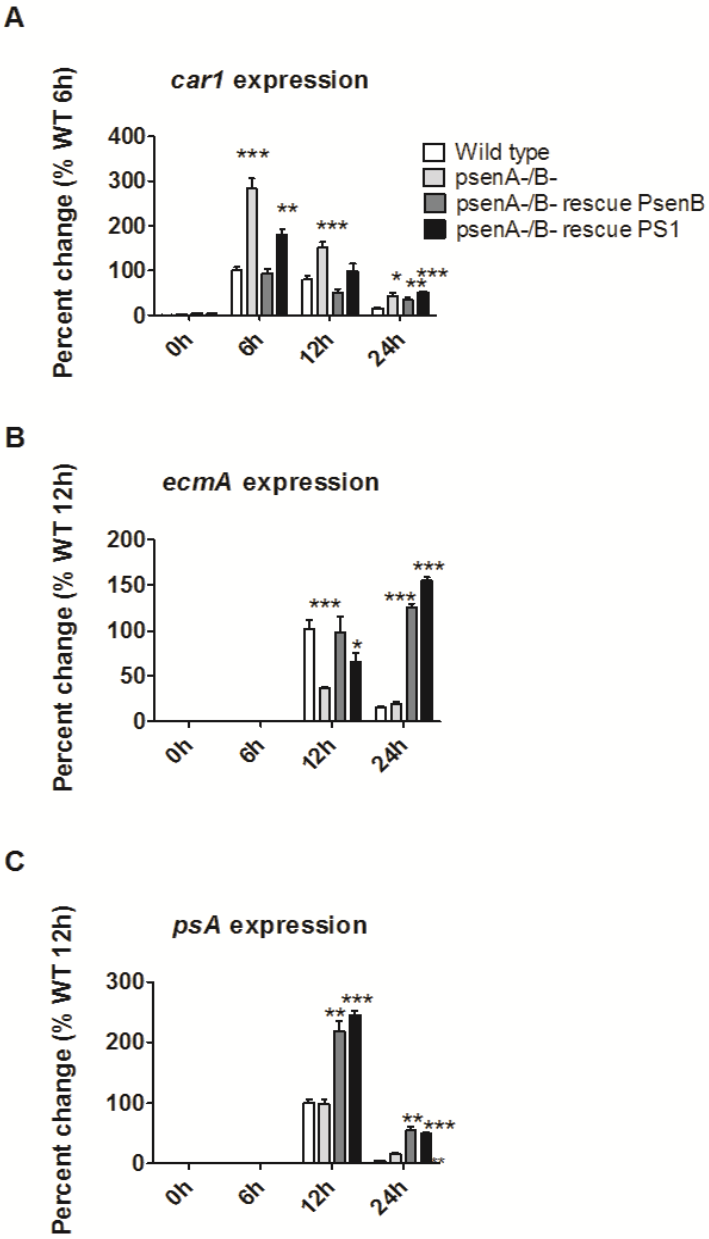

Fig.5.9 Quantitative PCR analysis of three developmentally regulated genes in wild type, *psenB*$^{-}$*/A*$^{-}$ mutant cells and *psenB*$^{-}$*/A*$^{-}$ mutant cells expressing either *psenB* or *ps1*. (A) *car1* (early aggregation marker), (B) *ecmA* (stalk cell marker) and (B) *psA* (spore cell marker) transcription levels were assessed and *ig7* was employed as a loading control. (A) *car1* transcription was significantly upregulated in *psenB*$^{-}$*/A*$^{-}$ mutant cells. (B) *ecmA* transcription was significantly lower in *psenB*$^{-}$*/A*$^{-}$ cells when compared to wild type cells. (C) No significant changes were observed in *psA* transcription of *psenB*$^{-}$*/A*$^{-}$ cells. (A) *car1* and (B) *ecmA* transcription levels were partially restored in overexpressing mutant cells when compared to *psenB*$^{-}$*/A*$^{-}$ cells. Both rescued strains displayed a significantly upregulation in (B) *ecmA* and (C) *psA* at 12 and 24h when compared to wild type and *psenB*$^{-}$*/A*$^{-}$ mutant cells. Values shown are means (±S.E.M; n=3; technical duplicates) *** p<0.001; ** p<0.01; * p<0.05.

5.6 Western blot analysis

In higher organisms, presenilin is cleaved through endoproteolysis of the intracellular loop in order to carry out γ-secretase functions and only very little full length presenilin protein can be found in cell lysates (Honda et al., 2000; Haass and De Strooper, 1999). In order to establish whether PsenB-GFP and PS1-GFP undergo cleavage in *D. discoideum*, Western blot analysis was carried out. Since both PsenB and PS1 were tagged with a GFP, protein lysates of *psenB*$^-$*/A*$^-$ overexpressing PsenB or PS1 cells were analysed by Western blotting using an anti-GFP antibody. The isoform 2 of PS1 consists of 463 amino acids and gives rise to a molecular weight of ~52kDa. PsenB encodes 473 amino acids also accounting for a molecular weight of ~52kDa. Both proteins contain a GFP tag (~28kDa) which together with PsenB or PS1 gives rise to an expected molecular weight of ~100kDa (rather than 80kDa). However, it should be noted that an increase in the molecular weight is often found when proteins are expressed with a GFP tag. Western blot analysis showed that both PsenB-GFP and PS1-GFP were expressed in *psenB*$^-$*/A*$^-$ cells but neither protein underwent endoproteolysis in *D.* discoideum. The presence of only full length ~80kDa proteins suggests a lack of endoproteolytic presenilin cleavage in *D. discoideum* (Fig. 5.10).

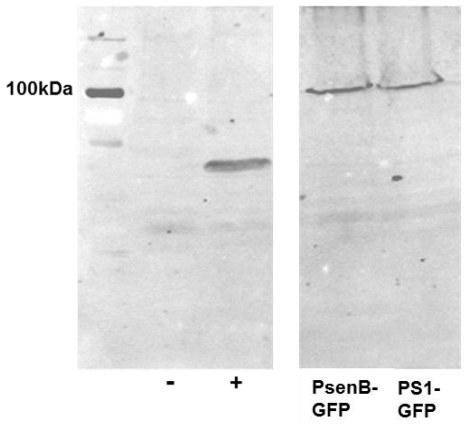

Fig.5.10 Western blot analysis of lysates from *psenB*$^-$*/A*$^-$ overexpressing either PsenB-GFP or PS1-GFP. An anti-GFP antibody was employed to probe for the GFP tag of PsenB-GFP (~80kDa) and PS1-GFP (~80kDa) in *psenB*$^-$*/A*$^-$ overexpressing mutants. Probing untransformed wild type cell lysate (-) for GFP showed no unspecific binding, whereas probing for GFP in lysates of cells overexpressing Crac PH domain-GFP (~41kDa) showed specificity of the antibody (+). Probing for GFP in lysates of cells overexpressing either PsenB or PS1, identified a single ~100kDa protein band.

5.7 Human presenilin 1 can rescue *psenB⁻/A⁻* phenotype independent of catalytic aspartic acid

Since no endoproteolytic cleavage of either PsenB-GFP or PS1-GFP was detected in *D. discoideum*, the ability of human PS1 to function in *D. discoideum* development lacking endoproteolytic activity was examined. Human PS1 possesses two active catalytic aspartic acid residues (D257 and D385) which are required for endoproteolysis and to catalyse γ-secretase functions (Wolfe et al., 1999). Mutation of either one of these aspartic acids leads to loss of γ-secretase function and thus proteolytic activity (Wolfe et al., 1999). In this experiment an endoproteolytic dead PS1 ($PS1^{D385A}$) was expressed in the *psenB⁻/A⁻* mutant cell line and developmental phenotype was assessed. To do so, human $PS1^{D385A}$ cDNA was cloned into the *D. discoideum* expression vector pDM448 and transformed into *psenB⁻/A⁻* cells. Transformants were developed on nitrocellulose filters and morphology assessment showed that the endoproteolytic dead $PS1^{D385A}$-GFP rescued the altered developmental phenotype observed in *psenB⁻/A⁻* cells (Fig. 5.11). The rescue using $PS1^{D385A}$ confirms an endoproteolytic independent function for presenilin proteins in *D. discoideum* development.

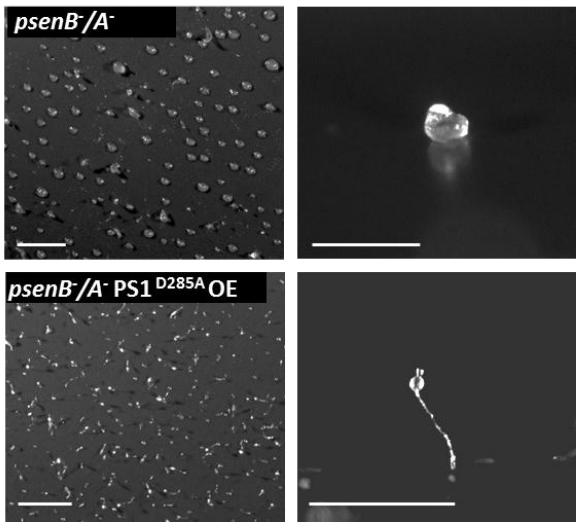

Fig.5.11 Developmental rescue of *psenB⁻/A⁻* mutant cells by $PS1^{D385A}$ overexpression. *psenB⁻/A⁻* and *psenB⁻/A⁻* $PS1^{D385A}$ overexpressing cells (N-terminal tagged GFP) were developed on nitrocellulose filters and developmental morphology was assessed using an aerial view (left) and side view (right). Overexpression of $PS1^{D385A}$ in the *psenB⁻/A⁻* cell line allowed development of mature fruiting bodies. Size bar=1mm.

To investigate whether localisation of human PS1 to the ER and nuclear envelope is dependent upon the catalytic aspartic acid residue (D385), live cell microscopy of *psenB*$^{-}$/*A*$^{-}$ PS1^{D385A} overexpressing cells was carried out. This proteolytic inactive protein, like the wild type protein was found to localise to structures resembling the ER and nuclear envelope (Fig. 5.12).

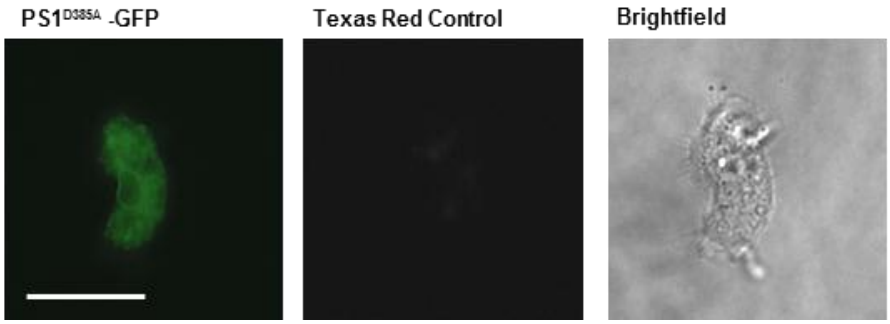

Fig.5.12 Live cell fluorescence images of *psenB*$^{-}$/*A*$^{-}$ PS1^{D385A} overexpressing cells 4h into starvation. PS1 ^{D385A} was tagged with an N -terminal GFP to allow visualisation. The protein was found to localise to structures resembling the ER and nuclear envelope. Texas red channel (615nm) shows auto-fluorescence caused by residual media within the cell. Size bar=10µm.

5.8 Notch-1 cleavage assay

So far, this study has shown that human presenilin is able to rescue the *D. discoideum* developmental phenotype caused by deletion of both endogenous presenilin genes. This result suggests that human and *D. discoideum* have functionally conserved roles. To examine the functionality of *D. discoideum* presenilin proteins in mammalian cells, both *D. discoideum* presenilin proteins were expressed in mouse blastocysts lacking all presenilin proteins (BD8 cells; PS1$^{-/-}$PS2$^{-/-}$) or all but one PS1 allele (BD3 cell; PS1$^{+/-}$PS2$^{-/-}$) whilst expressing a human truncated version of Notch-1 (Den1) (Donoviel et al., 1999). In this experiment, presenilin proteins, as part of the γ-secretase complex, were required to cleave human Notch-1 and the activity was assessed using a C-promoter binding factor-1 reporter assay as described by Hooper et al. (2006). In order to assess Notch-1 cleavage through *D. discoideum* presenilin proteins, full length *psenA* and *psenB* cDNA was cloned into a mammalian pFLAG-CMV 5a vector enabling expression of either wild type or FLAG tagged proteins. These constructs were transfected into BD8 and BD3 cells and Notch-1 cleavage was assessed.

As a positive control, *D. discoideum* presenilin proteins and human PS1 were expressed in BD3 cells. Analysis of BD3 cells showed that Notch-1 was successfully cleaved by the endogenous mouse PS1 and was similar to the cleavage levels observed in cells transfected with human PS1 (Fig. 5.13 A; p≤ 0.05). Analysis of Notch-1 cleavage by *D. discoideum* presenilin proteins revealed that both, Flag tagged and untagged, presenilin proteins were able to cleave Notch-1 more efficiently than human and mouse PS1 in the BD3 background (p≤ 0.01). Analysis of cleavage in a BD8 cell background revealed that human PS1 cleaved Notch-1 successfully (Fig. 5.13 B, p≤ 0.01). Furthermore, Notch-1 was also successfully cleaved by PsenA (p≤ 0.05) and PsenB (p≤ 0.01) when compared to the negative control. It should be noted that the Flag tagged did not interfere with the ability of *D. discoideum* presenilin proteins to cleave Notch-1. These results showed that *D. discoideum* presenilin proteins are able to cleave human Notch-1, thus revealing functional conservation between both *D. discoideum* and human PS1.

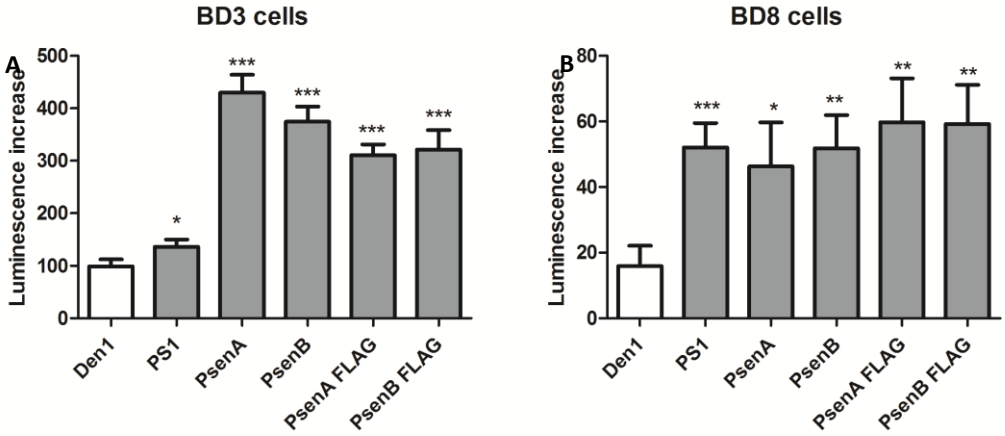

Fig.5.13 Notch-1 cleavage by human and *D. discoideum* presenilin proteins. Presenilin dependant Notch-1 S3 cleavage was assessed by increase in luminescence when compared to the Den1 control (reporter and truncated Notch-1 only), human PS1 and *D. discoideum* presenilin proteins. (A) Human PS1 cleaved Notch-1 (Den1) in BD3 mouse blastocyst cells ($PS1^{+/-}PS2^{-/-}$) as successful as the endogenous mouse PS1. Both tagged and untagged PsenA and PsenB cleaved Notch-1. (B) In BD8 mouse blastocyst cells, PS1 cleaved Notch-1 as well as both Flag tagged and untagged PsenA and PsenB. Values shown are means (±S.E.M; n=3) *** p<0.001; ** p<0.01; *p<0.05.

5.9 Discussion

This chapter investigated whether there is a functional relationship between *D. discoideum* and human PS1. Here it was shown that human PS1-GFP rescues the *psenB⁻/A⁻* developmental phenotype and localises to the same cellular structures as PsenB-GFP. This functional relationship was then independently confirmed by stalk, spore and qPCR assays. Further, analysis of presenilin protein endoproteolysis and developmental assessment of human PS1 with an inactive catalytic site revealed that the role for presenilin proteins in *D. discoideum* development is independent of endoproteolytic cleavage of presenilin proteins. To investigate the reverse relationship, *D. discoideum* presenilin proteins were expressed in mouse blastocysts, where it was shown that the amoeba proteins are capable of cleaving human Notch-1.

5.9.1 Functional relationship and localisation between human *D. discoideum* presenilin proteins

This current study employed human PS1 to rescue the *D. discoideum* developmental phenotype caused by deletion of both presenilin genes. In order to express PS1 in the *D. discoideum psenB⁻/A⁻* mutant, a vector containing full length PS1 was created and into *psenB⁻/A⁻* cells transformed. A development assay of *psenB⁻/A⁻* cells overexpressing PS1-GFP revealed that human presenilin is able to rescue the developmental defect, where mature fruiting bodies with stalks and sori and no gross changes in morphology were observed when compared to wild type fruiting bodies. This work, for the first time, describes that human PS1 is able to rescue *D. discoideum* development in a presenilin null background and suggest a functional relatedness between human and *D. discoideum* presenilin proteins.

Several other groups have attempted to establish a functional relatedness of presenilin throughout kingdoms. The most commonly used presenilin model are mice lacking either one or both presenilin genes (with both alleles deleted) (van Tijn et al., 2011). The deletion of *ps1⁻/⁻* leads to perinatal death, whereas deletion of *ps1⁻/⁻* and *ps2⁻/⁻* leads to lethality at embryonic stages. Both mouse presenilin models can be rescued by introduction of human PS1 (Wang et al.,

2003; Qian et al., 1998). In *C. elegans*, deletion of *sel-12* leads to an egg-laying deficiency through a down regulation of the Notch-1 pathway. Upon introduction of human PS1, this developmental phenotype is rescued, thus showing a functional conservation between the nematode and human presenilin proteins (Levitan et al., 1996). The biomedical model *D. melanogaster* possesses only one presenilin gene and deletion leads to lethality at the larval-pupal transition (Seidner et al., 2006). However, expression of either human PS1 or PS2 did not rescue the phenotype despite relative high conservation between human and *D. melanogaster* presenilin proteins (52% identities) (Seidner et al., 2006). The early land plant *P. patens* which also possesses only one presenilin gene, displays growth and light response defects upon gene deletion and these defects were rescued by introduction of human PS1 (Khandelwal et al., 2007).

When overexpressing human proteins in *D. discoideum*, which genome has a higher adenosine and tyrosine content, an altered codon bias of *D. discoideum* to mammalian genes can lead to a reduction in translation rate (Sharp and Devine, 1989). *D. discoideum* researchers are therefore in favour of synthesising heterologous cDNA using a *D. discoideum* codon bias to ensure expression in this amoeba. For example, modification of the nucleotide sequence of human chorionic gonadotropin for expression in *D. discoideum* leads to 6-8 fold higher expression levels than the non-modified gene (Vervoort et al., 2000). This current study did not adapt this codon bias but yet successfully expressed human PS1-GFP in *D. discoideum* at sufficient levels to rescue the developmental phenotype of *psenB⁻/A⁻* mutant. Expression of human PS1-GFP in *D. discoideum* wild type cells did not alter wild type development, which may suggest that presenilin proteins regulate downstream molecules through an ‘on/off’ effect. Future work could include expression of PS2 in a *D. discoideum* presenilin null background to fully understand functional conservation between human and *D. discoideum* presenilin proteins.

Presenilin protein was shown to localise to the ER and nuclear envelope in higher organisms and *D. discoideum* (Li et al., 1997; Walter et al., 1996; Tekirian et al., 2001). Fluorescence microscopy revealed a common localisation of PsenB-GFP and PS1-GFP to the *D. discoideum* ER and nuclear envelope, supporting a conserved functional role between these proteins. Since PS1

localises to the ER, it may enable analysis of FAD mutations and their effect on localisation and cellular effects. In higher systems, wild type presenilin proteins and their aberrant forms have been linked to ER leak channels and therefore Ca^{2+} dysregulation (Parks and Curtis, 2007; Tu et al., 2006a). Therefore, *D. discoideum* may offer a suitable system to investigate the effect of FAD mutation on Ca^{2+} signalling in the absence of APP or Notch-1 dysregulation. Furthermore, it would be of interest to investigate localisation of PS2 and PsenA *D. discoideum* to further explore the relatedness between these presenilin proteins.

5.9.2 Functional redundancy of *D. discoideum* presenilin

After showing that human PS1-GFP is able to rescue the developmental defect in the *psenB*$^{-}$*/A*$^{-}$ mutant, the reverse relationship was examined. *D. discoideum* does not possess a defined Notch homologue nor have any other endogenous γ-secretase cleavage targets been identified. Because of this, it is highly problematic to assess γ-secretase activity in this model. This proteolytic activity was therefore assessed in a mammalian cell line. *D. discoideum* and human presenilin proteins were expressed in mouse blastocysts lacking either all presenilin genes or all but one *ps1* allele. The assay showed that both human and *D. discoideum* presenilin proteins are capable of functioning within the mammalian γ-secretase complex to cleave Notch-1. This result confirms functional redundancy of presenilin protein activity between *D. discoideum* and humans. Further, this result represents one of the first examples of *D. discoideum* complementing an aberrant phenotype in a mammalian system.

Most biomedical models used in presenilin research possess a Notch-1 homologue (Levitan and Greenwald, 1995; Ye and Fortini, 1998). However, *P. patens* possesses homologues of all γ-secretase subunits (Nicastrin, Aph-1, Pen2) whilst possessing only *one copy of presenilin and lacking a Notch-1 homologue* (Khandelwal et al., 2007). Khandelwal et al. (2007) tried to rescue Notch-1 cleavage in mouse fibroblasts (lacking all presenilin activity) using this highly diverged presenilin protein but found that *P. patens* protein is unable to associate with the mammalian γ-secretase subunits and cleave human Notch-1.

The authors conclude that the *P. patens* presenilin protein cannot perform γ-secretase cleavage events in mouse fibroblasts. The work presented here suggests that, despite the evolutionary distance between *D. discoideum* and humans, *D. discoideum* presenilin proteins are able to integrate into the mammalian γ-secretase complex and perform Notch-1 cleavage.

5.9.3 Stalk and Spore cell analysis

Since deletion of both presenilin genes in *D. discoideum* leads to a severe developmental phenotype with no obvious stalk or spore structures, a more detailed analysis was carried out to establish the role of presenilin proteins in *D. discoideum* development. To do so, stalk cell monolayer assays were performed on wild type, presenilin single and double null mutant strains as well as the rescued strains. Analysis revealed that *psenB*$^-$*/A*$^-$ mutant cells did produce significantly fewer stalk cells when compared to wild type, single presenilin knock-out and rescued strains. The presence of cAMP has been shown to inhibit stalk cell production in wild type cells but allows around 10-20% of all cells to develop into stalk cells. Furthermore, it was shown that *psenB*$^-$*/A*$^-$ cells produce less stalk cells in the presence of cAMP. This suggests that deletion of presenilin genes in *D. discoideum* affects transcription of a gene regulating stalk cell production (*ecmB*) via a Gsk-A regulated pathway (Fig. 1.8) (Schilde et al., 2004). Furthermore, functional redundancy and a compensatory effect of both presenilin proteins were demonstrated in this assay as the PsenB-GFP and PS1-GFP overexpression in the *psenB*$^-$*/A*$^-$ background restored stalk cell production back to single presenilin knock-out and wild type cells levels.

Stalk cell production was as well assessed by McMains et al. (2010), where the authors have shown that deletion of *psenA* (*ps2*) results in a ~55% decrease in spore cell production, whereas deletion of *psenB* (*ps1*) shows no significant reduction in spore cell numbers when compared to wild type cells. Deletion of both presenilin genes leads to a ~50% reduction in spore cells, similar to that observed in their *ps2*$^-$ strain. However, the work here presented shows proof for a compensatory process of both *D. discoideum* presenilin proteins on developmental, stalk and spore cell level.

5.9.4 Developmental gene regulation in presenilin gene mutants

Analysis of *D. discoideum* developmental morphology and cell type specific differentiation of stalks and spore cells of *psenB⁻/A⁻* cells suggest that presenilin proteins play a critical role in multiple signalling pathways involved in *D. discoideum* development. To independently confirm a developmental dysregulation caused by presenilin gene ablation, developmentally regulated gene transcription was analysed by qPCR. Analysis of the early developmental marker (*car1*) revealed a 200% upregulation in *psenB⁻/A⁻* cells throughout development when compared to wild type cells. This early developmental marker is a cAMP surface G-coupled receptor which binds extracellular cAMP causing adenylyl cyclase A (ACA) activation, cAMP production and downstream PKA activation (Loomis, 1998). PKA in turn stimulates *aca* and *car1* transcription and inhibits ERK2 allowing internal cAMP to be hydrolysed by a phosphodiesterase (RegA) which results in a sophisticated feedback loop ensuring adequate response to external cAMP (Fig. 5.14) (Soderbom and Loomis, 1998).

A range of molecular mechanisms for presenilin proteins in *D. discoideum* may explain these observed phenotypes. One possible explanation for the upregulation of *car1* in the presenilin null background might be a compensatory mechanism via PKA. PKA may upregulate *car1* gene transcription as it tries to compensate for the lack of activation or protein levels of downstream signalling molecules such as the cAMP response element-binding protein (CREB/BZPF) or GATA-binding transcription factor (STKA) which is required for spore cell induction (Chang et al., 1996; Huang et al., 2011). Another explanation might be that presenilin proteins are a negative regulator of cAR1 or other signalling molecules of this complex signal relay (Fig. 5.14). Evidence that may support the latter theory is that *psenA* transcription is upregulated at 4h whilst *car1* transcription peaks around the same time and decreases from there onwards, suggesting negative regulatory mechanism between these molecules (Chubb et al., 2006). Further, the increased *car1* transcription levels may cause the streaming deficient phenotype observed in *psenB⁻/A⁻* allowing cells to accumulate in small aggregates with what appears to be smaller cell numbers. In order to unravel the role which presenilin proteins play in *car1* transcriptional

regulation, further analysis needs to be carried out such as cAR1 receptor quantification and immunoprecipitation of *D. discoideum* presenilin.

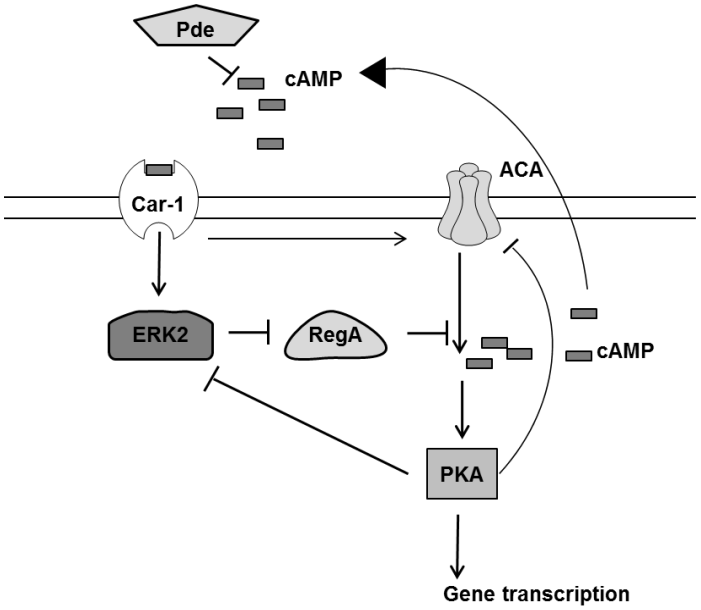

Fig.5.14 Schematic of *D. discoideum* aggregation network and feedback loop. cAMP binds Car1 which in turn activates ACA and ERK2. ACA synthesises cAMP which activates PKA or is excreted to act as a chemoattractant. PKA inhibits ERK2 which allows the phoshodiesterase, RegA, to hydrolyse cAMP preventing PKA activation. Extracellular cAMP is broken down by another phosphodiesterase (Pde) which permits Car-1 to return to its high-affinity state, allowing cAMP binding. This self-regulated circuit allows wavelike aggregation of *D. discoideum* cells. Adapted from Soderbom and Loomis (1998) & Loomis (1998).

Analysis of *ecmA* transcription levels, a marker for stalk cells (mid-development), revealed a highly significant downregulation in *psenB*$^{-}$*/A*$^{-}$ cells, suggesting a role for presenilin proteins in stalk cell formation. Transcription of *psenA* peaks at 12h whilst *ecmA* levels start to increase, which may indicate a positive regulatory role for this presenilin protein in stalk cell production (Chang et al., 1996).

Further, gene transcriptional analysis revealed that presenilin proteins appear to regulate spore cell production since the pre-spore marker was upregulated at 24h in *psenB*$^{-}$*/A*$^{-}$ cells when compared to wild type cells. Transcription of *psA* is a pre-spore marker, is induced at around 12h and is required, in addition of many other genes such as *spiA* and *cotB* for spore cell production (Loomis, 1998). Presenilin proteins may therefore negatively regulate the expression of *psA*.

Gene transcriptional analysis of *psenB⁻/A⁻* overexpressing PsenB-GFP or PS1-GFP revealed that both strains showed a reverse of the increase in *car1* and a decrease in *ecmA* transcription back to wild type levels. Here it was shown that PsenB-GFP was able to restore wild type transcription levels more efficiently than PS1-GFP which may be due some structural differences in the amino acid sequences. Furthermore, analysis of both rescued strains revealed highly significant upregulation in *psA* gene transcription at 12h and *ecmA* gene transcription at 24h in comparison to the wild type and *psenB⁻/A⁻* strain. On the genetic level, these results indicate that presenilin proteins regulate gene transcription of these genes as positive effector at 12h and 24h.

Transcriptional analysis of developmentally regulated genes revealed that presenilin proteins appear to have critical roles in multiple pathways of *D. discoideum* development. However, it should be noted that protein levels and activity should be assessed, as gene transcription does not necessary translate into protein function. Here again, the lack of commercially available antibodies makes analysis on protein level difficult. Furthermore, this qPCR analysis confirmed that PS1-GFP rescued the transcriptional dysregulation in *psenB⁻/A⁻* cells suggesting a functional redundancy for presenilin proteins in *D. discoideum*.

5.9.5 Endoproteolysis of presenilin proteins in *D. discoideum*

In higher organisms, presenilin is cleaved within the intracellular loop with only small amounts of full length presenilin detectable (Haass and De Strooper, 1999). The small amounts of full length PS1 are found mostly in the nuclear envelop, whereas processed PS1 has been associated with the ER (Honda et al., 2000). Presenilin of higher organisms showed cleavage of the intracellular loop giving rise to a ~34kDa amino and ~22kDa carboxyl fragment (Haass and De Strooper, 1999).

To investigate whether presenilin proteins undergo endoproteolysis in *D. discoideum*, Western blot analysis carried out on lysates of *psenB⁻/A⁻* overexpressing PsenB-GFP or PS1-GFP revealed that there is no evidence of endoproteolytic cleavage of either human or *D. discoideum* presenilin proteins

in this model. McMains et al. (2010) have independently shown that *D. discoideum* PsenA is not cleaved, however the importance of this finding was not further discussed in their publication. As the importance of presenilin protein cleavage was demonstrated in higher organisms, these results suggest that the role for presenilin proteins in *D. discoideum* may be γ-secretase independent (Spasic and Annaert, 2008).

Perhaps the best way to further investigate an endoproteolytic-independent function is to examine developmental rescue with a catalytic inactive presenilin protein the function of presenilin proteins in *D. discoideum* development. In mammalian systems, two aspartic acids (257 and 385) are required for cleavage of presenilin protein and proper γ-secretase function (Wolfe et al., 1999). Therefore, PS1 lacking one catalytic aspartic acid was transformed into the *psenB⁻/A⁻* to assess an endoproteolytic independent role for presenilin proteins in *D. discoideum* development. As seen in *psenB⁻/A⁻* cells overexpressing PS1, PS1^{D385A} was able to rescue the developmental phenotype observed in the *psenB⁻/A⁻* mutant. Furthermore, live cell imaging revealed that PS1^{D385A} also localised to the ER and nuclear envelope. These results suggest the role of presenilin proteins in *D. discoideum* does not require endoproteolytic cleavage of presenilin proteins. If by extension to that shown in mammalian systems, this blocks correct formation of the γ-secretase complex, this also suggests that the developmental in *D. discoideum* is independent of γ-secretase activity.

Mutation of either one of these active sites results in loss of γ-secretase, thus disruption in Notch-1 cleavage in mouse fibroblasts and reduction of APP cleavage in mouse neuroblastoma cells (Kim et al., 2001; Kim et al., 2005). However, mature fruiting bodies of *psenB⁻/A⁻* cells overexpressing PS1^{D385A} suggest that development of *D. discoideum* requires presenilin protein but not a γ-secretase catalytic aspartic residue and endoproteolysis. This result is in agreement with a study by Khandelwal et al. (2007) where both human PS1 and PS1^{D385A} were able to rescue the growth phenotype observed in *P. patens* lacking presenilin protein. Thus, the authors come to the conclusion that growth regulation in this organism is a γ-secretase independent function. This current study suggests that the role of presenilin proteins in *D. discoideum* development

may also be a γ-secretase independent function due to the lack of endoproteolytic cleavage and requirement of the catalytic residue. Further, in mammalian γ-secretase complexes, the aspartic acids represent the catalytic core for the cleavage of type I integral membrane proteins which in turn supports a γ-secretase independent function for presenilin proteins in *D. discoideum* development (Haass and De Strooper, 1999; Spasic and Annaert, 2008).

The results of the current study suggest a γ-secretase independent role for presenilin proteins in *D. discoideum* development in contrast to that suggested by McMains et al. (2010). They expressed *D. discoideum* PsenA$^{DD/AA}$ (PS2$^{DD/AA}$) in the developmentally defective *psenA*$^{-}$ (*ps2*$^{-}$) presenilin mutant. Development was not rescued in *psenA*$^{-}$ overexpressing PsenA$^{DD/AA}$ cells, thus the authors concluded that the presenilin function in *D. discoideum* development is γ-secretase dependent. Aspartic acid residues in human PS1 are located at amino acid residues 257 and 385 (Small, 2001), whereas corresponding residues in *D. discoideum* are located at residues 351, 543 (PsenA) and 348, 394 (PsenB). However, McMains et al. (2010) mutated aspartic acid residues 237 and 429 to alanine residues. As these residues do not correspond to aspartic acids, it is unclear if either the wrong amino acids were mutated or if the reporting of the work was incorrect. *D. discoideum* possesses homologues of all subunits required for the γ-secretase complex (Nicastrin, Aph-1 and Pen-2). McMains et al. (2010) showed that this γ-secretase complex cleaved truncated human APP expressed in *D. discoideum* cells. These results suggest that *D. discoideum* possesses γ-secretase dependant proteolytic functions. They also ablated other members of the γ-secretase complex which produced a phenotype similar to the psenB^{-}/A^{-} mutant cell line reported in this thesis. This would suggest that the γ-secretase complex is required for *D. discoideum* development without depending on endoproteolytic cleavage of presenilin proteins.

Chapter 6

After showing that the role of presenilin protein in *D. discoideum* development is independent of endoproteolysis, this chapter presents work to develop a new knock-in method which allows expression of FAD associated mutations in the endogenous *D. discoideum* presenilin gene. In addition, GSK-A, PKA and calcium pathways downstream of presenilin were examined.

6.1 FAD mutation knock in into *D. discoideum* presenilin gene

A new method was developed to knock-in FAD mutations into the endogenous *psenB*. The knock-in method was based on knocking in a blasticidin resistant cassette flanked by a loxP site enabling cassette excision. The knock-in plasmid was generated using pLPBLP where flanking target regions were derived from gDNA, starting from within the intron into the open reading frame of one flanking region with the other flanking region bearing a FAD mutation (Fig. 6.1). A control knock-in plasmid was generated which did not contain a FAD mutation. Integration of the knock-in cassette, followed by a blasticidin resistance cassette excision allows FAD mutation expression from an endogenous presenilin gene.

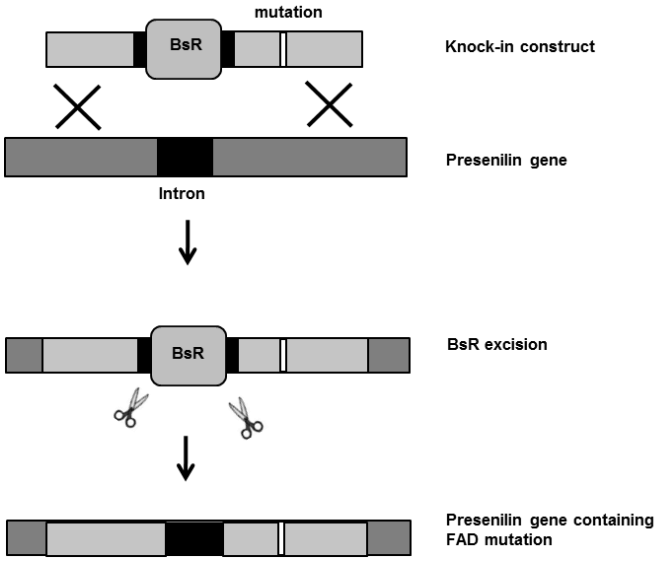

Fig.6.1 Schematic of homologous integration of a knock-in construct bearing a FAD mutation. Two flanking regions were amplified by PCR, where both flanking regions started in the first intron of *psenB* and reaching into the coding region of *psenB*, with the 3' end containing a FAD (L285V). The knock-in construct was digested and transformed into *D. discoideum* cells. Upon homologous integration of the knock-in construct, the blasticidin resistance cassette (BsR) was inserted into the first intron of *psenB*. Excision of the blasticidin resistance cassette allowed endogenous expression of *psenB* bearing a FAD mutation.

Two knock-in constructs were created to test this novel method of knock-in constructs in *D. discoideum*. The first generated knock-in construct did not contain a FAD associated mutation and was transformed as a negative control, whereas the second construct contained a mutation changing leucine to valine which corresponds to the FAD L286V mutation (Furukawa et al., 1998). Transformation of both constructs was performed in a wild type and *psenB*$^{-}$/*A*$^{-}$ background, and transformants growing in the presence of the antibiotic selection were screened by PCR for homologous integration of the knock-in construct (as described in Chapter 3). The frequency of homologous integration events for both knock-in constructs into *psenB* was very low. Despite screening in excess of 1500 transformants, only one homologously integrated transformant was identified (Fig. 6.2). This transformant was from a wild type cell line using the *psenB* control knock-in construct. Subsequently, the blasticidin resistance cassette of this transformant was excised and gDNA/cDNA of *psenB* was sequenced to assess splicing efficiency (Fig. 6.3, A, B). Sequencing of the gDNA revealed the presence of 50 additional nucleotides in the intron that include a translational stop codon and one loxP site consistent

with excision of the blasticidin resistance cassette. Sequence analysis of the derived cDNA showed that the RNA was correctly spliced, despite the 50 additional nucleotides contained in the gDNA.

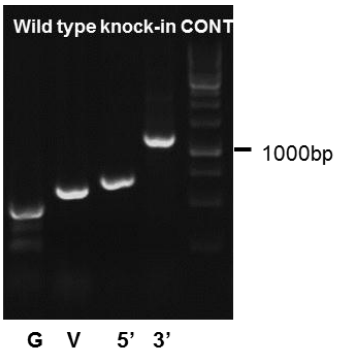

Fig.6.2 PCR identifications of wild type *psenB* knock-in mutant. For the *psenB* control knock-in in a wild type background, 5' and 3' termini were screened for homologous integration with four primer sets (genomic (G) control, vector (V) controls, and 5' and 3' knock-in diagnostic bands).

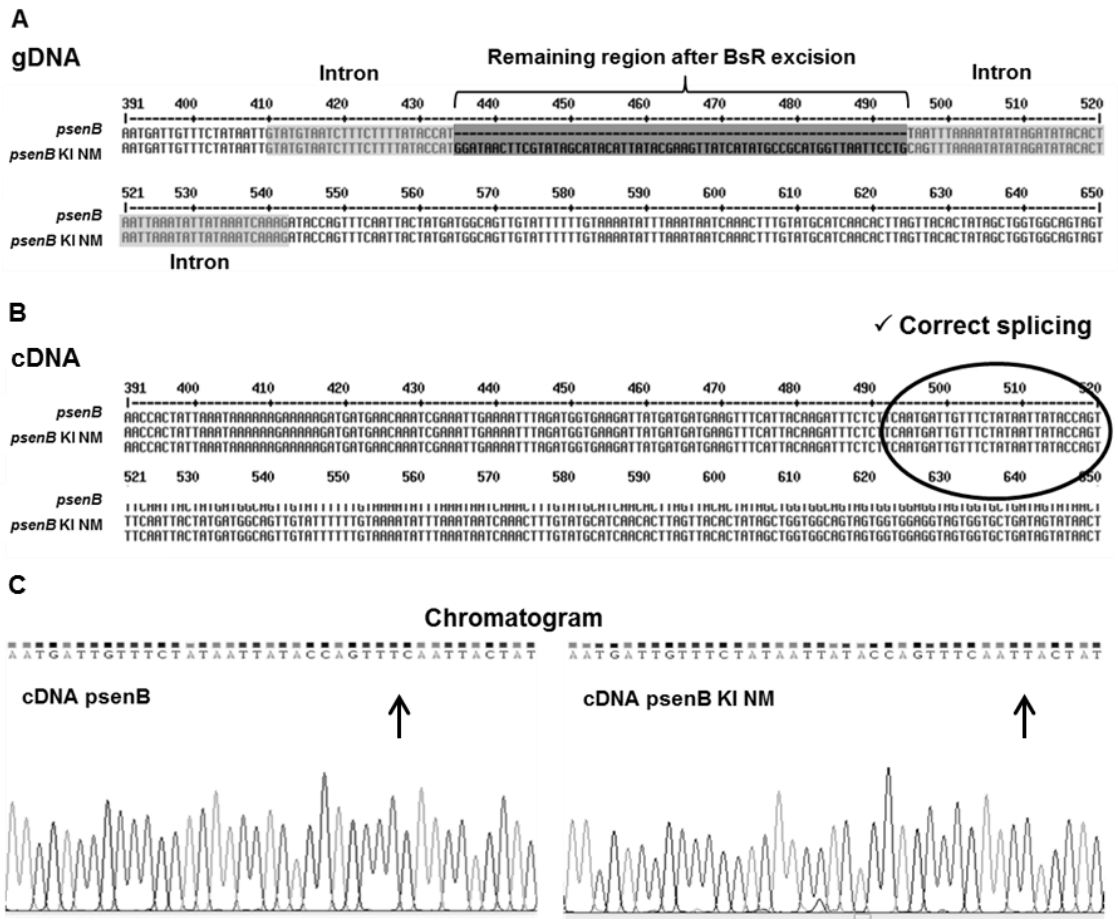

Fig.6.3 *psenB* sequence results of a wild type and control knock-in transformant. (A) Sequence analysis of gDNA from wild type (untransformed) and wild type control knock-in showed that after excision of the blasticidin resistance cassette, 50 additional nucleotides were present in the *psenB* intron. (B) Sequence analysis of cDNA from wild type (untransformed) and wild type control knock-in showed no difference between the two cDNA sources, indicating correct inton excision. (C) The chromatogram of cDNA sequencing reactions shows resolved peaks indicating a high confidence in the sequencing results. Arrows indicate splicing sites.

After confirmation of correct splicing in the wild type cell line containing the negative control *psenB* knock-in construct, development of this transformant was assessed to establish a potential developmental defect caused by this novel knock-in method. To do so, fruiting body morphology was assessed after 24h, revealing that the mutant cells were able to aggregate and form mature fruiting bodies (Fig. 6.4). No gross changes in stalks and sori structures were observed when compared to wild type fruiting body morphology.

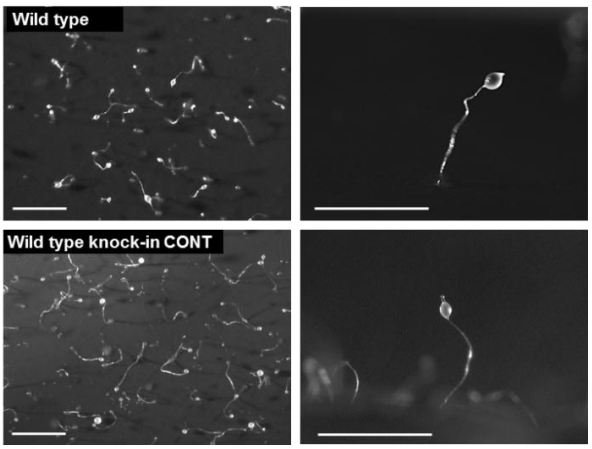

Fig.6.4 Effects of presenilin knock-in on development of *D. discoideum*. Wild type and knock-in control (wild type background with blasticidin resistance cassette removed) cell lines were developed on nitrocellulose filters and fruiting body morphology was assessed. Both cell lines developed mature fruiting bodies within 24h with no gross changes in development; shown from an aerial view at low magnification (left) and from a side angle at high magnification (right). Size bar= 1mm.

6.2 Glycogen synthase kinase as a possible downstream target of *D. discoideum* presenilin proteins

In mammals, PS1 has been shown to interact with and regulate GSK-3β (Chapter 1). The work presented here therefore investigated whether the altered developmental phenotype of *psenB*$^-$*/A*$^-$ mutant cells was caused by a lack of GSK-3β signalling. Therefore, the *D. discoideum* GSK-3β homologue (GSK-A) was expressed from a constitutively active promoter, giving expression in all cell types in *psenB*$^-$*/A*$^-$ mutant cells and development was assessed and compared to that of wild type and *psenB*$^-$*/A*$^-$ cells. *psenB*$^-$*/A*$^-$ overexpressing GSK-A-GFP (provided by Annette Muller-Taubenberger) were not able to form mature fruiting bodies as observed in wild type cells (Fig. 6.5). This result suggests the developmental defect caused by loss of both presenilin genes in *D. discoideum* was not caused by a loss of GSK-A levels.

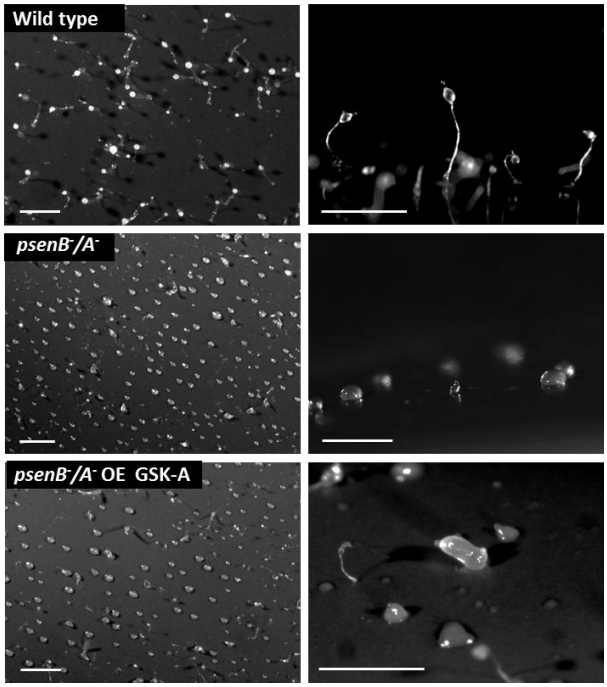

Fig.6.5 Overexpression of GSK-A-GFP in *psenB⁻/A⁻* mutant cells. Wild type, *psenB⁻/A⁻* and *psenB⁻/A⁻* overexpressing GSK-A-GFP were developed on nitrocellulose filters and developmental morphology was assessed after 24h, shown from an aerial view at low magnification (left) and from a side angle at high magnification (right). Overexpression of GSK-A-GFP did not rescue the developmental phenotype observed in *psenB⁻/A⁻* mutant cells. Size bar= 1mm.

6.3 Protein Kinase A as a potential downstream target of *D. discoideum* presenilin proteins

In mammalian systems, PKA regulates GSK-3β with presenilin proteins acting as a scaffold protein (Kang et al., 2002). The work presented here therefore investigated whether the altered developmental phenotype of *psenB⁻/A⁻* mutant cells was caused by a lack of PKA signalling.

To do so, active PKA (catalytic domain) was expressed from vectors under the control of developmental regulated promoters. These promoters, *ecmA* (pre-stalk) and *psA* (pre-spore) were employed to allow cell type specific expression of active PKA. Furthermore, it was shown that expression of a truncated active PKA protein allows a more stable expression in *D. discoideum* (personal communication with Jeff Williams, University of Dundee). Therefore, the study presented here expressed full length as well as truncated active PKA in *psenB⁻/A⁻* mutant cells. Upon transformation of these plasmids, transformants were developed on nitrocellulose filters and fruiting body morphology was assessed

(Fig. 6.6). This analysis revealed that neither full nor truncated length of the active PKA was able to rescue the aberrant developmental phenotype observed in *psenB⁻/A⁻* mutant cells. These results suggest that the developmental defect caused by deletion of both presenilin genes in *D. discoideum* is not caused by an activation of PKA.

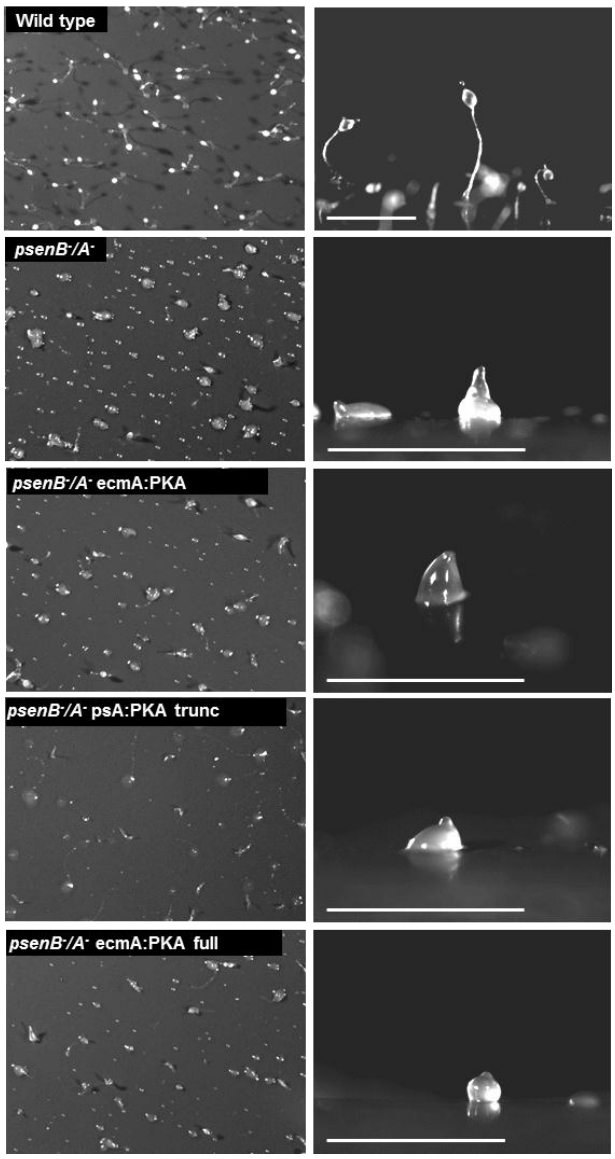

Fig.6.6 Overexpression of the catalytic, active, domain of PKA in *psenB⁻/A⁻* mutant cells. Wild type, *psenB⁻/A⁻*, *psenB⁻/A⁻* ecmA:PKA full length, *psenB⁻/A⁻* psA:PKA full length, *psenB⁻/A⁻* psA:PKA truncated were developed on nitrocellulose filters and fruiting body morphology was assessed. All cell lines expressing PKA cat full or truncated length did form aggregates within 24h but lacked stalk cells and sori when compared to wild type cells. The mutant phenotypes did resemble that seen in *psenB⁻/A⁻* mutant cells. Developmental structures are seen from an aerial view at low magnification (left) and from a side angle at high magnification (right). Size bar= 1mm.

6.4 Calcium homeostasis in presenilin mutants

Presenilin proteins have been associated with calcium homeostasis in mammalian systems (Chapter 1). The work presented here investigates a role for presenilin proteins in calcium signalling regulation in *D. discoideum*. In these experiments, calcium influx upon cAMP stimulation was assessed in single and double presenilin knock-out cell lines. These calcium measurements were carried out by employing the aequorin method which involved transforming a plasmid encoding the calcium sensitive photoprotein apoaequorin (lacking the prosthetic group) into cells. Cytosolic calcium levels were measured in cells, starved in shaking suspension for 7h, loaded with the coelenterazine where a transient increase in luminescence was measured (Allan and Fisher, 2009). Using this approach, calcium response upon cAMP stimulation was recorded and calcium kinetics were assessed in wild type and presenilin knock-out mutants (Fig. 6.7).

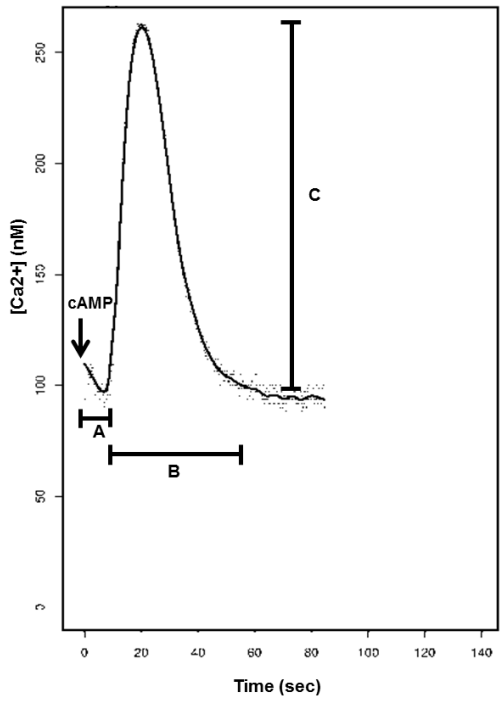

Fig.6.7 Representative graph of a calcium response recording upon cAMP stimulation. In addition to basal calcium level measurements, three other measurements were taken: (A) Length until calcium response after cAMP stimulation; (B) Length of calcium response; (C) Magnitude of calcium response. Recording duration was 90 seconds.

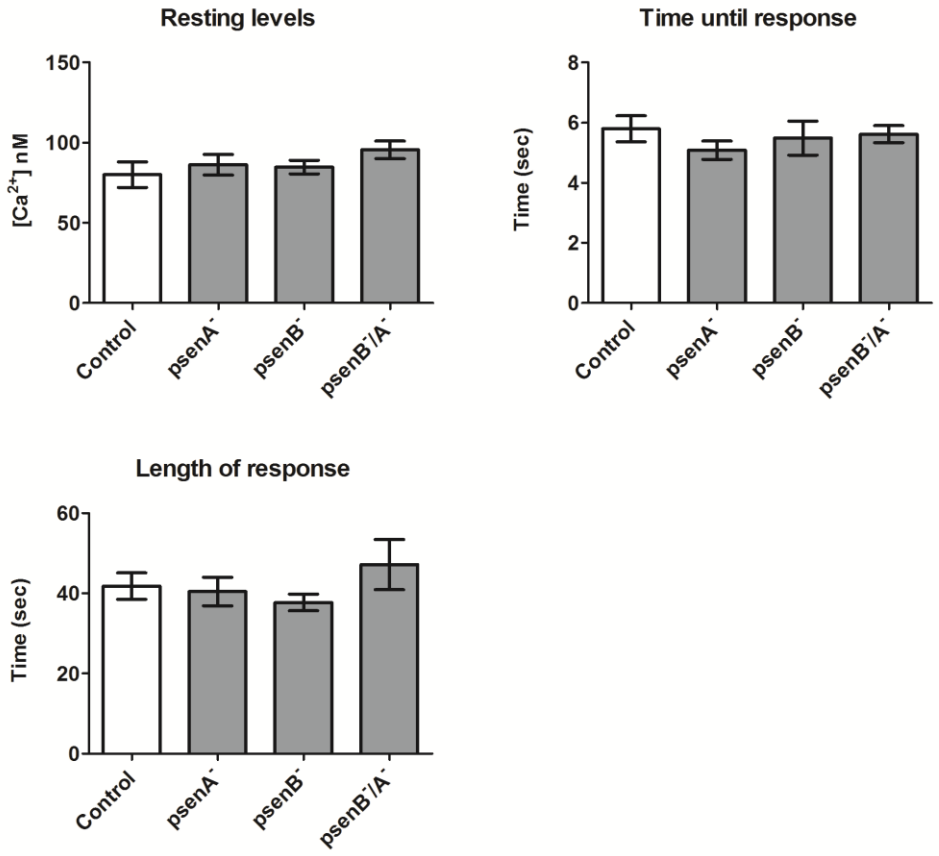

Fig.6.8 Kinetics of calcium responses in wild type and presenilin knock-out cell lines. Resting levels, time until the calcium response and the length of the calcium response were analysed. None of these parameters were significantly different in presenilin mutant cell lines when compared to wild type cell kinetics. Values shown are means (±S.E.M; n≥5). No values were found to be significantly different from wild type controls.

Analysis of the basal calcium levels revealed that presenilin single and double null mutant cell lines do not have altered levels when compared to the wild type cell line (Fig. 6.8). Furthermore, the time from cAMP stimulation until calcium release and the length of the response did not show significant changes in presenilin mutant cell lines when compared to wild type cells (Fig. 6.8). However, the magnitude of the cAMP induced calcium response was elevated in the single as well as the double presenilin knock-out cell lines when compared to that of wild type cells (Fig. 6.9). In these experiments, the *psenA*$^-$ mutant showed a 2 fold ($p < 0.05$) increase in the calcium response when compared to the wild type cell line. Analysis of the calcium kinetics in *psenB*$^-$ and *psenB*$^-$*/A*$^-$ mutant cell lines showed a 2 - 2.5 fold increase ($p < 0.01$) in the

magnitude of the calcium response. These results suggest a role for presenilin proteins in *D. discoideum* signal-induced calcium homeostasis.

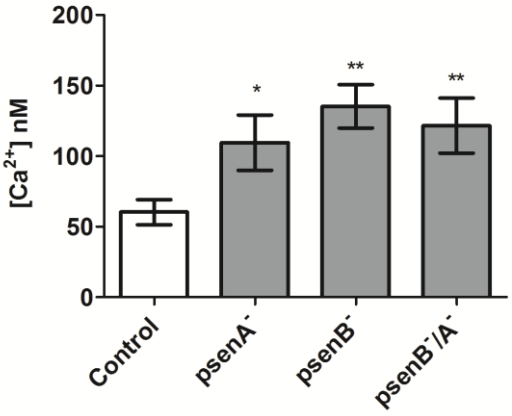

Fig.6.9 Magnitude of cAMP induced calcium response in wild type and presenilin mutant cell lines. The magnitude of calcium response is significantly upregulated in *psenA*$^-$, *psenB*$^-$ and *psenB*$^-$/*A*$^-$ cell lines when compared to wild type levels. Values shown are means (±S.E.M; n≥5) *** p<0.001; ** p<0.01; *p<0.05.

6.5 Discussion

This chapter described the development of a novel knock-in method in *D. discoideum* exemplified by *psenB* and the analysis of a role for presenilin proteins in regulating GSK-A, PKA and calcium signalling pathways in *D. discoideum*.

6.5.1 Endogenous FAD mutation expression in *D. discoideum*

A goal of biomedical research in biomedical systems is to better understand human diseases. In FAD, research would involve the characterisation of FAD-inducing mutations and the effects on signalling pathways in *D. discoideum*. Expression of these mutations could be achieved through overexpression from a constitutively active promoter or integration into the endogenous presenilin gene locus, thus allowing endogenous expression of the mutation.

The regions of high conservation of *D. discoideum* and human presenilin proteins enable the engineering of FAD mutations into the endogenous presenilin genes of *D. discoideum*. To do so, two knock-in constructs were designed which allowed integration into *psenB* without altering the coding or intergenic regions adjacent to the gene. Insertion of the blasticidin resistance cassette into the first intron of *psenB* upon homologous integration ensured intact gene transcription and splicing following blasticidin resistance gene excision using Cre recombinase. The lack of homologous integration events prevented an analysis of an endogenous expressed FAD mutation (L286V) (Furukawa et al., 1998). Nevertheless, one wild type cell line containing the control knock-in construct was generated, showing that this novel knock-in method does not cause altered cDNA sequences in *D. discoideum*.

In *D. discoideum,* regularly employed knock-in methods involve insertion of the antibiotic resistant selection cassette into downstream intergenic regions as shown in the RacB mutants produced by Park et al. (2004). In other model organisms, FAD mutations are regularly expressed under a constitutively active promoter (actin 15) or under the endogenous presenilin promoter as shown in *D. melanogaster* (Seidner et al., 2006; Tu et al., 2006a). The endogenous

promoters of *psenA* and *psenB* have not been defined which currently prevents expression of these genes under an endogenous promoter control from a non-integrating vector, such as the pDM vector series (Veltman et al., 2009). However, since the present study showed that human PS1 is able to rescue the developmental phenotype of *psenB⁻/A⁻*, it is feasible to express human PS1 bearing FAD mutations in *psenB⁻/A⁻* mutant cells, allowing analysis of biochemical changes caused by these mutations.

This method prevents phenotypic changes due to overexpression of proteins at toxic levels. Furthermore, despite the drawback of a low frequency of homologous integration into *psenB*, this novel method opens new ways of expressing endogenous proteins containing mutations or proteins tags in *D. discoideum*.

6.5.2 Glycogen synthase kinase regulation through presenilin proteins in *D. discoideum*

GSK-3β is a serine/threonine kinase that phosphorylates a multitude of downstream targets such as the cyclic AMP responsive binding element (CREB) and tau which can lead to tau tangle formation as observed in AD (Wang et al., 2010; Rankin et al., 2007). In mammalian systems, it was proposed that presenilin may interact with GSK-3β as a scaffold independent of γ-secretase function (Martinez, 2010). The work presented here, investigated whether GSK-A acts downstream of presenilin proteins in *D. discoideum* and whether it can rescue the aberrant developmental phenotype observed in *psenB⁻/A⁻* by constitutively expressing GSK-A-GFP. Developmental assessment of *psenB⁻/A⁻* cells overexpressing GSK-A-GFP showed that the phenotype was not rescued, thus further work will be required to establish whether GSK-A acts downstream of presenilin proteins in *D. discoideum*.

In humans, presenilin proteins directly interact with GSK-3β affecting several downstream signalling pathways including tau and β-catenin (Takashima et al., 1998). *D. discoideum* does not possess a tau homologue but a β-catenin homologue and a Wnt-like pathway has been proposed in this amoeba (Sun and Kim, 2011). In *D. discoideum*, inhibition of GSK-A is required for cells to

undergo stalk cell differentiation (Schilde et al., 2004). However, it is still unknown whether GSK-A is inactivated via phosphorylation or through removal from the nucleus where it controls *ecmB* transcription and therefore stalk cell production. It was shown that cAMP binding to cAR3 results in increased GSK-A activity (substrate phosphorylation) resulting in an increased inhibition of stalk cell production (Plyte et al., 1999). Therefore, deletion of cAR3 or GSK-A leads to in increased proportion of stalk cells, confirming a common signalling pathway for these molecules. Furthermore, overexpression of GSK-A in wild type background does not alter development nor stalk cell production, suggesting a tight control of the GSK-A pathway by other signalling molecules where *D. discoideum* presenilin proteins may play a role as previously suggested in mammalian systems (De Strooper and Annaert, 2001). To confirm an interaction between *D. discoideum* presenilin proteins and GSK-A, immunoprecipitation of PsenA and PsenB may show direct binding to GSK-A. Furthermore, identification of altered GSK-A phosphorylation and kinase activity could be performed in *psenB*$^-$*/A*$^-$ mutant cells to further identify a signalling interaction (Ryves et al., 1998; Plyte et al., 1999).

6.5.3 Protein kinase A regulation through presenilin proteins in *D. discoideum*

PKA is a holoprotein which consists of a regulatory and a catalytic subunit. Upon cAMP binding to the regulatory subunit, the catalytic subunit is released which in turn regulates downstream signalling such as CREB (Beglopoulos and Shen, 2006). Activated PKA is a key signalling molecule in *D. discoideum* development and required for spore cell production (Escalante and Vicente, 2000). Therefore, in a collaboration with Pauline Schaap and Christina Schilde (University of Dundee) analysed intracellular cAMP levels in wild type, *psenB*$^-$*/A*$^-$ *psenB*$^-$*/A*$^-$ overexpressing PsenB-GFP and *psenB*$^-$*/A*$^-$ overexpressing PS1-GFP. These experiments identified a ~3 fold increase ($p \leq 0.005$) in cytosolic cAMP in the *psenB*$^-$*/A*$^-$ mutant cells at 8h into development when compared to wild type cells (Fig. 6.10). PsenB-GFP restored cAMP levels back to wild type levels in *psenB*$^-$*/A*$^-$ cells, whereas PS1-GFP only partially restored this level. The increase in cytosolic cAMP would suggest an increased PKA activity and thus

elevated spore cell production as observed in the *regA*$^-$ (phosphodiesterase) mutants where elevated cAMP levels led to precocious development and spore production (Thomason et al., 1999b). However, as previously shown *psenB*$^-$*/A*$^-$ mutant cells did not show an accelerated development nor increased spore cells production. These data imply that the activation of PKA activity may be inhibited in *psenB*$^-$*/A*$^-$ cells. Therefore, active PKA was expressed in *psenB*$^-$*/A*$^-$ mutant cells under developmentally regulated promoters. Developmental assessment of active PKA transformants showed that the altered phenotype of *psenB*$^-$*/A*$^-$ mutant cells was not rescued.

In mammals, presenilin proteins have been shown to interact with PKA and GSK-3β as a scaffold protein providing structural support rather than a catalytic γ-secretase function (Kang et al., 2002). Presenilin proteins positively regulate CREB via PKA which has been associated with memory formation and neuronal survival in mammals (Beglopoulos and Shen, 2006). *D. discoideum* possesses a CREB-like transcription factor (BzpF) that binds a cAMP response element homologue that acts downstream of PKA and *bzpf*$^-$ mutant displays a delayed development with aberrant spore structures (Huang et al., 2011). Future work may include expressing the CREB-like protein in the *psenB*$^-$*/A*$^-$ mutant to assess whether the aberrant developmental phenotype can be rescued using this approach to establish a common signalling pathway. It should be noted that PKA is localised in the cytosol as well as nucleus (Woffendin et al., 1986). Therefore, considering that presenilin proteins are found to localise not only to the ER but also to the nuclear envelope, a role for presenilin in the shuttling of PKA into the nucleus may be investigated. This could be achieved through localisation studies of PKA in *psenB*$^-$*/A*$^-$ and wild type cells. Further experiments are required to establish if presenilin proteins have a role in PKA regulation in *D. discoideum*.

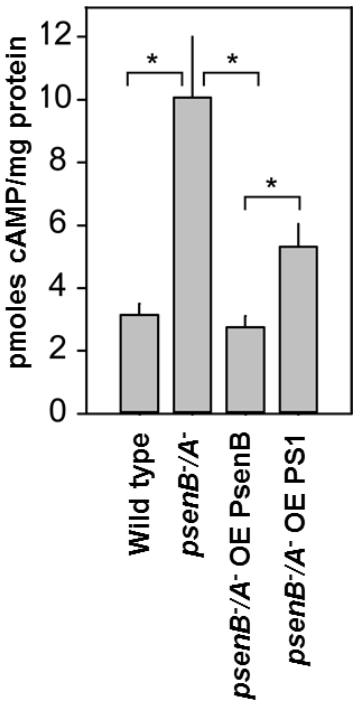

Fig.6.10 cAMP levels in wild type, *psenB*$^{-}$*/A*$^{-}$, *psenB*$^{-}$*/A*$^{-}$ overexpressing PsenB-GFP or overexpressing PS1-GFP. Bars connected by lines represent data sets that were significantly different from each other at P<0.005. Unlinked sets were not significantly different at P<0.05. Values are shown are means (±S.E.M; n=5; technical triplicate).

6.5.4 A role for presenilin in *D. discoideum* calcium signalling

Calcium is involved in many signalling pathways such as CREB and protein kinase C signalling and neuronal calcium dysregulation contributes to the biochemical alterations observed in debilitating diseases such as AD (Marambaud et al., 2009). Presenilin proteins have been proposed to regulate calcium homeostasis in mammalian systems (Chapter 1), which led to the work carried out here, where calcium measurements were performed in *D. discoideum* presenilin protein mutant strains. Analysis of the generated strains revealed that calcium influx into the cytosol upon cAMP stimulation was significantly elevated in presenilin mutant strains, suggesting an inhibitory role for presenilin proteins in *D. discoideum* signal-induced calcium homeostasis.

In recent years, the calcium leak hypothesis has been a favoured model for the role of presenilin proteins in calcium dysregulation observed in FAD. It was suggested that presenilin proteins regulate calcium stores through forming calcium leak channels, independent of γ-secretase, and that deletion of

presenilin proteins or introduction of FAD mutations lead to an overload of these stores which resulted in an increased calcium response upon stimulation (Tu et al., 2006a). However, one recent commentary suggests that there is insufficient evidence for presenilin proteins forming leak channels (Shilling et al., 2012). Another hypothesis has been proposed, where presenilin proteins directly interact with the IP_3 receptor leading to altered receptor gating, resulting in elevated calcium responses in the presence of FAD mutations (Cheung et al., 2008). Calcium dysregulation in *D. discoideum* presenilin null mutants supports a negative regulatory role for presenilin proteins in calcium homeostasis and potentially an IP_3 receptor interaction. *D. discoideum* possess a homologue of IP_3 receptor (IPLA) which is situated at the ER and the localisation of presenilin proteins to the ER in *D. discoideum* provides evidence for an interaction. However, in order to support an interaction between presenilin proteins and IPLA, an immunoprecipitation experiment would also need to be performed. Nevertheless, the data gathered in *D. discoideum* presenilin mutants and evidence from mammalian systems supports the hypothesis that presenilin proteins negatively regulate calcium homeostasis.

Since this work presented here provides evidence supporting previous reports from mammalian systems that presenilin proteins play a role in calcium homeostasis, *D. discoideum* offers a novel system to further investigate this hypothesis. Furthermore, since reports have shown that calcium dysregulation leads to neuronal death in AD and FAD, *D. discoideum* offers a novel drug screen system to identify compounds that reverse calcium dysregulation.

Conclusion

Structure and phylogeny of presenilin proteins in *D. discoideum*

Presenilin proteins are conserved in a multitude of organisms, ranging from human to *A. thaliana*. *D. discoideum* possesses two presenilin protein homologues which contain regions of high homology to human presenilin proteins. These regions are predominantly found in transmembrane regions, which include two aspartic acid residues and the 'PAL' sequence that are required for proper γ-secretase function in mammalian systems. The conservation throughout evolution in many organisms and expression in development and adulthood suggests a critical role for presenilin proteins in survival of the organism.

Presenilin proteins regulate development in *D. discoideum*

Presenilin proteins have been shown to regulate many signalling pathways in multicellular organisms (van Tijn et al., 2011). Specifically, a role for presenilin proteins has been proposed in Notch signalling leading to lethal developmental abnormalities in several biomedical models such as *M. musculus* and *C. elegans* (Woo et al., 2009). The work presented here investigated a role for presenilin proteins in *D. discoideum* development. As observed in other model organisms, deletion of both presenilin proteins led to a severe developmental phenotype in *D. discoideum* which was not observed in cell lines lacking only one presenilin gene. This suggested a compensatory mechanism in which PsenA can compensate for PsenB and vice versa despite differing gene transcription throughout development. The hypothesis of a compensatory mechanism was confirmed by the rescue of the developmental phenotype observed in *psenB⁻/A⁻* cells overexpressing PsenB-GFP. Furthermore, stalk cell and spore cell assays, where deletion of both presenilin genes resulted in a downregulation of specific cell type differentiation, supported an underlying compensatory mechanism of both presenilin proteins in *D. discoideum* (Chapter

5). These findings mirror those observed in *C. elegans* where deletion of a single presenilin gene led to a milder phenotype than the more severe phenotype upon deletion of both presenilin genes (Westlund et al., 1999). The work presented here showed that presenilin proteins play a regulatory role in *D. discoideum* as development is severely altered upon deletion of both presenilin genes.

Conserved function of *D. discoideum* and human presenilin proteins

The development of the *D. discoideum* cell line lacking both presenilin genes was rescued by overexpression of human PS1-GFP, similar to the growth phenotype rescue observed in *P. patens* when complemented with human PS1 (Khandelwal et al., 2007). Despite evolutionary distance, expression of PS1-GFP allowed development of mature fruiting bodies in the absence of endogenous presenilin proteins in *D. discoideum*. Not only was the developmental rescue shown through fruiting body morphology but also by employing stalk, spore cell and gene transcription analysis (Chapter 5). However, the overall rescue with PS1-GFP was not as efficient as observed when overexpressing PsenB-GFP. This may be due to differences in amino acid sequence of presenilin proteins of human and *D. discoideum*.

Since human PS1 rescues *D. discoideum* development, this amoeba offers a novel system to analyse interacting partners and identify novel presenilin-regulated signalling pathways. Furthermore, the effects of PS1 containing FAD mutations can be readily assessed in this model in isogenic cell lines produced without the need of continuous transfection or animal usage.

Presenilin proteins have a role in calcium signalling of *D. discoideum*

In higher organisms, presenilin proteins regulate calcium homeostasis and expression of FAD mutations leads to an increased influx into the cytosol from calcium stores (Tu et al., 2006a; Cheung et al., 2008). Analysis of *D.*

discoideum revealed that deletion of either presenilin protein led to an increased calcium influx into the cytosol upon cAMP stimulation. Since these results mirror results obtained in higher organisms, three possible hypotheses of the role or roles of presenilin proteins in *D. discoideum* can be proposed (Fig. 7.1): (1) Interaction of presenilin with the IP_3 receptor may negatively regulate calcium release upon IP_3 binding, thus leading to a higher influx of calcium into the cytosol upon presenilin protein deletion. (2) Presenilin proteins may form passive calcium leak channels which lead to an intracellular calcium store overload, which in turn upon cAMP stimulation results in a greater calcium influx from stores into the cytosol. (3) Gene transcriptional analysis revealed that *car1* was significantly upregulated in *psenB*$^-$*/A*$^-$ cells. Assuming that the mRNA was translated into proteins, more cAR1 would be present on the cell membrane leading to activity of phospholipase C, using PIP_2 to produce more diacylglycerol and IP_3 which then causes binding to the IP_3 receptor and calcium release. However, this hypothesis does not involve presenilin proteins directly but instead a compensatory transcriptional upregulation of *car1* upon presenilin deletion.

Whether all, one or none of these mechanisms can be attributed to presenilin proteins in *D. discoideum* is yet to be answered. Nevertheless, *D. discoideum* may provide a model to further investigate the calcium store overloading hypothesis reported in AD and FAD as well as the effects of human PS1 bearing FAD mutations on calcium homeostasis as part of a translational biology study.

Role of presenilin proteins in development is endoproteolytic independent

In higher organisms, presenilin proteins require endoproteolysis, in order to integrate into the γ-secretase complex (Haass and De Strooper, 1999). Western blot analysis of PsenB-GFP and PS1-GFP showed that neither of these proteins were cleaved in *D. discoideum* unlike in mammalian systems, where only small amounts of full length protein can be found (Honda et al., 2000). To support these findings, human PS1-GFP lacking a catalytic site and unable to undergo

endoproteolytic cleavage was expressed in the *psenB⁻/A⁻* mutant cells. Developmental studies showed that this altered protein rescued the developmental phenotype. These findings revealed that presenilin proteins are not required to undergo endoproteolysis in order to function in *D. discoideum* development.

To assess whether the reverse relationship between *D. discoideum* and human presenilin proteins is true, a Notch cleavage assay was performed in mouse blastocysts using *D. discoideum* presenilin proteins. Here it was shown, that both *D. discoideum* presenilin proteins were capable of cleaving human Notch expressed in mouse blastocysts. This work presented here showed that human and *D. discoideum* presenilin proteins have common cellular functions, as predicted in the bioinformatic analysis (Chapter 3).

Since the role for *D. discoideum* presenilin was demonstrated to be independent of endoproteolytic cleavage of presenilin proteins, it is unclear if this ancient homologue is capable of a γ-secretase assembly. No endogenous proteolytic target has been identified by McMains et al. (2010) but the authors have shown that *D. discoideum* presenilin proteins are capable of cleaving human APP, suggesting a γ-secretase cleavage function. It is possible that the γ-secretase function in *D. discoideum* does not require endoproteolytic cleavage of presenilin proteins in order to function.

Presenilin proteins may act as a scaffold protein in *D. discoideum* development

The aberrant developmental phenotype observed in the *psenB⁻/A⁻* mutant lacked all stalk and spore head structures found in mature wild type fruiting bodies. GSK-A, cAMP and PKA are the major signalling molecules involved in stalk and spore cell production which initiated the analysis of these pathways.

The data provided by Pauline Schaap and Christina Schilde showed that intracellular cAMP levels were significantly raised in *psenB⁻/A⁻* cells at 8h into development, which would suggest an increase in PKA activity and early spore production as observed in *regA⁻* cells (Thomason et al., 1999b). However, the

lack of a precocious development of *psenB*$^{-}$*/A*$^{-}$ cells suggests that presenilin gene deletion may reduce PKA activation and that the elevated cAMP levels may be a compensatory mechanism. This compensation may be regulated through an upregulation of *car1* transcription level in the early stages of development (6h-12h). A role for reduced PKA activation in the presenilin double null mutant was investigated by overexpressing the activated form of PKA (catalytic domain). This did not rescue the developmental phenotype (Chapter 6).

In mammalian systems, presenilin proteins interact with GSK-3β as a scaffold protein, facilitating activation and/or phosphorylation of downstream targets (Martinez, 2010). Therefore, the aberrant developmental phenotype of *psenB*$^{-}$*/A*$^{-}$ cells may have arisen through decreased GSK-A activity or target phosphorylation. Overexpression of GSK-A in these cells did not rescue the altered phenotype, thus suggesting that deletion of presenilin proteins does not downregulate the levels of GSK-A. In mammalian systems, GSK-3β has been shown to be phosphorylated and therefore inhibited by PKA in a complex where presenilin proteins have a scaffold function independent of γ-secretase activity (Fang et al., 2000; Doble and Woodgett, 2003). If presenilin proteins in *D. discoideum* development act as a scaffold protein to GSK-A and PKA, overexpression of GSK-A and PKA (activated protein) would not rescue the aberrant phenotype. This is due to the lack of presenilin proteins and their scaffold function *psenB*$^{-}$*/A*$^{-}$ cells, preventing inhibition of GSK-A activity by PKA, thus preventing stalk cell production.

Furthermore, this lack of scaffold function may also interfere with the activation or downstream signalling of PKA in spore cell production (Fig. 7.1). In order to support this hypothesis, presenilin protein, PKA and GSK-A immunoprecipitation, PKA and GSK-A phosphorylation assays and specific kinase activity assays need to be performed in single and double presenilin null mutants and complemented presenilin protein cell lines.

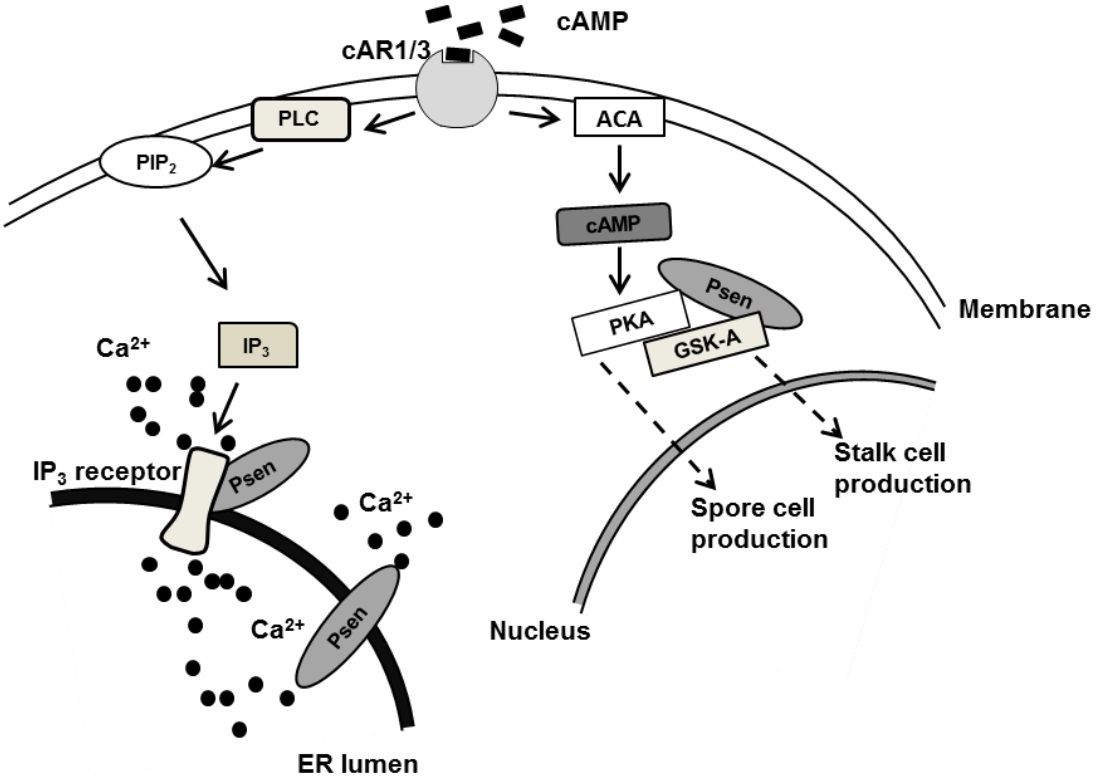

Fig.7.1 Schematic diagram of proposed cellular roles for presenilin proteins in *D. discoideum*. cAMP binding to cAR1/3 activates phospholipase C (PLC) and adenylate cyclase (ACA), allowing PIP_2 and cAMP production which regulates several downstream targets. The role for presenilin proteins in calcium homeostasis could be regulated through three functions: Presenilin proteins regulate negatively the IP_3 receptor; presenilin proteins form calcium leak channels; presenilin regulates *car1* transcription and therefore calcium release. The role for presenilin proteins in *D. discoideum* development could be a structural scaffold function through which it regulates PKA, GSK and therefore stalk and spore production.

D. discoideum could provide a greater insight into presenilin protein signalling and familial Alzheimer's disease

Microorganisms such as *Escherichia coli* and *Saccharomyces cerevisiae* have provided a great insight into the molecular basis of a multitude of signalling molecules, cell cycle regulation, immune cell function and dysregulation in human disease. The importance of biological research using simple model organisms and translational biology has been acknowledged by the wide scientific community, as microorganisms are featured in Nobel prizes almost every year since 2001 (except 2004 and 2010). All living organisms originate from one common ancestor with molecular and cellular functions often being conserved throughout evolution. Studies in microorganisms and biomedical

models provided great insights into underlying mechanisms of human disease as for example employing *C. elegans* provided a first link between presenilin protein and Notch (Levitan and Greenwald, 1995). Therefore, the evidence reported here for conservation of presenilin protein functions in *D. discoideum* may open new research avenues for investigations into presenilin protein function and FAD related signalling.

References

Adley,K.E., Keim,M., and Williams,R.S. (2006). Pharmacogenetics: defining the genetic basis of drug action and inositol trisphosphate analysis. Methods Mol. Biol. *346*, 517-534.

Allan,C.Y. and Fisher,P.R. (2009). In vivo measurements of cytosolic calcium in Dictyostelium discoideum. Methods Mol. Biol. *571*, 291-308.

Altschul,S.F., Gish,W., Miller,W., Myers,E.W., and Lipman,D.J. (1990). Basic local alignment search tool. J. Mol. Biol. *215*, 403-410.

Alzheimer, A. Über eine eigenartige Erkrankung der Hirnrinde. [64. Band]. 1907. Allgemeine Zeitschrift für Psychiatrie und psychisch-gerichtliche Medizin, Verlag von Georg Reimer.
Ref Type: Generic

Annesley,S.J. and Fisher,P.R. (2009). Dictyostelium discoideum--a model for many reasons. Mol. Cell Biochem. *329*, 73-91.

Arduengo,P.M., Appleberry,O.K., Chuang,P., and L'Hernault,S.W. (1998). The presenilin protein family member SPE-4 localizes to an ER/Golgi derived organelle and is required for proper cytoplasmic partitioning during Caenorhabditis elegans spermatogenesis. J. Cell Sci. *111 (Pt 24)*, 3645-3654.

Aubry,L. and Firtel,R. (1999). Integration of signaling networks that regulate Dictyostelium differentiation. Annu. Rev. Cell Dev. Biol. *15*, 469-517.

Bapteste,E., Brinkmann,H., Lee,J.A., Moore,D.V., Sensen,C.W., Gordon,P., Durufle,L., Gaasterland,T., Lopez,P., Muller,M., and Philippe,H. (2002). The analysis of 100 genes supports the grouping of three highly divergent amoebae: Dictyostelium, Entamoeba, and Mastigamoeba. Proc. Natl. Acad. Sci. U. S. A *99*, 1414-1419.

Beglopoulos,V. and Shen,J. (2006). Regulation of CRE-dependent transcription by presenilins: prospects for therapy of Alzheimer's disease. Trends Pharmacol. Sci. *27*, 33-40.

Berezovska,O., Xia,M.Q., and Hyman,B.T. (1998). Notch is expressed in adult brain, is coexpressed with presenilin-1, and is altered in Alzheimer disease. J. Neuropathol. Exp. Neurol. *57*, 738-745.

Bertram,L., Lill,C.M., and Tanzi,R.E. (2010). The genetics of Alzheimer disease: back to the future. Neuron *68*, 270-281.

Boonen,R.A., van,T.P., and Zivkovic,D. (2009). Wnt signaling in Alzheimer's disease: up or down, that is the question. Ageing Res. Rev. *8*, 71-82.

Bozzaro,S. and Ponte,E. (1995). Cell adhesion in the life cycle of Dictyostelium. Experientia *51*, 1175-1188.

Briscoe,C. and Firtel,R.A. (1995). Intercellular signaling. A kinase for cell-fate determination? Curr. Biol. *5*, 228-231.

Brookmeyer,R., Johnson,E., Ziegler-Graham,K., and Arrighi,H.M. (2007). Forecasting the global burden of Alzheimer's disease. Alzheimers. Dement. *3*, 186-191.

Casley,C.S., Canevari,L., Land,J.M., Clark,J.B., and Sharpe,M.A. (2002). Beta-amyloid inhibits integrated mitochondrial respiration and key enzyme activities. J. Neurochem. *80*, 91-100.

Chang,P., Orabi,B., Deranieh,R.M., Dham,M., Hoeller,O., Shimshoni,J.A., Yagen,B., Bialer,M., Greenberg,M.L., Walker,M.C., and Williams,R.S. (2012). The antiepileptic drug valproic acid and other medium-chain fatty acids acutely reduce phosphoinositide levels independently of inositol in Dictyostelium. Dis. Model. Mech. *5*, 115-124.

Chang,W.T., Newell,P.C., and Gross,J.D. (1996). Identification of the cell fate gene stalky in Dictyostelium. Cell *87*, 471-481.

Chenna,R., Sugawara,H., Koike,T., Lopez,R., Gibson,T.J., Higgins,D.G., and Thompson,J.D. (2003). Multiple sequence alignment with the Clustal series of programs. Nucleic Acids Res. *31*, 3497-3500.

Cheung,K.H., Shineman,D., Muller,M., Cardenas,C., Mei,L., Yang,J., Tomita,T., Iwatsubo,T., Lee,V.M., and Foskett,J.K. (2008). Mechanism of Ca2+ disruption in Alzheimer's disease by presenilin regulation of InsP3 receptor channel gating. Neuron *58*, 871-883.

Chisholm,R.L., Gaudet,P., Just,E.M., Pilcher,K.E., Fey,P., Merchant,S.N., and Kibbe,W.A. (2006). dictyBase, the model organism database for Dictyostelium discoideum. Nucleic Acids Res. *34*, D423-D427.

Chubb,J.R., Bloomfield,G., Xu,Q., Kaller,M., Ivens,A., Skelton,J., Turner,B.M., Nellen,W., Shaulsky,G., Kay,R.R., Bickmore,W.A., and Singer,R.H. (2006). Developmental timing in Dictyostelium is regulated by the Set1 histone methyltransferase. Dev. Biol. *292*, 519-532.

Cruts,M. and Van,B.C. (1998). Presenilin mutations in Alzheimer's disease. Hum. Mutat. *11*, 183-190.

Cserzo,M., Eisenhaber,F., Eisenhaber,B., and Simon,I. (2002). On filtering false positive transmembrane protein predictions. Protein Eng *15*, 745-752.

De Strooper,B. (2003). Aph-1, Pen-2, and Nicastrin with Presenilin generate an active gamma-Secretase complex. Neuron *38*, 9-12.

De Strooper,B. and Annaert,W. (2001). Where Notch and Wnt signaling meet. The presenilin hub. J. Cell Biol. *152*, F17-F20.

De Strooper,B. and Annaert,W. (2010). Novel research horizons for presenilins and gamma-secretases in cell biology and disease. Annu. Rev. Cell Dev. Biol. *26*, 235-260.

Delrieu,J., Ousset,P.J., Caillaud,C., and Vellas,B. (2012). 'Clinical trials in Alzheimer's disease': immunotherapy approaches. J. Neurochem. *120 Suppl 1*, 186-193.

Doble,B.W. and Woodgett,J.R. (2003). GSK-3: tricks of the trade for a multi-tasking kinase. J. Cell Sci. *116*, 1175-1186.

Donoviel,D.B., Hadjantonakis,A.K., Ikeda,M., Zheng,H., Hyslop,P.S., and Bernstein,A. (1999). Mice lacking both presenilin genes exhibit early embryonic patterning defects. Genes Dev. *13*, 2801-2810.

Eichinger,L., Pachebat,J.A., Glockner,G., Rajandream,M.A., Sucgang,R., Berriman,M., Song,J., Olsen,R., Szafranski,K., Xu,Q., Tunggal,B., Kummerfeld,S., Madera,M., Konfortov,B.A., Rivero,F., Bankier,A.T., Lehmann,R., Hamlin,N., Davies,R., Gaudet,P., Fey,P., Pilcher,K., Chen,G., Saunders,D., Sodergren,E., Davis,P., Kerhornou,A., Nie,X., Hall,N., Anjard,C., Hemphill,L., Bason,N., Farbrother,P., Desany,B., Just,E., Morio,T., Rost,R., Churcher,C., Cooper,J., Haydock,S., van,D.N., Cronin,A., Goodhead,I., Muzny,D., Mourier,T., Pain,A., Lu,M., Harper,D., Lindsay,R., Hauser,H., James,K., Quiles,M., Madan,B.M., Saito,T., Buchrieser,C., Wardroper,A., Felder,M., Thangavelu,M., Johnson,D., Knights,A., Loulseged,H., Mungall,K., Oliver,K., Price,C., Quail,M.A., Urushihara,H., Hernandez,J., Rabbinowitsch,E., Steffen,D., Sanders,M., Ma,J., Kohara,Y., Sharp,S., Simmonds,M., Spiegler,S., Tivey,A., Sugano,S., White,B., Walker,D., Woodward,J., Winckler,T., Tanaka,Y., Shaulsky,G., Schleicher,M., Weinstock,G., Rosenthal,A., Cox,E.C., Chisholm,R.L., Gibbs,R., Loomis,W.F., Platzer,M., Kay,R.R., Williams,J., Dear,P.H., Noegel,A.A., Barrell,B., and Kuspa,A. (2005). The genome of the social amoeba Dictyostelium discoideum. Nature *435*, 43-57.

Escalante,R. and Vicente,J.J. (2000). Dictyostelium discoideum: a model system for differentiation and patterning. Int. J. Dev. Biol. *44*, 819-835.

Fagone,P. and Jackowski,S. (2009). Membrane phospholipid synthesis and endoplasmic reticulum function. J. Lipid Res. *50 Suppl*, S311-S316.

Faix,J., Kreppel,L., Shaulsky,G., Schleicher,M., and Kimmel,A.R. (2004). A rapid and efficient method to generate multiple gene disruptions in Dictyostelium discoideum using a single selectable marker and the Cre-loxP system. Nucleic Acids Res. *32*, e143.

Fang,X., Yu,S.X., Lu,Y., Bast,R.C., Jr., Woodgett,J.R., and Mills,G.B. (2000). Phosphorylation and inactivation of glycogen synthase kinase 3 by protein kinase A. Proc. Natl. Acad. Sci. U. S. A *97*, 11960-11965.

Feng,R., Wang,H., Wang,J., Shrom,D., Zeng,X., and Tsien,J.Z. (2004). Forebrain degeneration and ventricle enlargement caused by double knockout

of Alzheimer's presenilin-1 and presenilin-2. Proc. Natl. Acad. Sci. U. S. A *101*, 8162-8167.

Fisher,P.R. and Wilczynska,Z. (2006). Contribution of endoplasmic reticulum to Ca(2+) signals in Dictyostelium depends on extracellular Ca(2+). FEMS Microbiol. Lett. *257*, 268-277.

Furukawa,K., Guo,Q., Schellenberg,G.D., and Mattson,M.P. (1998). Presenilin-1 mutation alters NGF-induced neurite outgrowth, calcium homeostasis, and transcription factor (AP-1) activation in PC12 cells. J. Neurosci. Res. *52*, 618-624.

Gotz,J. and Ittner,L.M. (2008). Animal models of Alzheimer's disease and frontotemporal dementia. Nat. Rev. Neurosci. *9*, 532-544.

Greenbaum,D., Colangelo,C., Williams,K., and Gerstein,M. (2003). Comparing protein abundance and mRNA expression levels on a genomic scale. Genome Biol. *4*, 117.

Guo,Q., Furukawa,K., Sopher,B.L., Pham,D.G., Xie,J., Robinson,N., Martin,G.M., and Mattson,M.P. (1996). Alzheimer's PS-1 mutation perturbs calcium homeostasis and sensitizes PC12 cells to death induced by amyloid beta-peptide. Neuroreport *8*, 379-383.

Haass,C. and De Strooper,B. (1999). The presenilins in Alzheimer's disease--proteolysis holds the key. Science *286*, 916-919.

Hall,A.M. and Roberson,E.D. (2011). Mouse models of Alzheimer's disease. Brain Res. Bull.

Handler,M., Yang,X., and Shen,J. (2000). Presenilin-1 regulates neuronal differentiation during neurogenesis. Development *127*, 2593-2606.

Hanger,D.P. and Noble,W. (2011). Functional implications of glycogen synthase kinase-3-mediated tau phosphorylation. Int. J. Alzheimers. Dis. *2011*, 352805.

Harwood,A.J. (2008). Use of the Dictyostelium stalk cell assay to monitor GSK-3 regulation. Methods Mol. Biol. *469*, 39-43.

Harwood,A.J., Plyte,S.E., Woodgett,J., Strutt,H., and Kay,R.R. (1995). Glycogen synthase kinase 3 regulates cell fate in Dictyostelium. Cell *80*, 139-148.

Hashimoto-Gotoh,T., Tsujimura,A., Watanabe,Y., Iwabe,N., Miyata,T., and Tabira,T. (2003). A unifying model for functional difference and redundancy of presenilin-1 and -2 in cell apoptosis and differentiation. Gene *323*, 115-123.

Hauptmann,S., Keil,U., Scherping,I., Bonert,A., Eckert,A., and Muller,W.E. (2006). Mitochondrial dysfunction in sporadic and genetic Alzheimer's disease. Exp. Gerontol. *41*, 668-673.

Henricson,A., Kall,L., and Sonnhammer,E.L. (2005). A novel transmembrane topology of presenilin based on reconciling experimental and computational evidence. FEBS J. *272*, 2727-2733.

Herreman,A., Hartmann,D., Annaert,W., Saftig,P., Craessaerts,K., Serneels,L., Umans,L., Schrijvers,V., Checler,F., Vanderstichele,H., Baekelandt,V., Dressel,R., Cupers,P., Huylebroeck,D., Zwijsen,A., Van,L.F., and de,S.B. (1999). Presenilin 2 deficiency causes a mild pulmonary phenotype and no changes in amyloid precursor protein processing but enhances the embryonic lethal phenotype of presenilin 1 deficiency. Proc. Natl. Acad. Sci. U. S. A *96*, 11872-11877.

Ho,S.N., Hunt,H.D., Horton,R.M., Pullen,J.K., and Pease,L.R. (1989). Site-directed mutagenesis by overlap extension using the polymerase chain reaction. Gene *77*, 51-59.

Honda,T., Nihonmatsu,N., Yasutake,K., Ohtake,A., Sato,K., Tanaka,S., Murayama,O., Murayama,M., and Takashima,A. (2000). Familial Alzheimer's disease-associated mutations block translocation of full-length presenilin 1 to the nuclear envelope. Neurosci. Res. *37*, 101-111.

Hooper,C., Tavassoli,M., Chapple,J.P., Uwanogho,D., Goodyear,R., Melino,G., Lovestone,S., and Killick,R. (2006). TAp73 isoforms antagonize Notch signalling in SH-SY5Y neuroblastomas and in primary neurones. J. Neurochem. *99*, 989-999.

Huang,E., Talukder,S., Hughes,T.R., Curk,T., Zupan,B., Shaulsky,G., and Katoh-Kurasawa,M. (2011). BzpF is a CREB-like transcription factor that regulates spore maturation and stability in Dictyostelium. Dev. Biol. *358*, 137-146.

Huang,Y. and Mucke,L. (2012). Alzheimer mechanisms and therapeutic strategies. Cell *148*, 1204-1222.

Iranfar,N., Fuller,D., and Loomis,W.F. (2003). Genome-wide expression analyses of gene regulation during early development of Dictyostelium discoideum. Eukaryot. Cell *2*, 664-670.

Ito,E., Oka,K., Etcheberrigaray,R., Nelson,T.J., McPhie,D.L., Tofel-Grehl,B., Gibson,G.E., and Alkon,D.L. (1994). Internal Ca2+ mobilization is altered in fibroblasts from patients with Alzheimer disease. Proc. Natl. Acad. Sci. U. S. A *91*, 534-538.

Ittner,A., Ke,Y.D., van,E.J., Gladbach,A., Gotz,J., and Ittner,L.M. (2011). Brief update on different roles of tau in neurodegeneration. IUBMB. Life *63*, 495-502.

Jaffe,L.F. (1999). Organization of early development by calcium patterns. Bioessays *21*, 657-667.

Kang,D.E., Soriano,S., Xia,X., Eberhart,C.G., de,S.B., Zheng,H., and Koo,E.H. (2002). Presenilin couples the paired phosphorylation of beta-catenin

independent of axin: implications for beta-catenin activation in tumorigenesis. Cell *110*, 751-762.

Khandelwal,A., Chandu,D., Roe,C.M., Kopan,R., and Quatrano,R.S. (2007). Moonlighting activity of presenilin in plants is independent of gamma-secretase and evolutionarily conserved. Proc. Natl. Acad. Sci. U. S. A *104*, 13337-13342.

Kim,H., Ki,H., Park,H.S., and Kim,K. (2005). Presenilin-1 D257A and D385A mutants fail to cleave Notch in their endoproteolyzed forms, but only presenilin-1 D385A mutant can restore its gamma-secretase activity with the compensatory overexpression of normal C-terminal fragment. J. Biol. Chem. *280*, 22462-22472.

Kim,J.Y., Haastert,P.V., and Devreotes,P.N. (1996). Social senses: G-protein-coupled receptor signaling pathways in Dictyostelium discoideum. Chem. Biol. *3*, 239-243.

Kim,J.Y., Soede,R.D., Schaap,P., Valkema,R., Borleis,J.A., Van Haastert,P.J., Devreotes,P.N., and Hereld,D. (1997). Phosphorylation of chemoattractant receptors is not essential for chemotaxis or termination of G-protein-mediated responses. J. Biol. Chem. *272*, 27313-27318.

Kim,S.D. and Kim,J. (2008). Sequence analyses of presenilin mutations linked to familial Alzheimer's disease. Cell Stress. Chaperones. *13*, 401-412.

Kim,S.H., Leem,J.Y., Lah,J.J., Slunt,H.H., Levey,A.I., Thinakaran,G., and Sisodia,S.S. (2001). Multiple effects of aspartate mutant presenilin 1 on the processing and trafficking of amyloid precursor protein. J. Biol. Chem. *276*, 43343-43350.

King,J.S. (2012). Autophagy across the eukaryotes: Is S. cerevisiae the odd one out? Autophagy. *8*.

Kjeld, O. DNA analysis software. AcaClone software. 2006.
Ref Type: Generic

Knapp, M. and Prince, M. Dementia UK. 2007. Alzheimer's Society.
Ref Type: Generic

Koo,E.H. and Kopan,R. (2004). Potential role of presenilin-regulated signaling pathways in sporadic neurodegeneration. Nat. Med. *10 Suppl*, S26-S33.

Kumar,S., Nei,M., Dudley,J., and Tamura,K. (2008). MEGA: a biologist-centric software for evolutionary analysis of DNA and protein sequences. Brief. Bioinform. *9*, 299-306.

Laferla,F.M., Green,K.N., and Oddo,S. (2007). Intracellular amyloid-beta in Alzheimer's disease. Nat. Rev. Neurosci. *8*, 499-509.

Lai,M.T., Chen,E., Crouthamel,M.C., DiMuzio-Mower,J., Xu,M., Huang,Q., Price,E., Register,R.B., Shi,X.P., Donoviel,D.B., Bernstein,A., Hazuda,D.,

Gardell,S.J., and Li,Y.M. (2003). Presenilin-1 and presenilin-2 exhibit distinct yet overlapping gamma-secretase activities. J. Biol. Chem. *278*, 22475-22481.

Lam,D., Kosta,A., Luciani,M.F., and Golstein,P. (2008). The inositol 1,4,5-trisphosphate receptor is required to signal autophagic cell death. Mol. Biol. Cell *19*, 691-700.

Landman,N., Jeong,S.Y., Shin,S.Y., Voronov,S.V., Serban,G., Kang,M.S., Park,M.K., Di,P.G., Chung,S., and Kim,T.W. (2006). Presenilin mutations linked to familial Alzheimer's disease cause an imbalance in phosphatidylinositol 4,5-bisphosphate metabolism. Proc. Natl. Acad. Sci. U. S. A *103*, 19524-19529.

Lee,M.K., Slunt,H.H., Martin,L.J., Thinakaran,G., Kim,G., Gandy,S.E., Seeger,M., Koo,E., Price,D.L., and Sisodia,S.S. (1996). Expression of presenilin 1 and 2 (PS1 and PS2) in human and murine tissues. J. Neurosci. *16*, 7513-7525.

Levitan,D., Doyle,T.G., Brousseau,D., Lee,M.K., Thinakaran,G., Slunt,H.H., Sisodia,S.S., and Greenwald,I. (1996). Assessment of normal and mutant human presenilin function in Caenorhabditis elegans. Proc. Natl. Acad. Sci. U. S. A *93*, 14940-14944.

Levitan,D. and Greenwald,I. (1995). Facilitation of lin-12-mediated signalling by sel-12, a Caenorhabditis elegans S182 Alzheimer's disease gene. Nature *377*, 351-354.

Li,G., Alexander,H., Schneider,N., and Alexander,S. (2000). Molecular basis for resistance to the anticancer drug cisplatin in Dictyostelium. Microbiology *146 (Pt 9)*, 2219-2227.

Li,J., Xu,M., Zhou,H., Ma,J., and Potter,H. (1997). Alzheimer presenilins in the nuclear membrane, interphase kinetochores, and centrosomes suggest a role in chromosome segregation. Cell *90*, 917-927.

Li,Y., Liu,L., Liu,D., Woodward,S., Barger,S.W., Mrak,R.E., and Griffin,W.S. (2004). Microglial activation by uptake of fDNA via a scavenger receptor. J. Neuroimmunol. *147*, 50-55.

Logan,C.Y. and Nusse,R. (2004). The Wnt signaling pathway in development and disease. Annu. Rev. Cell Dev. Biol. *20*, 781-810.

Loomis,W.F. (1998). Role of PKA in the timing of developmental events in Dictyostelium cells. Microbiol. Mol. Biol. Rev. *62*, 684-694.

Ludtmann,M.H., Boeckeler,K., and Williams,R.S. (2011). Molecular pharmacology in a simple model system: implicating MAP kinase and phosphoinositide signalling in bipolar disorder. Semin. Cell Dev. Biol. *22*, 105-113.

Maccioni,R.B., Munoz,J.P., and Barbeito,L. (2001). The molecular bases of Alzheimer's disease and other neurodegenerative disorders. Arch. Med. Res. *32*, 367-381.

Magalhaes,L.G., de Castro-Borges,W., de Souza,G.M., Guerra-Sa,R., and Rodrigues,V. (2009). Molecular cloning, sequencing, and expression analysis of presenilin cDNA from Schistosoma mansoni. Parasitol. Res. *106*, 7-13.

Marambaud,P., Dreses-Werringloer,U., and Vingtdeux,V. (2009). Calcium signaling in neurodegeneration. Mol. Neurodegener. *4*, 20.

Martinez, A. Emerging Drugs and Targets for Alzheimer's Disease: Volume 1: Beta-Amyloid, Tau Protein and Glucose Metabolism. 2010. RSC Publishing. Ref Type: Generic

Martinez-Mir,A., Canestro,C., Gonzalez-Duarte,R., and Albalat,R. (2001). Characterization of the amphioxus presenilin gene in a high gene-density genomic region illustrates duplication during the vertebrate lineage. Gene *279*, 157-164.

Mattson,M.P. (2010). ER calcium and Alzheimer's disease: in a state of flux. Sci. Signal. *3*, e10.

Mattson,M.P. and Chan,S.L. (2003). Neuronal and glial calcium signaling in Alzheimer's disease. Cell Calcium *34*, 385-397.

McCarthy,J.V., Twomey,C., and Wujek,P. (2009). Presenilin-dependent regulated intramembrane proteolysis and gamma-secretase activity. Cell Mol. Life Sci. *66*, 1534-1555.

McMains,V.C., Myre,M., Kreppel,L., and Kimmel,A.R. (2010). Dictyostelium possesses highly diverged presenilin/gamma-secretase that regulates growth and cell-fate specification and can accurately process human APP: a system for functional studies of the presenilin/gamma-secretase complex. Dis. Model. Mech. *3*, 581-594.

Meredith,J.E., Jr., Wang,Q., Mitchell,T.J., Olson,R.E., Zaczek,R., Stern,A.M., and Seiffert,D. (2002). Gamma-secretase activity is not involved in presenilin-mediated regulation of beta-catenin. Biochem. Biophys. Res. Commun. *299*, 744-750.

Moehlmann,T., Winkler,E., Xia,X., Edbauer,D., Murrell,J., Capell,A., Kaether,C., Zheng,H., Ghetti,B., Haass,C., and Steiner,H. (2002). Presenilin-1 mutations of leucine 166 equally affect the generation of the Notch and APP intracellular domains independent of their effect on Abeta 42 production. Proc. Natl. Acad. Sci. U. S. A *99*, 8025-8030.

Mrak,R.E. (2012). Microglia in Alzheimer brain: a neuropathological perspective. Int. J. Alzheimers. Dis. *2012*, 165021.

Muirhead,K.E., Borger,E., Aitken,L., Conway,S.J., and Gunn-Moore,F.J. (2010). The consequences of mitochondrial amyloid beta-peptide in Alzheimer's disease. Biochem. J. *426*, 255-270.

Muller-Taubenberger,A., Lupas,A.N., Li,H., Ecke,M., Simmeth,E., and Gerisch,G. (2001). Calreticulin and calnexin in the endoplasmic reticulum are important for phagocytosis. EMBO J. *20*, 6772-6782.

Murayama,M., Tanaka,S., Palacino,J., Murayama,O., Honda,T., Sun,X., Yasutake,K., Nihonmatsu,N., Wolozin,B., and Takashima,A. (1998). Direct association of presenilin-1 with beta-catenin. FEBS Lett. *433*, 73-77.

Myre,M.A., Lumsden,A.L., Thompson,M.N., Wasco,W., MacDonald,M.E., and Gusella,J.F. (2011). Deficiency of huntingtin has pleiotropic effects in the social amoeba Dictyostelium discoideum. PLoS. Genet. *7*, e1002052.

Nicholson,A.M. and Ferreira,A. (2009). Increased membrane cholesterol might render mature hippocampal neurons more susceptible to beta-amyloid-induced calpain activation and tau toxicity. J. Neurosci. *29*, 4640-4651.

Nornes,S., Newman,M., Verdile,G., Wells,S., Stoick-Cooper,C.L., Tucker,B., Frederich-Sleptsova,I., Martins,R., and Lardelli,M. (2008). Interference with splicing of Presenilin transcripts has potent dominant negative effects on Presenilin activity. Hum. Mol. Genet. *17*, 402-412.

Nornes,S., Newman,M., Wells,S., Verdile,G., Martins,R.N., and Lardelli,M. (2009). Independent and cooperative action of Psen2 with Psen1 in zebrafish embryos. Exp. Cell Res. *315*, 2791-2801.

Page,M.J. and Di,C.E. (2008). Evolution of peptidase diversity. J. Biol. Chem. *283*, 30010-30014.

Parent,C.A. (2004). Making all the right moves: chemotaxis in neutrophils and Dictyostelium. Curr. Opin. Cell Biol. *16*, 4-13.

Parihar,M.S. and Hemnani,T. (2004). Alzheimer's disease pathogenesis and therapeutic interventions. J. Clin. Neurosci. *11*, 456-467.

Paris,D., Town,T., Mori,T., Parker,T.A., Humphrey,J., and Mullan,M. (2000). Soluble beta-amyloid peptides mediate vasoactivity via activation of a pro-inflammatory pathway. Neurobiol. Aging *21*, 183-197.

Park,K.C., Rivero,F., Meili,R., Lee,S., Apone,F., and Firtel,R.A. (2004). Rac regulation of chemotaxis and morphogenesis in Dictyostelium. EMBO J. *23*, 4177-4189.

Parks,A.L. and Curtis,D. (2007). Presenilin diversifies its portfolio. Trends Genet. *23*, 140-150.

Pawolleck,N. and Williams,R.S. (2009). Quantifying in vivo phosphoinositide turnover in chemotactically competent Dictyostelium cells. Methods Mol. Biol. *571*, 283-290.

Plyte,S.E., O'Donovan,E., Woodgett,J.R., and Harwood,A.J. (1999). Glycogen synthase kinase-3 (GSK-3) is regulated during Dictyostelium development via the serpentine receptor cAR3. Development *126*, 325-333.

Qian,S., Jiang,P., Guan,X.M., Singh,G., Trumbauer,M.E., Yu,H., Chen,H.Y., Van de Ploeg,L.H., and Zheng,H. (1998). Mutant human presenilin 1 protects presenilin 1 null mouse against embryonic lethality and elevates Abeta1-42/43 expression. Neuron *20*, 611-617.

Qing,H., He,G., Ly,P.T., Fox,C.J., Staufenbiel,M., Cai,F., Zhang,Z., Wei,S., Sun,X., Chen,C.H., Zhou,W., Wang,K., and Song,W. (2008). Valproic acid inhibits Abeta production, neuritic plaque formation, and behavioral deficits in Alzheimer's disease mouse models. J. Exp. Med. *205*, 2781-2789.

R Core Team. R: A Language and Environment for Statistical Computing. 2012. R Foundation for Statistical Computing.
Ref Type: Generic

Rankin,C.A., Sun,Q., and Gamblin,T.C. (2007). Tau phosphorylation by GSK-3beta promotes tangle-like filament morphology. Mol. Neurodegener. *2*, 12.

Rasband, W. C. ImageJ. 2007. U. S. National Institutes of Health, Bethesda, Maryland, USA.
Ref Type: Generic

Rasband, W. S. ImageJ. 1997. U. S. National Institutes of Health.
Ref Type: Generic

Readnower,R.D., Sauerbeck,A.D., and Sullivan,P.G. (2011). Mitochondria, Amyloid beta, and Alzheimer's Disease. Int. J. Alzheimers. Dis. *2011*, 104545.

Rehberg,M., Kleylein-Sohn,J., Faix,J., Ho,T.H., Schulz,I., and Graf,R. (2005). Dictyostelium LIS1 is a centrosomal protein required for microtubule/cell cortex interactions, nucleus/centrosome linkage, and actin dynamics. Mol. Biol. Cell *16*, 2759-2771.

Robey,E. (1997). Notch in vertebrates. Curr. Opin. Genet. Dev. *7*, 551-557.

Rogaeva,E.A., Fafel,K.C., Song,Y.Q., Medeiros,H., Sato,C., Liang,Y., Richard,E., Rogaev,E.I., Frommelt,P., Sadovnick,A.D., Meschino,W., Rockwood,K., Boss,M.A., Mayeux,R., and George-Hyslop,P. (2001). Screening for PS1 mutations in a referral-based series of AD cases: 21 novel mutations. Neurology *57*, 621-625.

Rot,G., Parikh,A., Curk,T., Kuspa,A., Shaulsky,G., and Zupan,B. (2009). dictyExpress: a Dictyostelium discoideum gene expression database with an explorative data analysis web-based interface. BMC. Bioinformatics. *10*, 265.

Ryves,W.J., Fryer,L., Dale,T., and Harwood,A.J. (1998). An assay for glycogen synthase kinase 3 (GSK-3) for use in crude cell extracts. Anal. Biochem. *264*, 124-127.

Salawu,F.K., Umar,J.T., and Olokoba,A.B. (2011). Alzheimer's disease: a review of recent developments. Ann. Afr. Med. *10*, 73-79.

Schenk,D., Barbour,R., Dunn,W., Gordon,G., Grajeda,H., Guido,T., Hu,K., Huang,J., Johnson-Wood,K., Khan,K., Kholodenko,D., Lee,M., Liao,Z., Lieberburg,I., Motter,R., Mutter,L., Soriano,F., Shopp,G., Vasquez,N., Vandevert,C., Walker,S., Wogulis,M., Yednock,T., Games,D., and Seubert,P. (1999). Immunization with amyloid-beta attenuates Alzheimer-disease-like pathology in the PDAPP mouse. Nature *400*, 173-177.

Scherer,A., Kuhl,S., Wessels,D., Lusche,D.F., Raisley,B., and Soll,D.R. (2010). Ca2+ chemotaxis in Dictyostelium discoideum. J. Cell Sci. *123*, 3756-3767.

Schilde,C., Araki,T., Williams,H., Harwood,A., and Williams,J.G. (2004). GSK3 is a multifunctional regulator of Dictyostelium development. Development *131*, 4555-4565.

Seidner,G.A., Ye,Y., Faraday,M.M., Alvord,W.G., and Fortini,M.E. (2006). Modeling clinically heterogeneous presenilin mutations with transgenic Drosophila. Curr. Biol. *16*, 1026-1033.

Selkoe,D. and Kopan,R. (2003). Notch and Presenilin: regulated intramembrane proteolysis links development and degeneration. Annu. Rev. Neurosci. *26*, 565-597.

Selkoe,D.J. (1997). Alzheimer's disease: genotypes, phenotypes, and treatments. Science *275*, 630-631.

Selkoe,D.J. (2011). Resolving controversies on the path to Alzheimer's therapeutics. Nat. Med. *17*, 1060-1065.

Sharma,R.P. and Chopra,V.L. (1976). Effect of the Wingless (wg1) mutation on wing and haltere development in Drosophila melanogaster. Dev. Biol. *48*, 461-465.

Sharp,P.M. and Devine,K.M. (1989). Codon usage and gene expression level in Dictyostelium discoideum: highly expressed genes do 'prefer' optimal codons. Nucleic Acids Res. *17*, 5029-5039.

Shen,J., Bronson,R.T., Chen,D.F., Xia,W., Selkoe,D.J., and Tonegawa,S. (1997). Skeletal and CNS defects in Presenilin-1-deficient mice. Cell *89*, 629-639.

Shilling,D., Mak,D.O., Kang,D.E., and Foskett,J.K. (2012). Lack of evidence for presenilins as endoplasmic reticulum Ca2+ leak channels. J. Biol. Chem.

Small,D.H. (2001). The role of presenilins in gamma-secretase activity: catalyst or cofactor? J. Neurochem. *76*, 1612-1614.

Soderbom,F. and Loomis,W.F. (1998). Cell-cell signaling during Dictyostelium development. Trends Microbiol. *6*, 402-406.

Soriano,S., Kang,D.E., Fu,M., Pestell,R., Chevallier,N., Zheng,H., and Koo,E.H. (2001). Presenilin 1 negatively regulates beta-catenin/T cell factor/lymphoid

enhancer factor-1 signaling independently of beta-amyloid precursor protein and notch processing. J. Cell Biol. *152*, 785-794.

Spasic,D. and Annaert,W. (2008). Building gamma-secretase: the bits and pieces. J. Cell Sci. *121*, 413-420.

Spasic,D., Tolia,A., Dillen,K., Baert,V., de,S.B., Vrijens,S., and Annaert,W. (2006). Presenilin-1 maintains a nine-transmembrane topology throughout the secretory pathway. J. Biol. Chem. *281*, 26569-26577.

Sun,T. and Kim,L. (2011). Tyrosine phosphorylation-mediated signaling pathways in dictyostelium. J. Signal. Transduct. *2011*, 894351.

Sun,T.J. and Devreotes,P.N. (1991). Gene targeting of the aggregation stage cAMP receptor cAR1 in Dictyostelium. Genes Dev. *5*, 572-582.

Supnet,C. and Bezprozvanny,I. (2011). Presenilins as endoplasmic reticulum calcium leak channels and Alzheimer's disease pathogenesis. Sci. China Life Sci. *54*, 744-751.

Swerdlow,R.H. (2011). Brain aging, Alzheimer's disease, and mitochondria. Biochim. Biophys. Acta *1812*, 1630-1639.

Takagi,S., Tominaga,A., Sato,C., Tomita,T., and Iwatsubo,T. (2010). Participation of transmembrane domain 1 of presenilin 1 in the catalytic pore structure of the gamma-secretase. J. Neurosci. *30*, 15943-15950.

Takashima,A., Murayama,M., Murayama,O., Kohno,T., Honda,T., Yasutake,K., Nihonmatsu,N., Mercken,M., Yamaguchi,H., Sugihara,S., and Wolozin,B. (1998). Presenilin 1 associates with glycogen synthase kinase-3beta and its substrate tau. Proc. Natl. Acad. Sci. U. S. A *95*, 9637-9641.

Tandon,A. and Fraser,P. (2002). The presenilins. Genome Biol. *3*, reviews3014.

Tang,Y. and Gomer,R.H. (2008). A protein with similarity to PTEN regulates aggregation territory size by decreasing cyclic AMP pulse size during Dictyostelium discoideum development. Eukaryot. Cell *7*, 1758-1770.

Tekirian,T.L., Merriam,D.E., Marshansky,V., Miller,J., Crowley,A.C., Chan,H., Ausiello,D., Brown,D., Buxbaum,J.D., Xia,W., and Wasco,W. (2001). Subcellular localization of presenilin 2 endoproteolytic C-terminal fragments. Brain Res. Mol. Brain Res. *96*, 14-20.

Thomason,P., Traynor,D., and Kay,R. (1999a). Taking the plunge. Terminal differentiation in Dictyostelium. Trends Genet. *15*, 15-19.

Thomason,P.A., Traynor,D., Stock,J.B., and Kay,R.R. (1999b). The RdeA-RegA system, a eukaryotic phospho-relay controlling cAMP breakdown. J. Biol. Chem. *274*, 27379-27384.

Traynor,D., Milne,J.L., Insall,R.H., and Kay,R.R. (2000). Ca(2+) signalling is not required for chemotaxis in Dictyostelium. EMBO J. *19*, 4846-4854.

Tsujimura,A., Yasojima,K., and Hashimoto-Gotoh,T. (1997). Cloning of Xenopus presenilin-alpha and -beta cDNAs and their differential expression in oogenesis and embryogenesis. Biochem. Biophys. Res. Commun. *231*, 392-396.

Tu,H., Nelson,O., Bezprozvanny,A., Wang,Z., Lee,S.F., Hao,Y.H., Serneels,L., de,S.B., Yu,G., and Bezprozvanny,I. (2006a). Presenilins form ER Ca2+ leak channels, a function disrupted by familial Alzheimer's disease-linked mutations. Cell *126*, 981-993.

Tu,H., Nelson,O., Bezprozvanny,A., Wang,Z., Lee,S.F., Hao,Y.H., Serneels,L., de,S.B., Yu,G., and Bezprozvanny,I. (2006b). Presenilins form ER Ca2+ leak channels, a function disrupted by familial Alzheimer's disease-linked mutations. Cell *126*, 981-993.

Tuppo,E.E. and Arias,H.R. (2005). The role of inflammation in Alzheimer's disease. Int. J. Biochem. Cell Biol. *37*, 289-305.

van Tijn,P., Kamphuis,W., Marlatt,M.W., Hol,E.M., and Lucassen,P.J. (2011). Presenilin mouse and zebrafish models for dementia: focus on neurogenesis. Prog. Neurobiol. *93*, 149-164.

Veltman,D.M., Akar,G., Bosgraaf,L., and Van Haastert,P.J. (2009). A new set of small, extrachromosomal expression vectors for Dictyostelium discoideum. Plasmid *61*, 110-118.

Vervoort,E.B., van,R.A., van Peij,N.N., Heikoop,J.C., Van Haastert,P.J., Verheijden,G.F., and Linskens,M.H. (2000). Optimizing heterologous expression in dictyostelium: importance of 5' codon adaptation. Nucleic Acids Res. *28*, 2069-2074.

Walter,J., Capell,A., Grunberg,J., Pesold,B., Schindzielorz,A., Prior,R., Podlisny,M.B., Fraser,P., Hyslop,P.S., Selkoe,D.J., and Haass,C. (1996). The Alzheimer's disease-associated presenilins are differentially phosphorylated proteins located predominantly within the endoplasmic reticulum. Mol. Med. *2*, 673-691.

Wang,J., Beher,D., Nyborg,A.C., Shearman,M.S., Golde,T.E., and Goate,A. (2006). C-terminal PAL motif of presenilin and presenilin homologues required for normal active site conformation. J. Neurochem. *96*, 218-227.

Wang,J.Z., Grundke-Iqbal,I., and Iqbal,K. (2007). Kinases and phosphatases and tau sites involved in Alzheimer neurofibrillary degeneration. Eur. J. Neurosci. *25*, 59-68.

Wang,P., Pereira,F.A., Beasley,D., and Zheng,H. (2003). Presenilins are required for the formation of comma- and S-shaped bodies during nephrogenesis. Development *130*, 5019-5029.

Wang,Y., Steimle,P.A., Ren,Y., Ross,C.A., Robinson,D.N., Egelhoff,T.T., Sesaki,H., and Iijima,M. (2011). Dictyostelium huntingtin controls chemotaxis

and cytokinesis through the regulation of myosin II phosphorylation. Mol. Biol. Cell *22*, 2270-2281.

Wang,Z., Iwasaki,M., Ficara,F., Lin,C., Matheny,C., Wong,S.H., Smith,K.S., and Cleary,M.L. (2010). GSK-3 promotes conditional association of CREB and its coactivators with MEIS1 to facilitate HOX-mediated transcription and oncogenesis. Cancer Cell *17*, 597-608.

Weijer,C.J. (2004). Dictyostelium morphogenesis. Curr. Opin. Genet. Dev. *14*, 392-398.

Weijer, C. J. and Williams, J. G. Dictyostelium: Cell Sorting and Patterning. 2009. ENCYCLOPEDIA OF LIFE SCIENCES, John Wiley & Sons.
Ref Type: Generic

Westlund,B., Parry,D., Clover,R., Basson,M., and Johnson,C.D. (1999). Reverse genetic analysis of Caenorhabditis elegans presenilins reveals redundant but unequal roles for sel-12 and hop-1 in Notch-pathway signaling. Proc. Natl. Acad. Sci. U. S. A *96*, 2497-2502.

Wilczynska,Z., Happle,K., Muller-Taubenberger,A., Schlatterer,C., Malchow,D., and Fisher,P.R. (2005). Release of Ca2+ from the endoplasmic reticulum contributes to Ca2+ signaling in Dictyostelium discoideum. Eukaryot. Cell *4*, 1513-1525.

Williams,R.S., Boeckeler,K., Graf,R., Muller-Taubenberger,A., Li,Z., Isberg,R.R., Wessels,D., Soll,D.R., Alexander,H., and Alexander,S. (2006). Towards a molecular understanding of human diseases using Dictyostelium discoideum. Trends Mol. Med. *12*, 415-424.

Williams,R.S., Eames,M., Ryves,W.J., Viggars,J., and Harwood,A.J. (1999). Loss of a prolyl oligopeptidase confers resistance to lithium by elevation of inositol (1,4,5) trisphosphate. EMBO J. *18*, 2734-2745.

Woffendin,C., Chambers,T.C., Schaller,K.L., Leichtling,B.H., and Rickenberg,H.V. (1986). Translocation of cAMP-dependent protein kinase to the nucleus during development of Dictyostelium discoideum. Dev. Biol. *115*, 1-8.

Wolfe,M.S., Xia,W., Ostaszewski,B.L., Diehl,T.S., Kimberly,W.T., and Selkoe,D.J. (1999). Two transmembrane aspartates in presenilin-1 required for presenilin endoproteolysis and gamma-secretase activity. Nature *398*, 513-517.

Woo,H.N., Park,J.S., Gwon,A.R., Arumugam,T.V., and Jo,D.G. (2009). Alzheimer's disease and Notch signaling. Biochem. Biophys. Res. Commun. *390*, 1093-1097.

Wray,S. and Noble,W. (2009). Linking amyloid and tau pathology in Alzheimer's disease: the role of membrane cholesterol in Abeta-mediated tau toxicity. J. Neurosci. *29*, 9665-9667.

Ye,Y. and Fortini,M.E. (1998). Characterization of Drosophila Presenilin and its colocalization with Notch during development. Mech. Dev. *79*, 199-211.

Zhang,Z., Hartmann,H., Do,V.M., Abramowski,D., Sturchler-Pierrat,C., Staufenbiel,M., Sommer,B., van de Wetering,M., Clevers,H., Saftig,P., de,S.B., He,X., and Yankner,B.A. (1998). Destabilization of beta-catenin by mutations in presenilin-1 potentiates neuronal apoptosis. Nature *395*, 698-702.